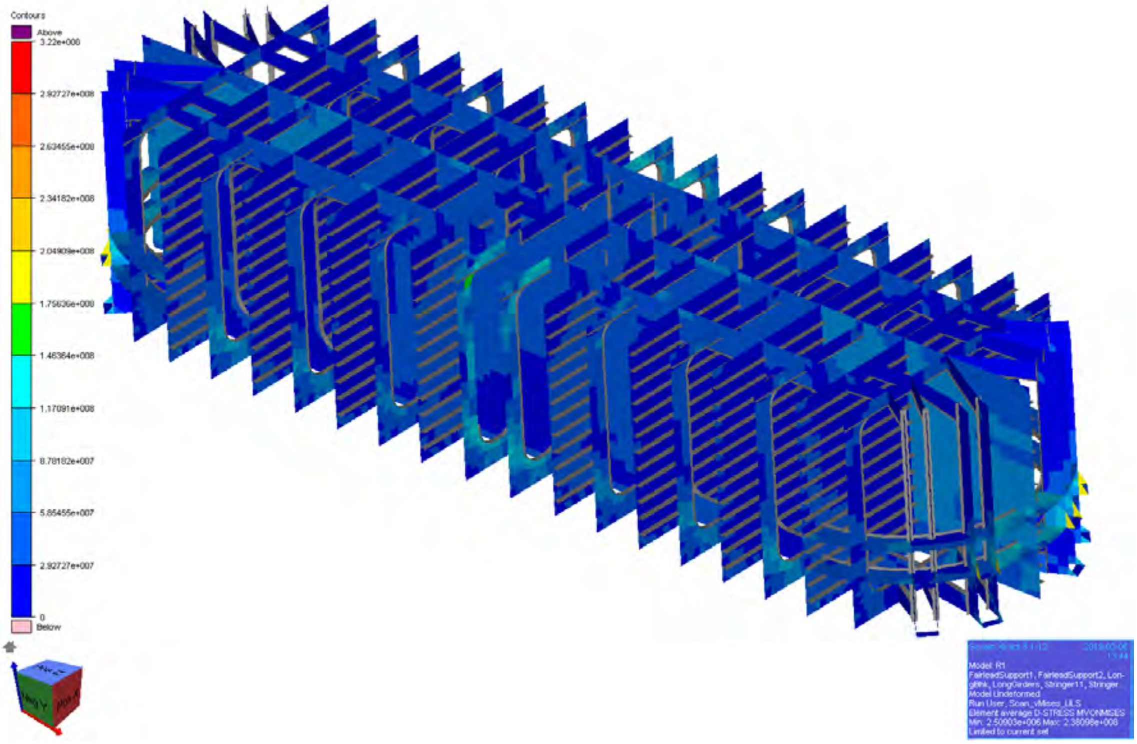

Figure 5-34 von Mises stresses for ULS load combinations [N/m^2] for internal structure

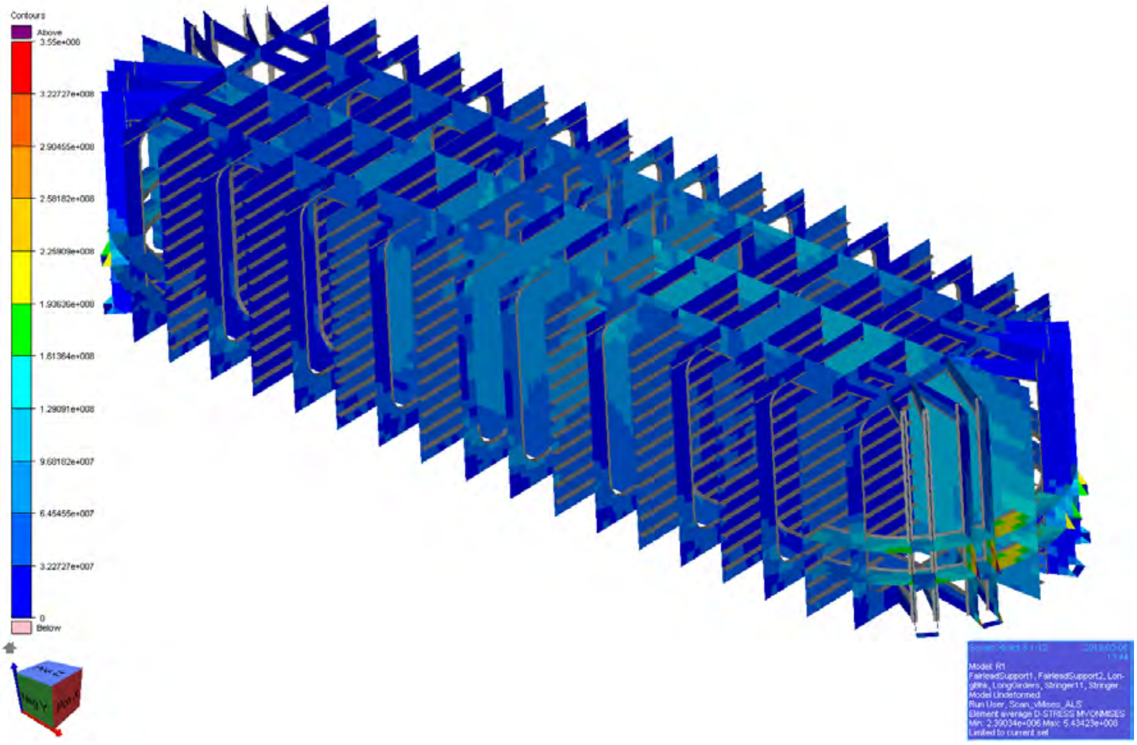

Figure 5-35 von Mises stresses for ALS load combinations [N/m^2] for internal structure

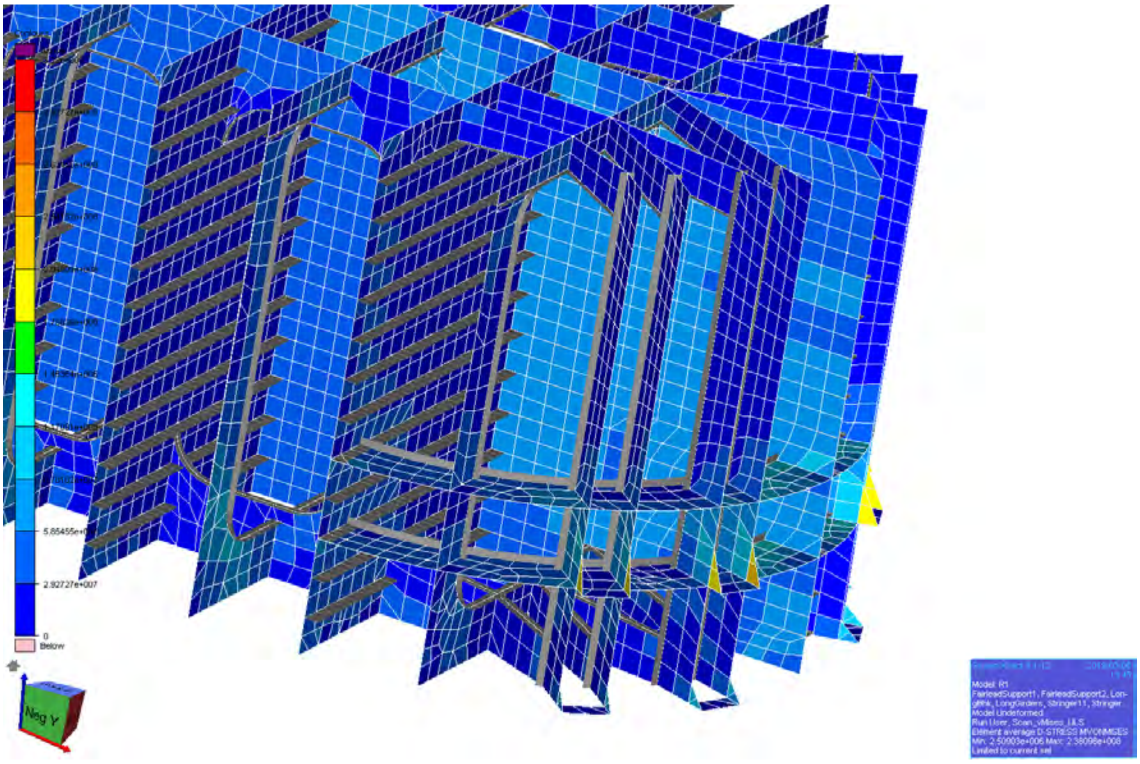

Figure 5-36 von Mises stresses for ULS load combinations [N/m²] for internal structure in way of fairlead supports

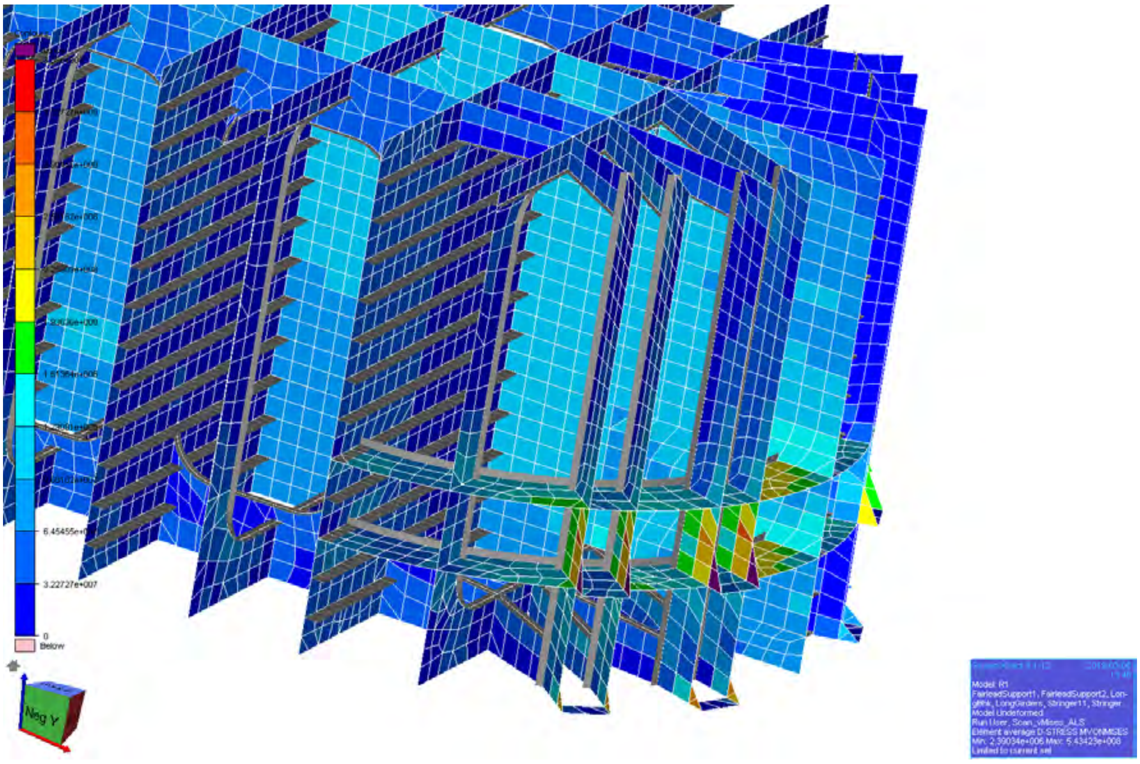

Figure 5-37 von Mises stresses for ALS load combinations [N/m²] for internal structure in way of fairlead supports

5.5.2 Buckling and minimum scantling assessment

The buckling assessment is performed according to DNVGL-RP-C203 and the minimum scantling check is performed according to DNVGL-OS-C101 by use of STIPLA software.

Identification of the structural items checked herein is shown in Figure 5-38, Figure 5-45, Figure 5-52, Figure 5-59, Figure 5-66, Figure 5-73 and Figure 5-80 for the “pontoon base case”.

The stress components in local x- and y- direction are taken from the result scans of the ULS and ALS load combinations respectively and shown herein.

The buckling and minimum scantling results are shown in Table 5-1 and Table 5-2, and the proposed structural scantling for the “pontoon base case” fulfil the rule requirements.

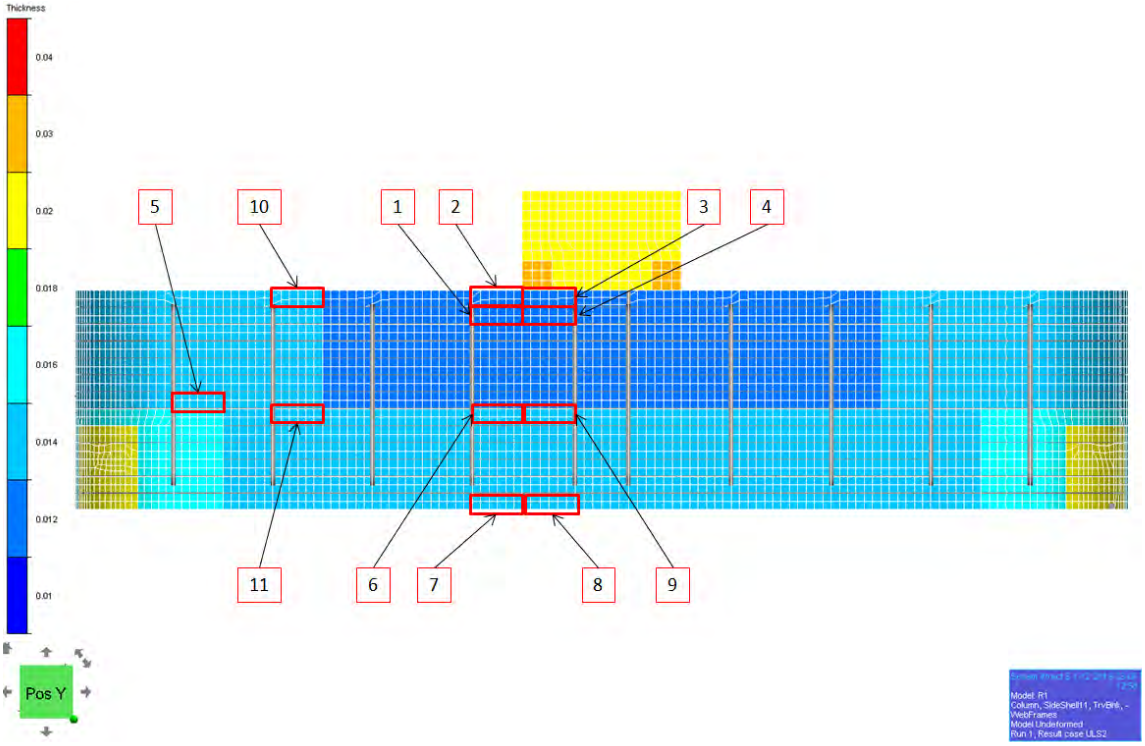

Figure 5-38 Identification of areas considered for buckling & scantling check for outer side shell

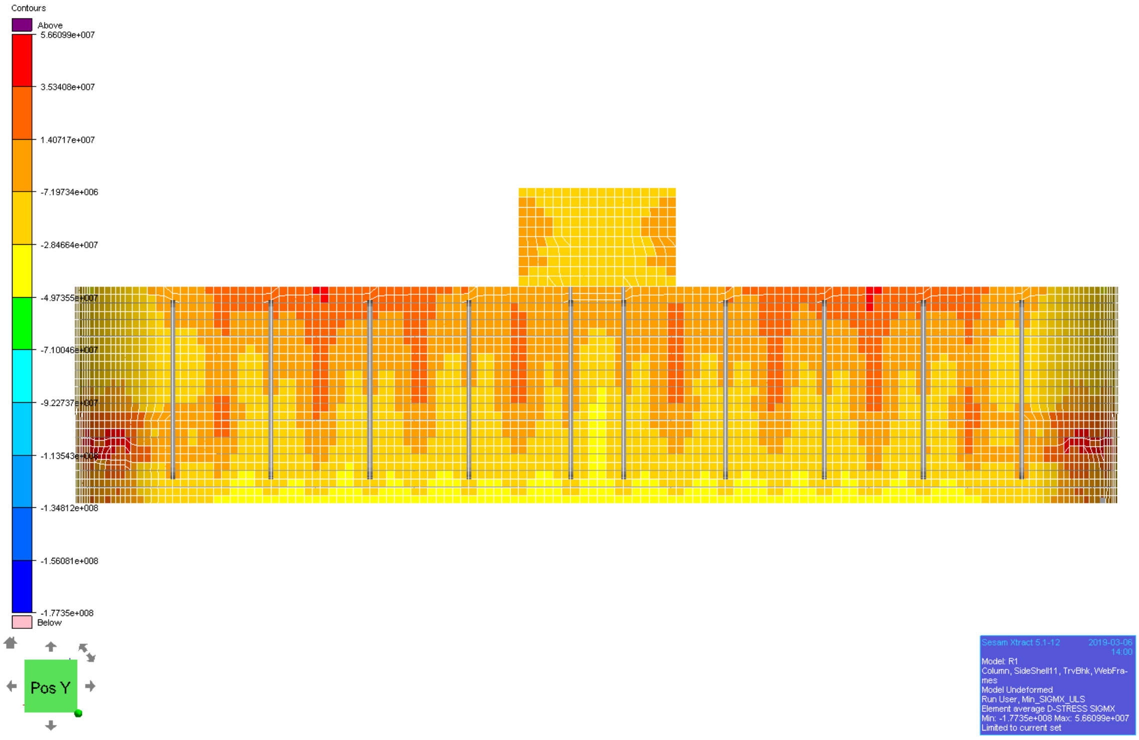

Sesam Xtract 5.1-12 2019-03-06 14:00
Model: R1
Column, SideShell11, TrvBhk, WebFrames
Model Undeformed
Run User, Min_SIGMX_ULS
Element average D-STRESS SIGMX
Min: -1.7735e+008 Max: 5.66099e+007
Limited to current set

Figure 5-39 SIGMX stresses for ULS load combinations [N/m^2], outer side shell

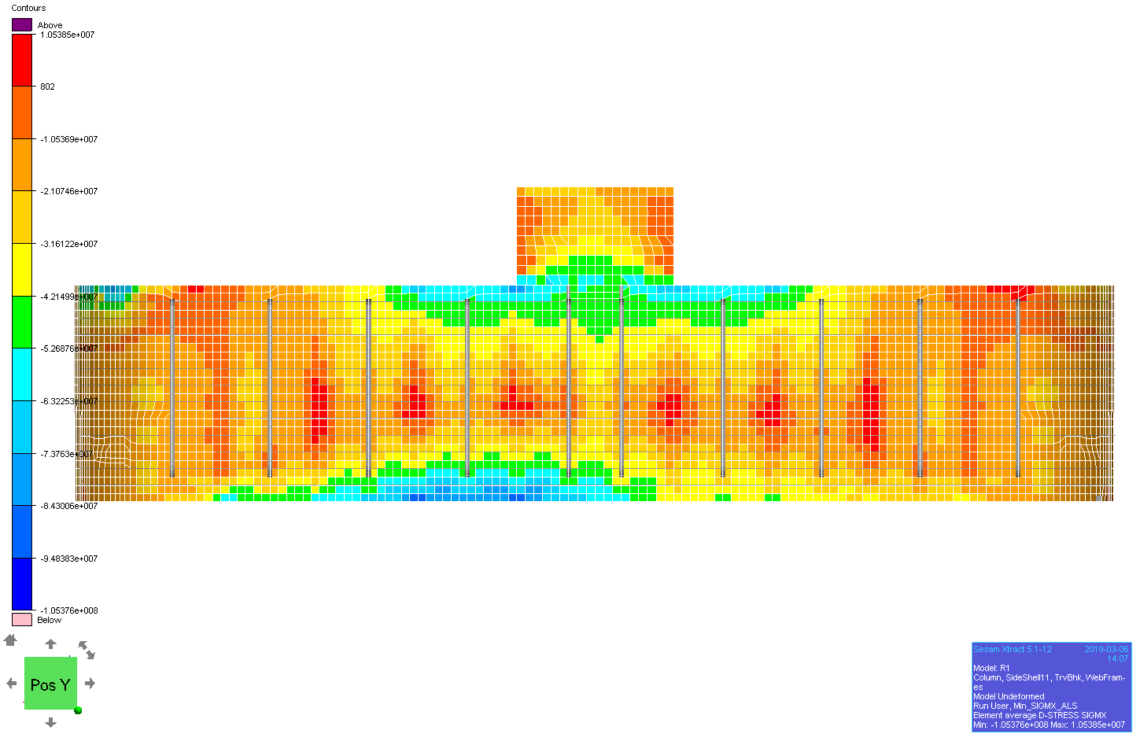

Sesam Xtract 5.1-12 2019-03-06 14:07
Model: R1
Column, SideShell11, TrvBhk, WebFrames
Model Undeformed
Run User, Min_SIGMX_ALS
Element average D-STRESS SIGMX
Min: -1.05376e+008 Max: 1.05385e+007

Figure 5-40 SIGMX stresses for ALS load combinations [N/m^2], outer side shell

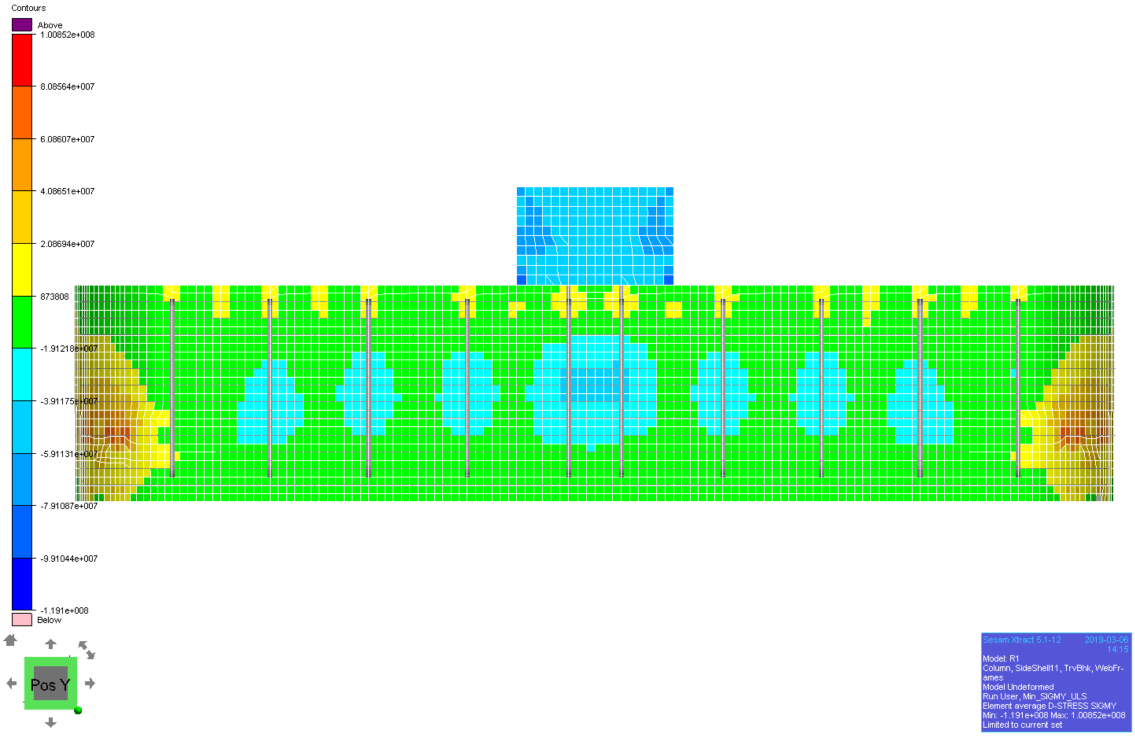

Sesam Xtract 5.1-12 2019-03-06 14:15
Model: R1
Column, SideShell11, TrvBhk, WebFr-ames
Model Undeformed
Run User, Min_SIGMY_ULS
Element average D-STRESS SIGMY
Min: -1.191e+008 Max: 1.00852e+008
Limited to current set

Figure 5-41 SIGMY stresses for ULS load combinations [N/m^2], outer side shell

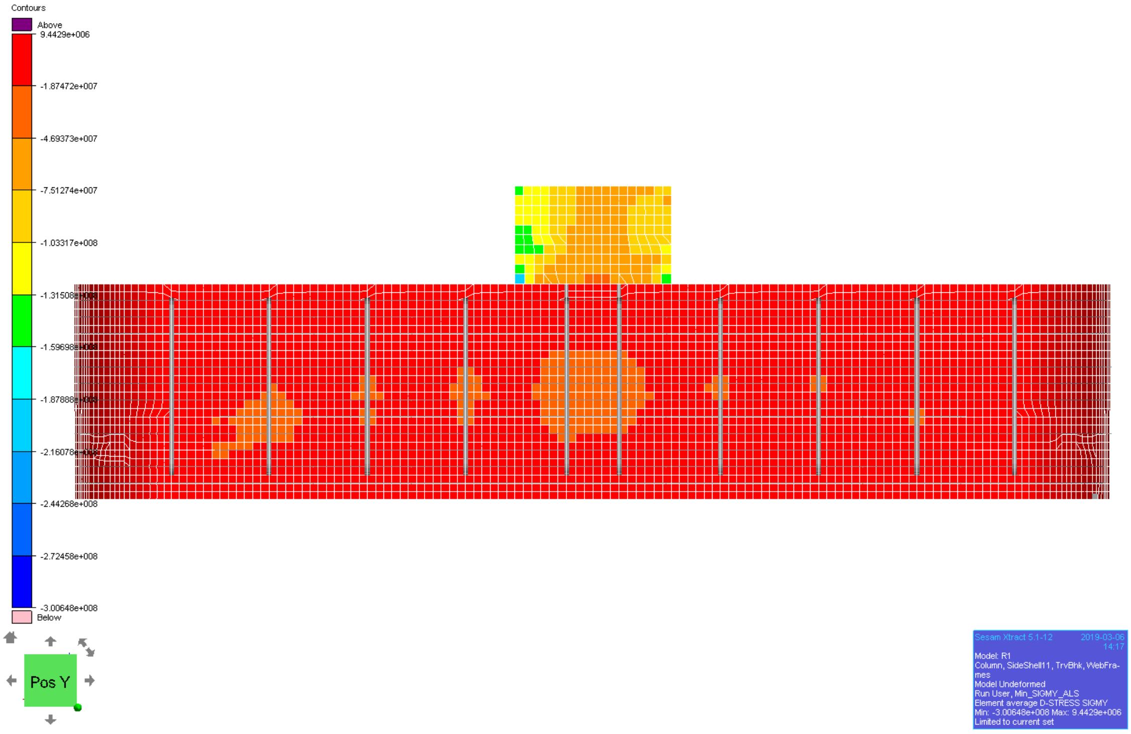

Sesam Xtract 5.1-12 2019-03-06 14:17
Model: R1
Column, SideShell11, TrvBhk, WebFra-mes
Model Undeformed
Run User, Min_SIGMY_ALS
Element average D-STRESS SIGMY
Min: -3.00648e+008 Max: 9.4429e+006
Limited to current set

Figure 5-42 SIGMY stresses for ALS load combinations [N/m^2], outer side shell

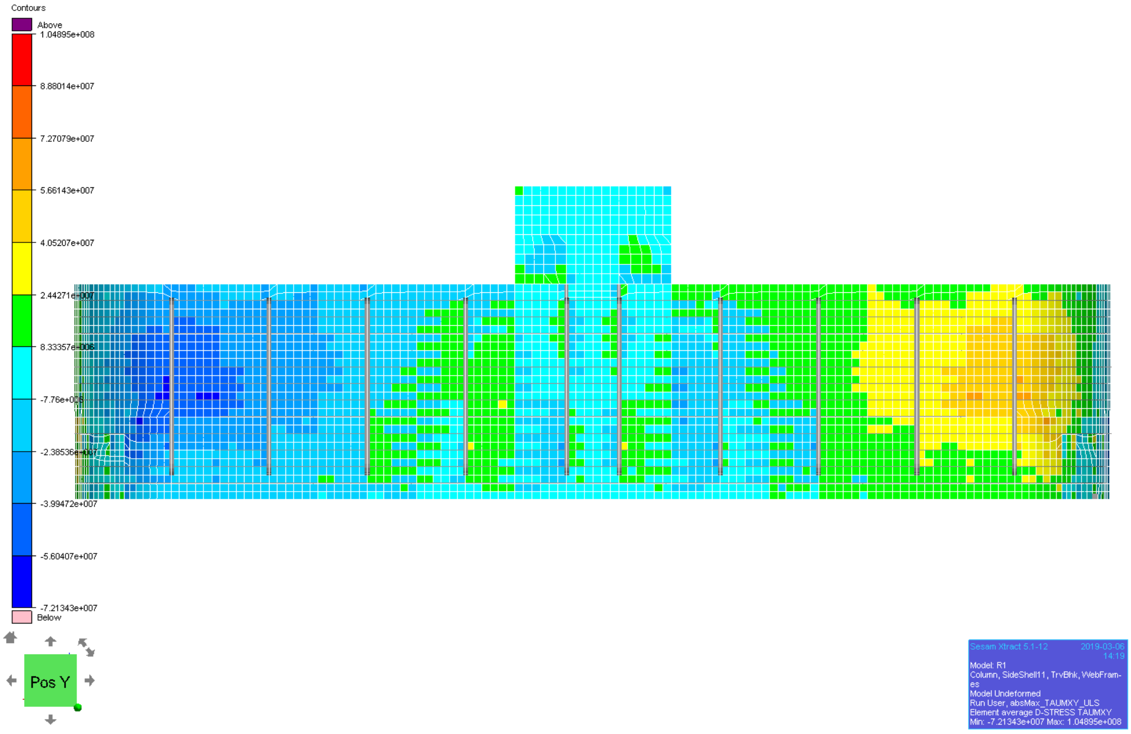

Figure 5-43 TAUMXY stresses for ULS load combinations [N/m^2], outer side shell

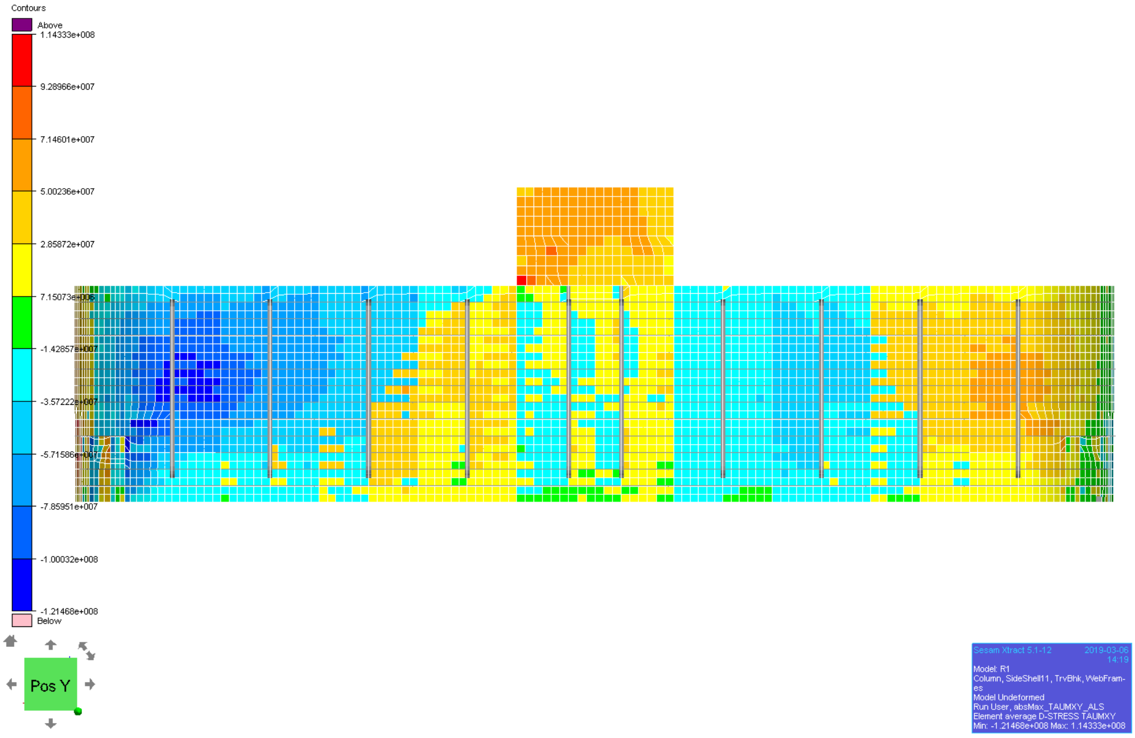

Figure 5-44 TAUMXY stresses for ALS load combinations [N/m^2], outer side shell

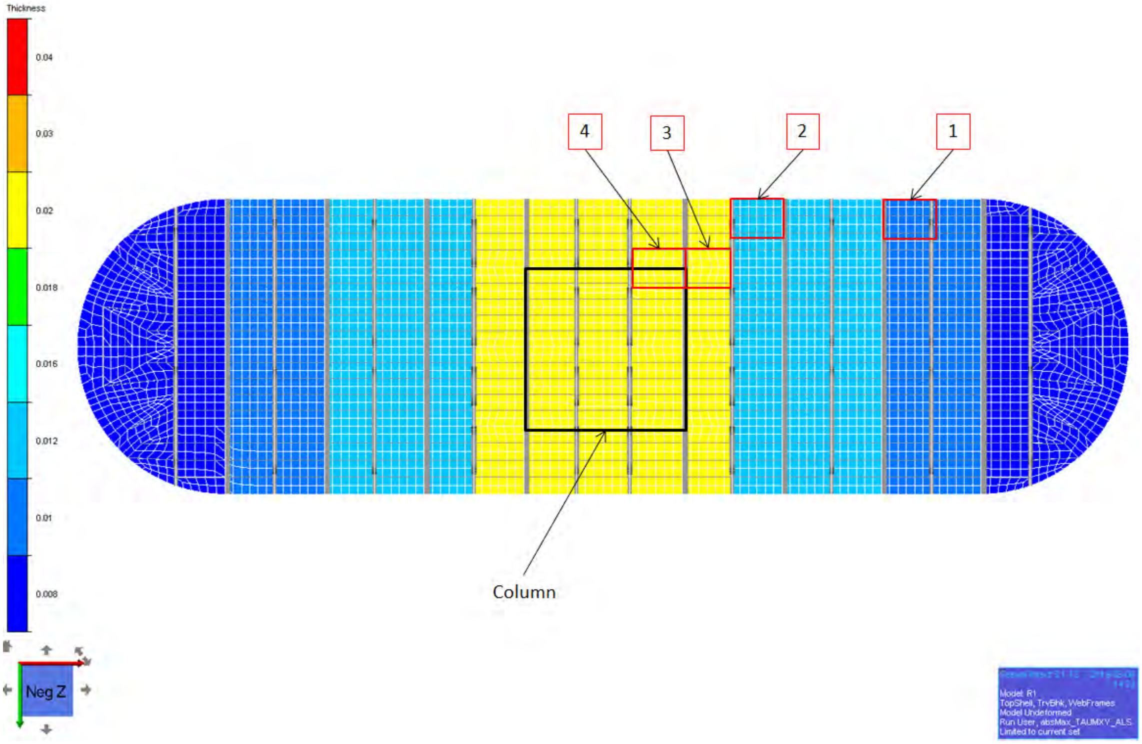

Figure 5-45 Identification of areas considered for buckling & scantling check for outer top shell

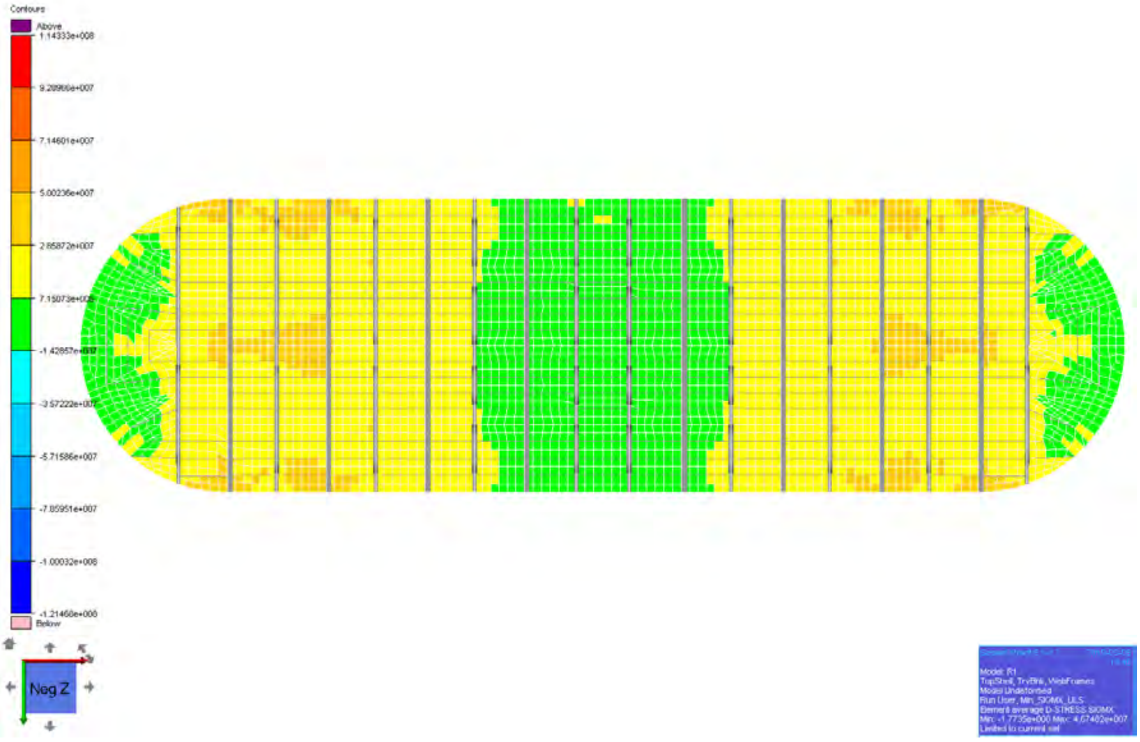

Figure 5-46 SIGMX stresses for ULS load combinations [N/m^2] for outer top shell

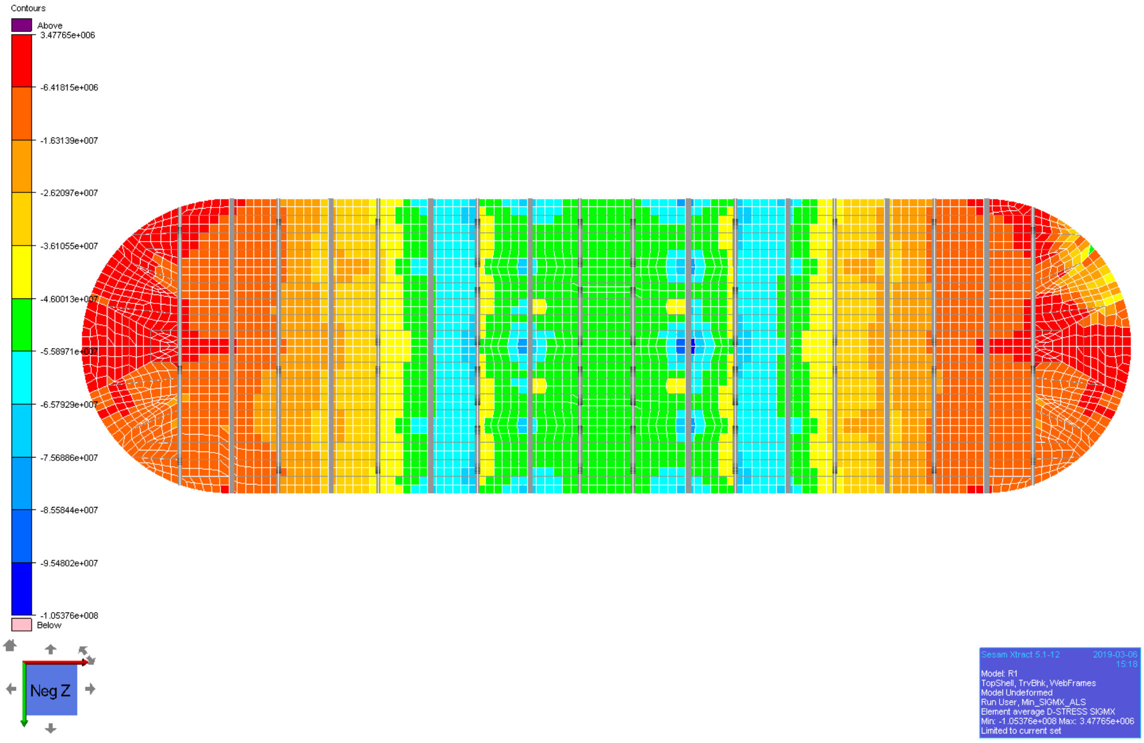

```
Sesam Xtract 5.1-12        2019-03-06
                                15:18
Model: R1
TopShell, TrvBhk, WebFrames
Model Undeformed
Run User, Min_SIGMX_ALS
Element average D-STRESS SIGMX
Min: -1.05376e+008 Max: 3.47765e+006
Limited to current set
```

Figure 5-47 SIGMX stresses for ALS load combinations [N/m^2] for outer top shell

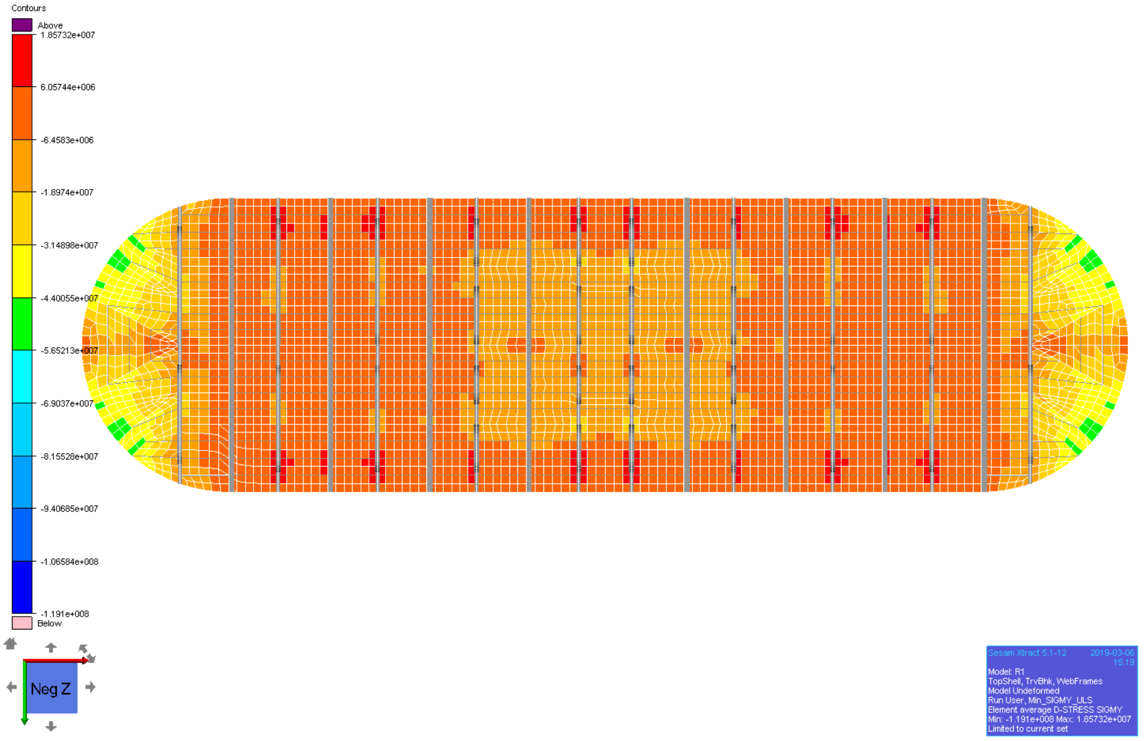

```
Sesam Xtract 5.1-12        2019-03-06
                                15:19
Model: R1
TopShell, TrvBhk, WebFrames
Model Undeformed
Run User, Min_SIGMY_ULS
Element average D-STRESS SIGMY
Min: -1.191e+008 Max: 1.85732e+007
Limited to current set
```

Figure 5-48 SIGMY stresses for ULS load combinations [N/m^2] for outer top shell

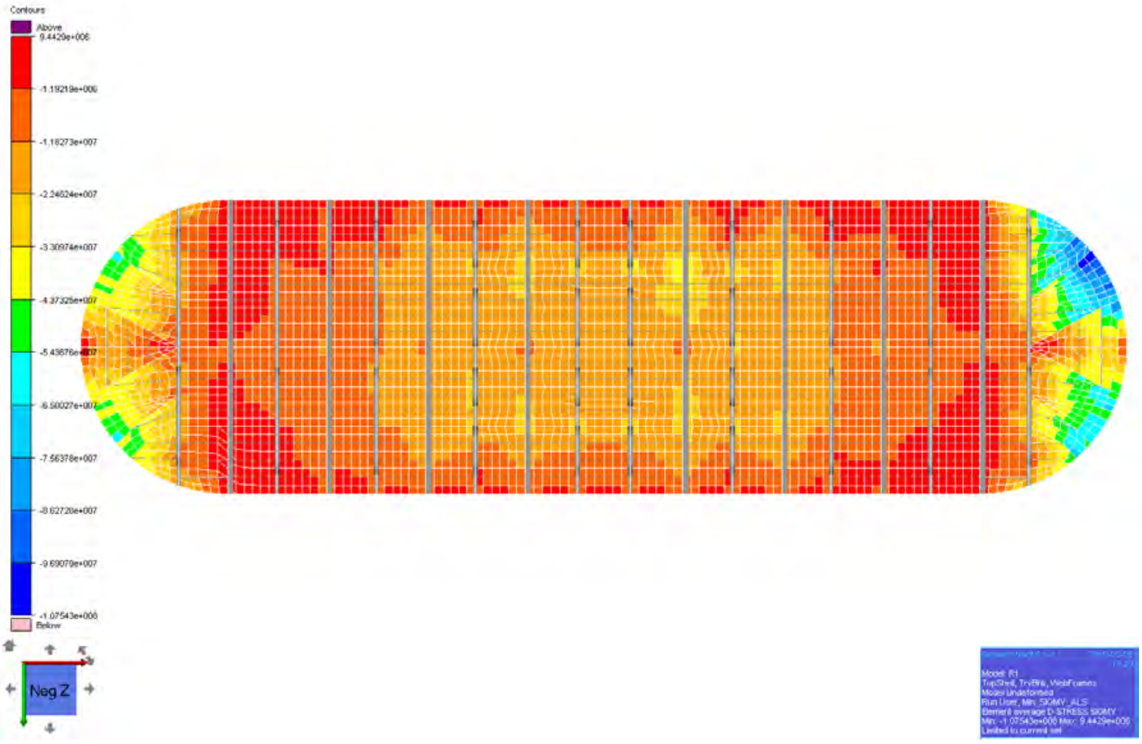

Figure 5-49 SIGMY stresses for ALS load combinations [N/m^2] for outer top shell

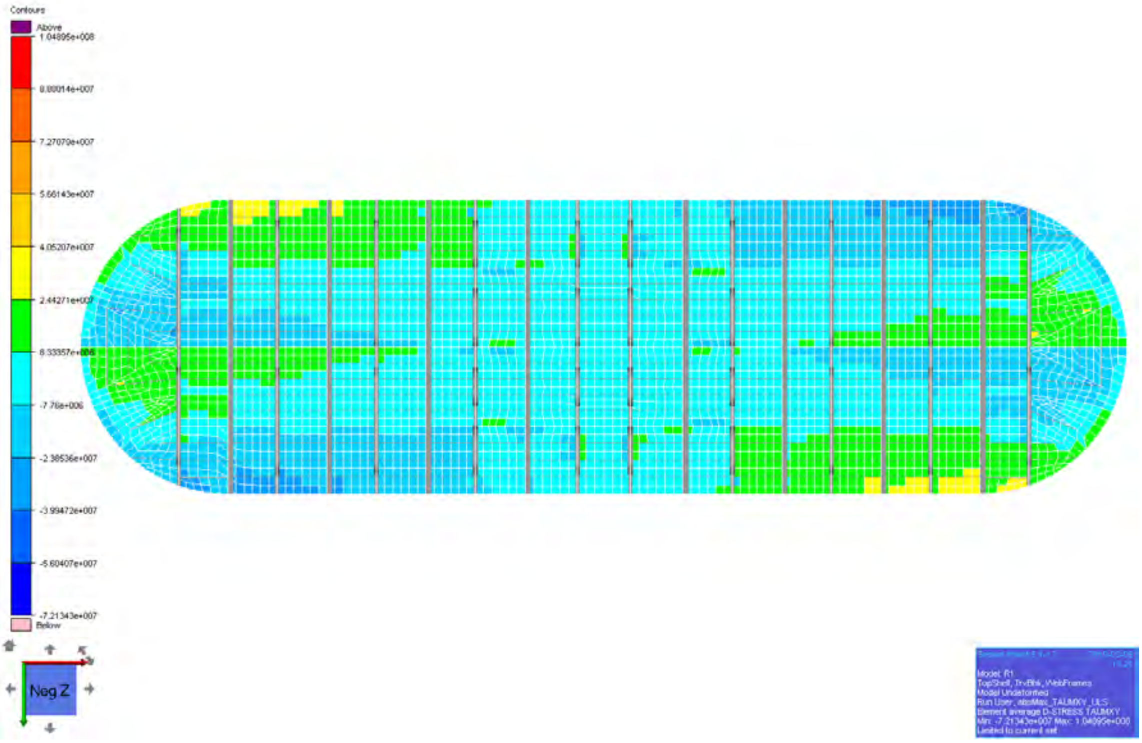

Figure 5-50 TAUMXY stresses for ULS load combinations [N/m^2] for outer top shell

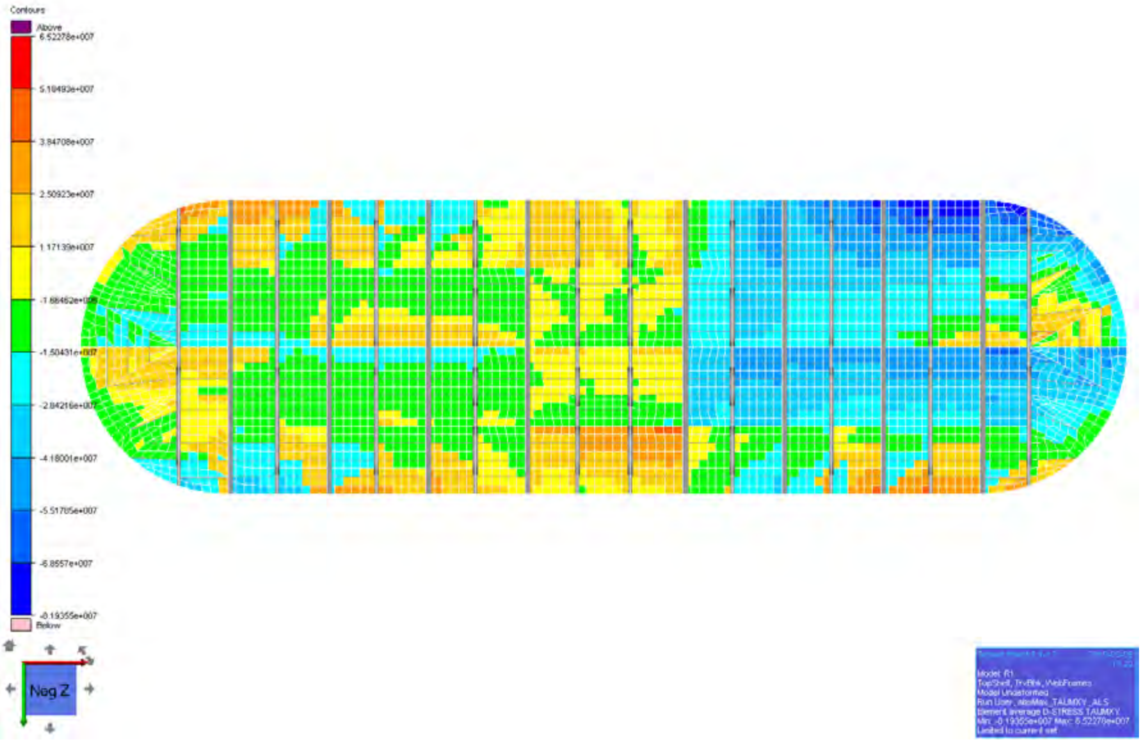

Figure 5-51 TAUMXY stresses for ALS load combinations [N/m^2] for outer top shell

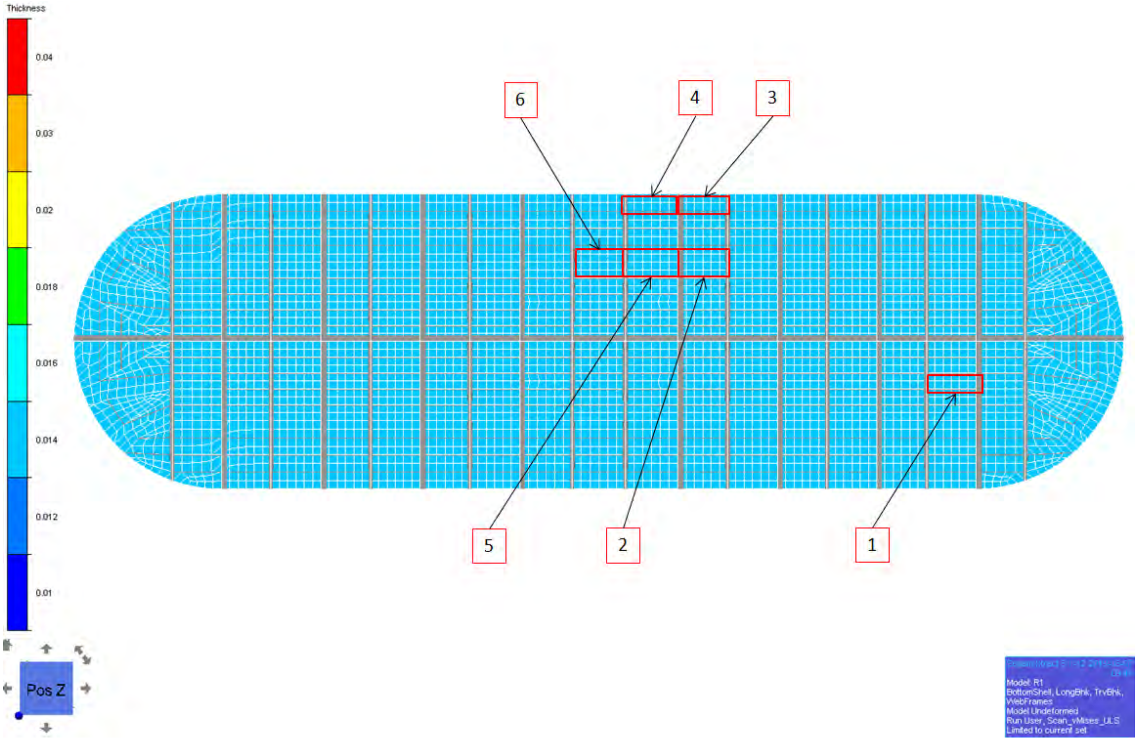

Figure 5-52 Identification of areas considered for buckling & scantling check for outer bottom shell

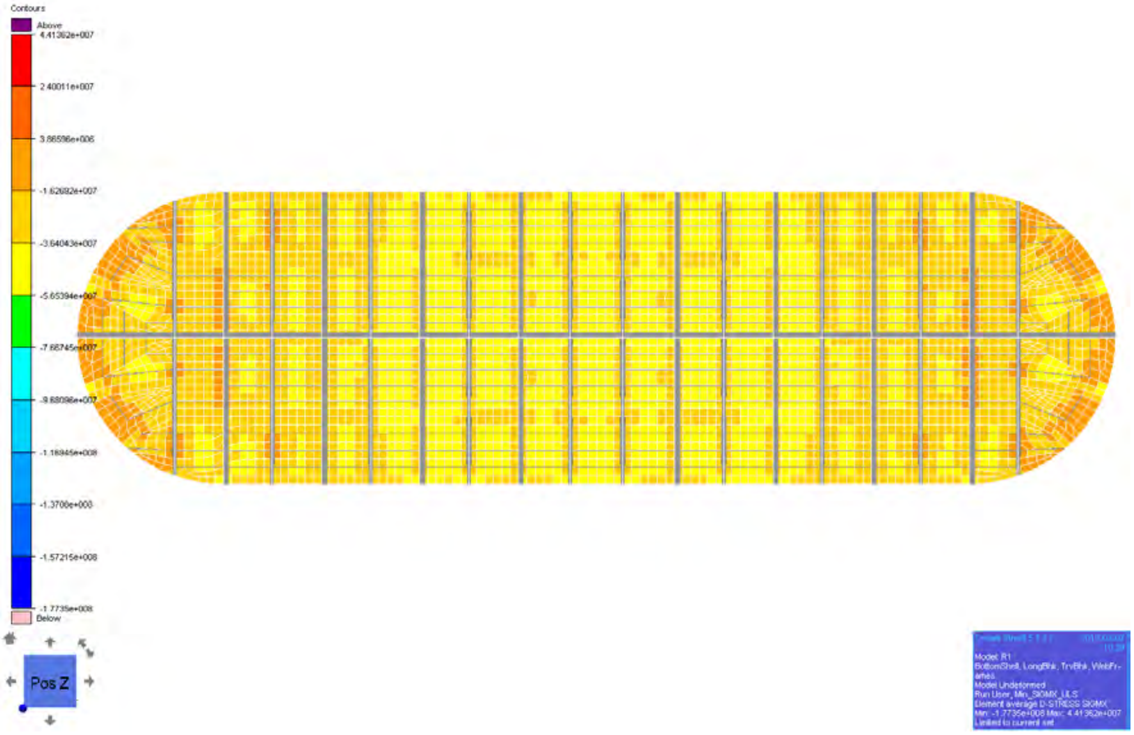

Figure 5-53 SIGMX stresses for ULS load combinations [N/m^2] for outer bottom shell

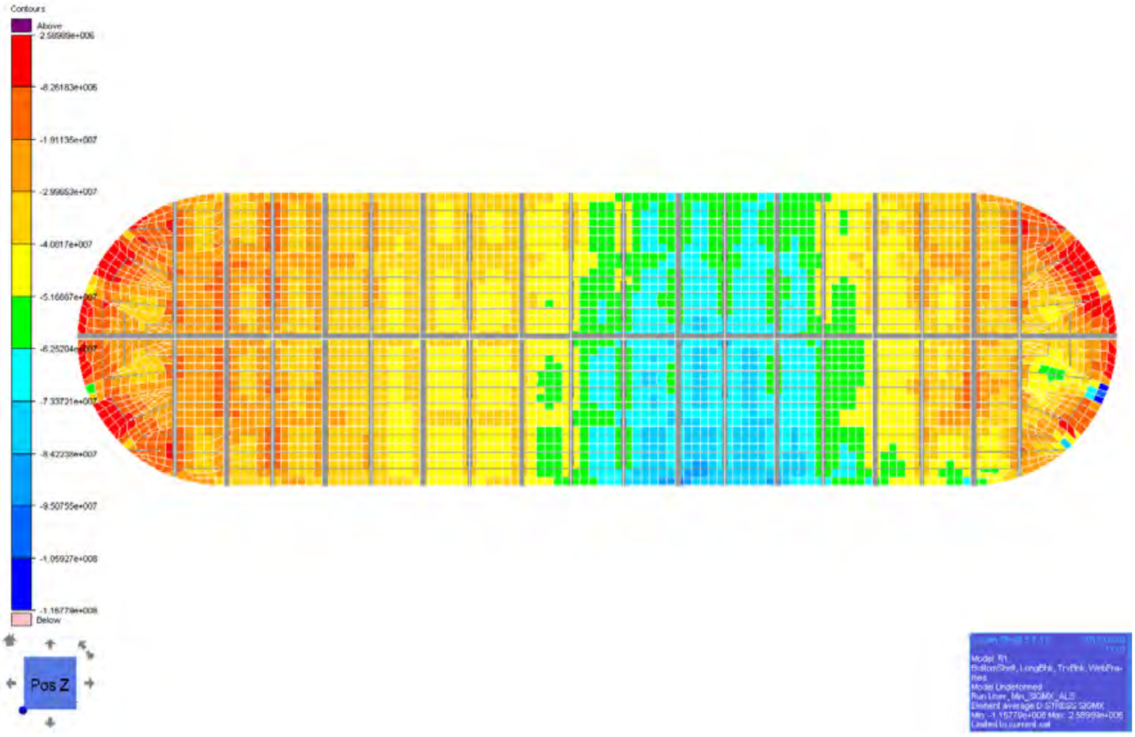

Figure 5-54 SIGMX stresses for ALS load combinations [N/m^2] for outer bottom shell

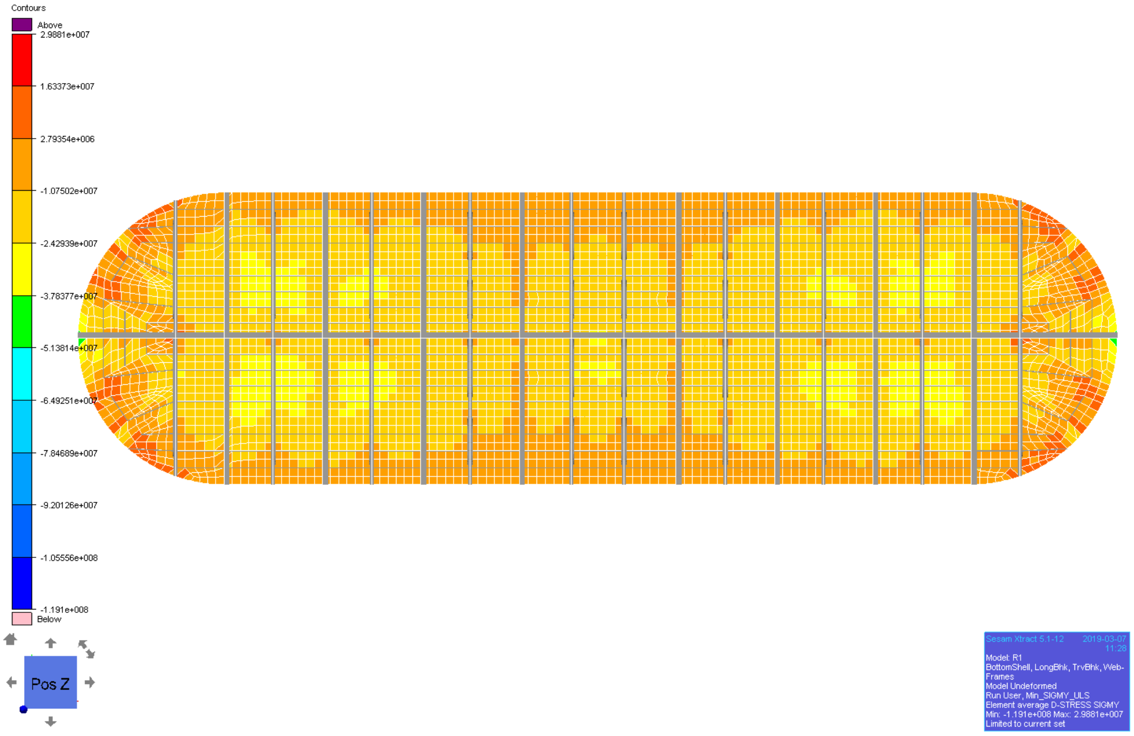

Figure 5-55 SIGMY stresses for ULS load combinations [N/m^2] for outer bottom shell

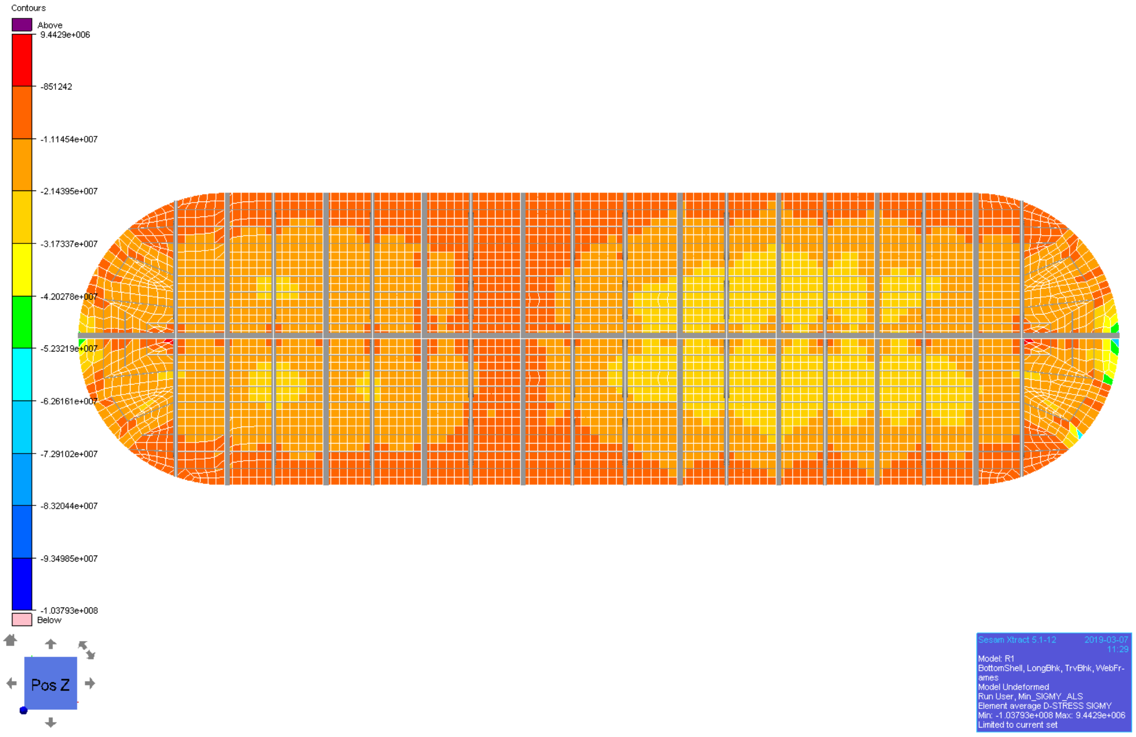

Figure 5-56 SIGMY stresses for ALS load combinations [N/m^2] for outer bottom shell

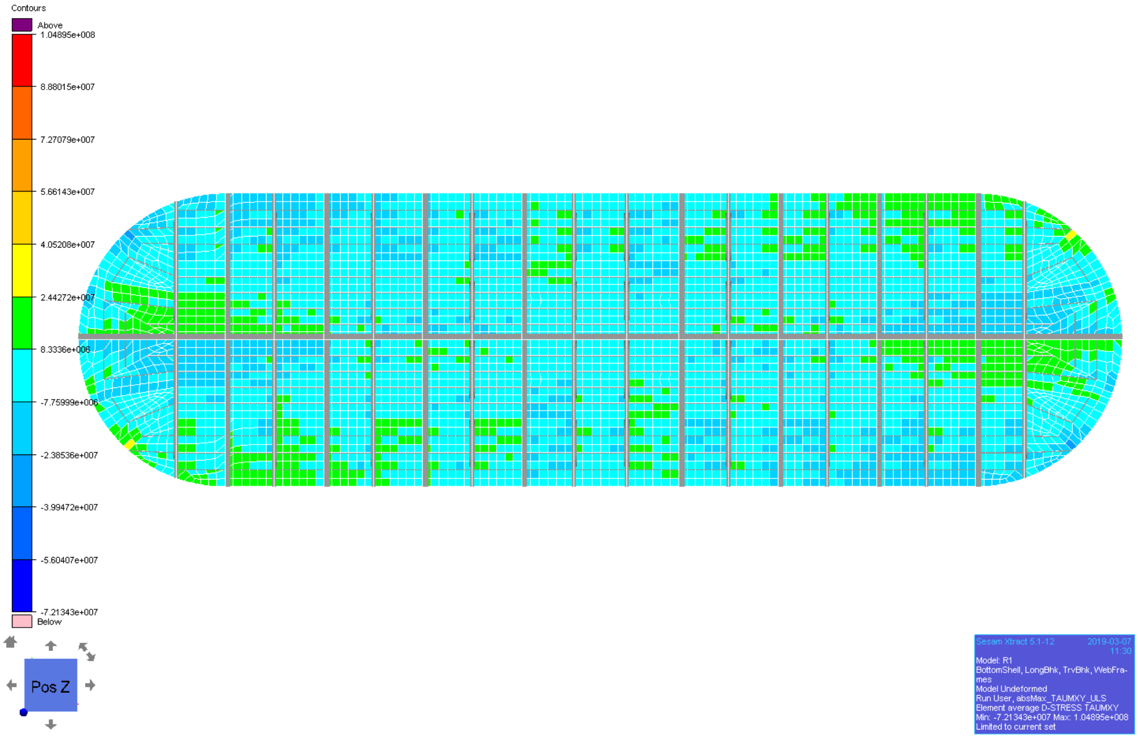

Figure 5-57 TAUMXY stresses for ULS load combinations [N/m^2] for outer bottom shell

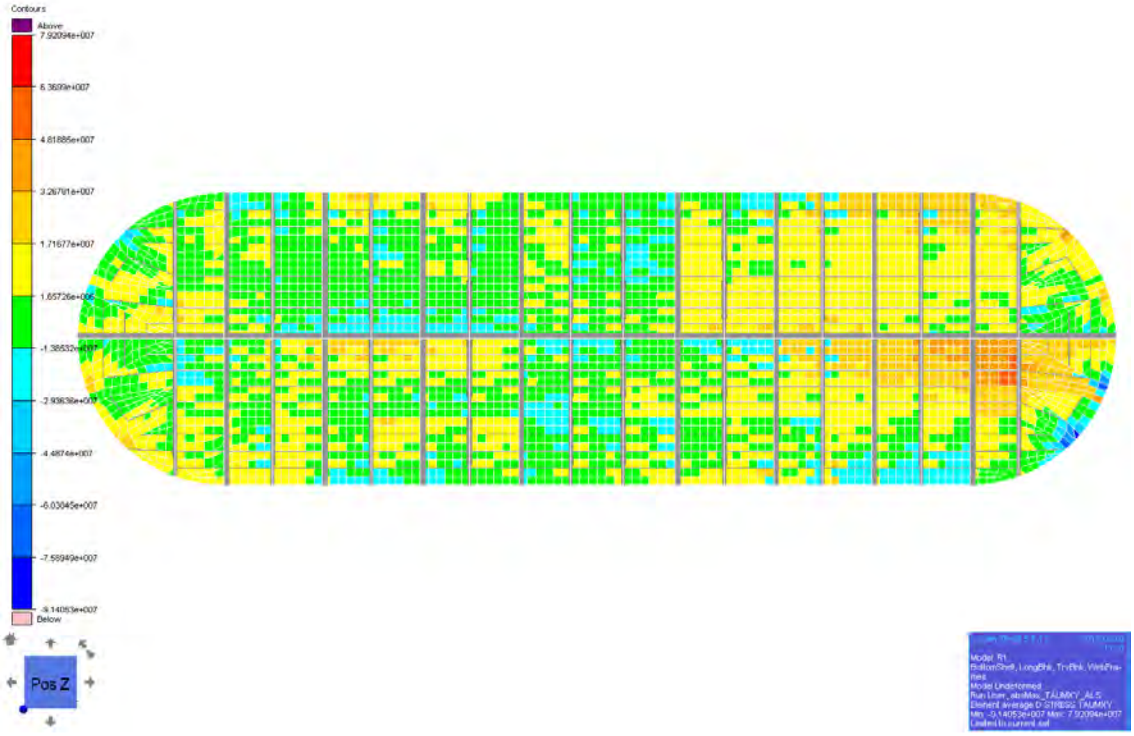

Figure 5-58 TAUMXY stresses for ALS load combinations [N/m^2] for outer bottom shell

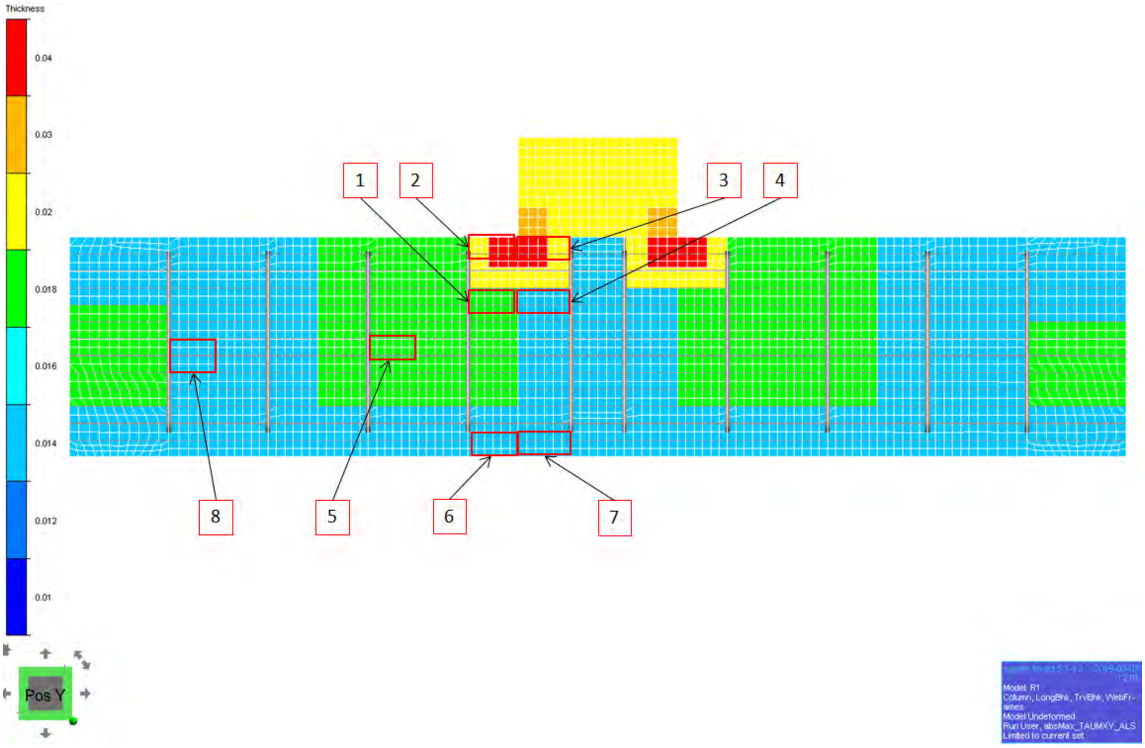

Figure 5-59 Identification of areas considered for buckling & scantling check for centreline bulkhead

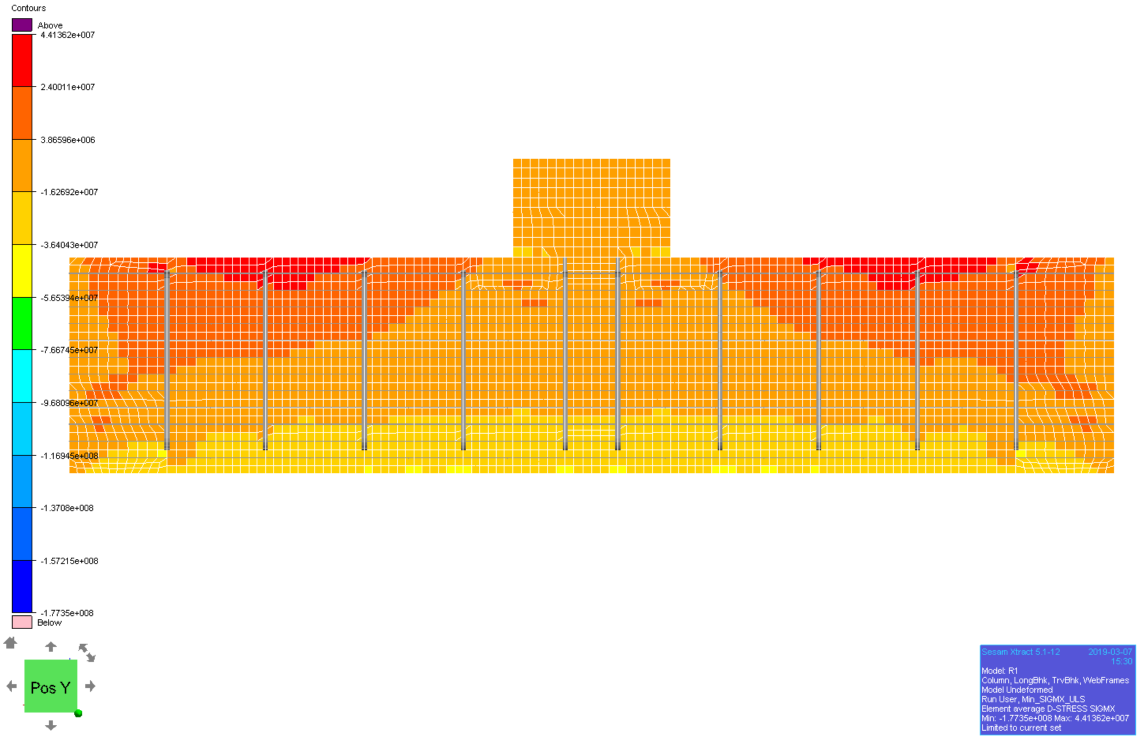

Figure 5-60 SIGMX stresses for ULS load combinations [N/m^2] for centreline bulkhead

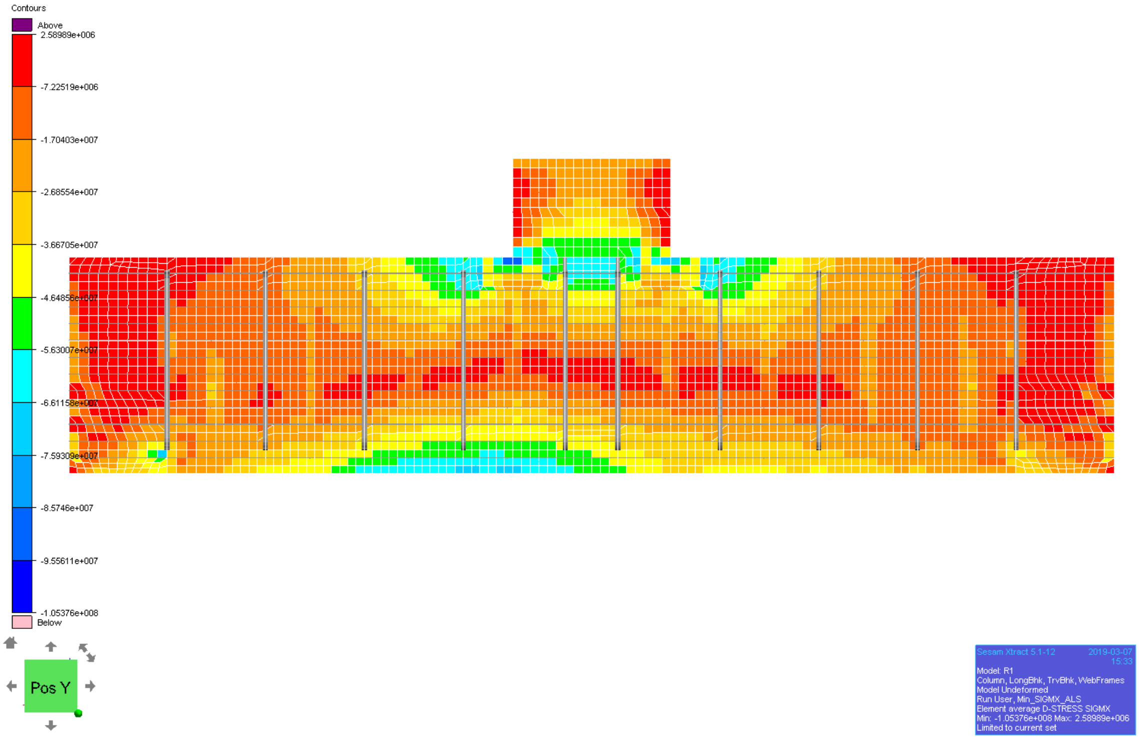

Figure 5-61 SIGMX stresses for ALS load combinations [N/m²] for centreline bulkhead

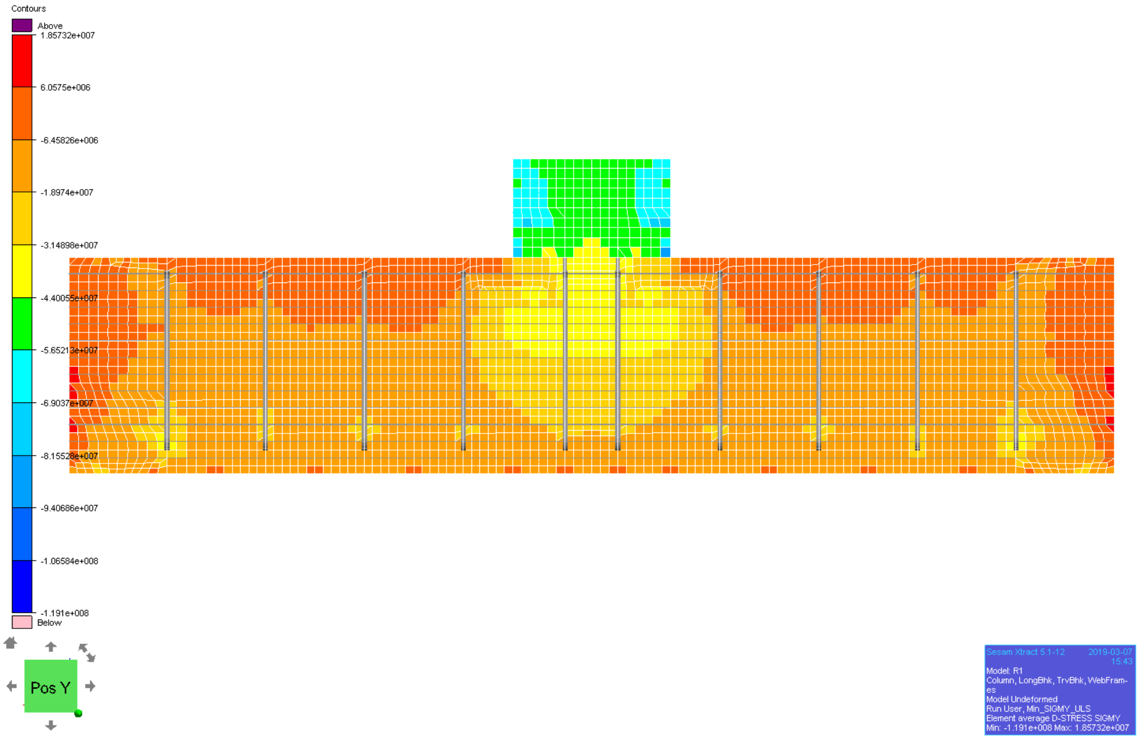

Figure 5-62 SIGMY stresses for ULS load combinations [N/m²] for centreline bulkhead

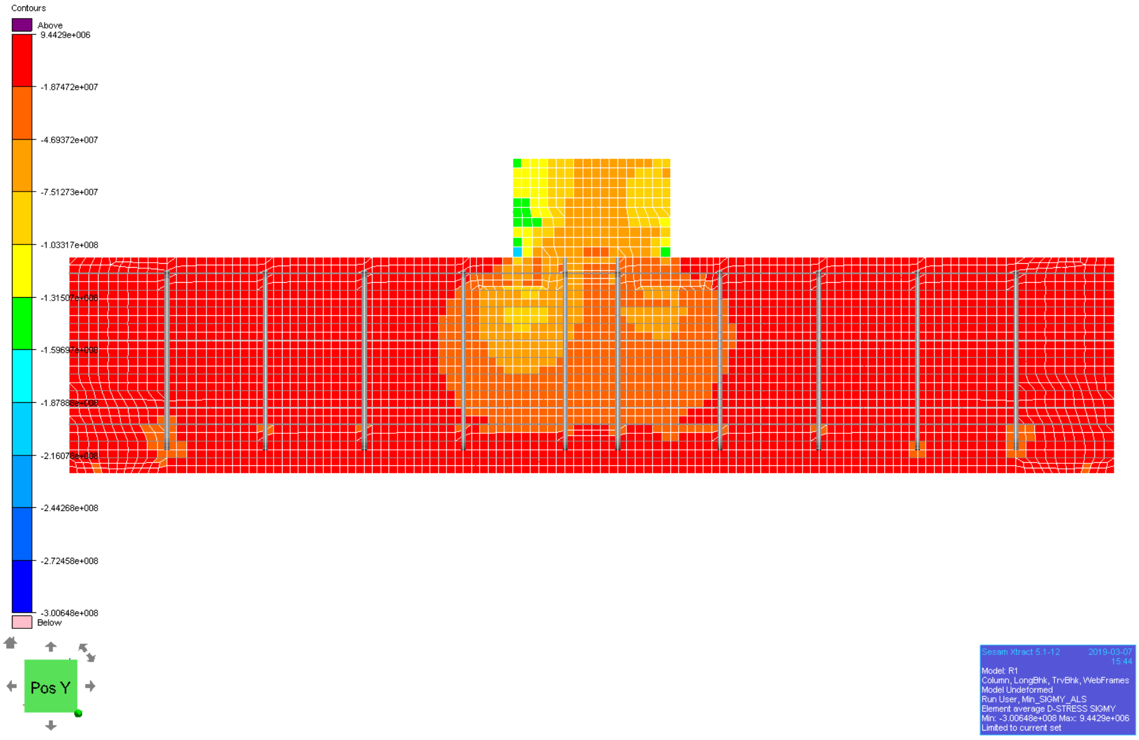

Sesam Xtract 5.1-12 2019-03-07 15:44
Model: R1
Column, LongBhk, TrvBhk, WebFrames
Model Undeformed
Run User, Min_SIGMY_ALS
Element average D-STRESS SIGMY
Min: -3.00648e+008 Max: 9.4429e+006
Limited to current set

Figure 5-63 SIGMY stresses for ALS load combinations [N/m^2] for centreline bulkhead

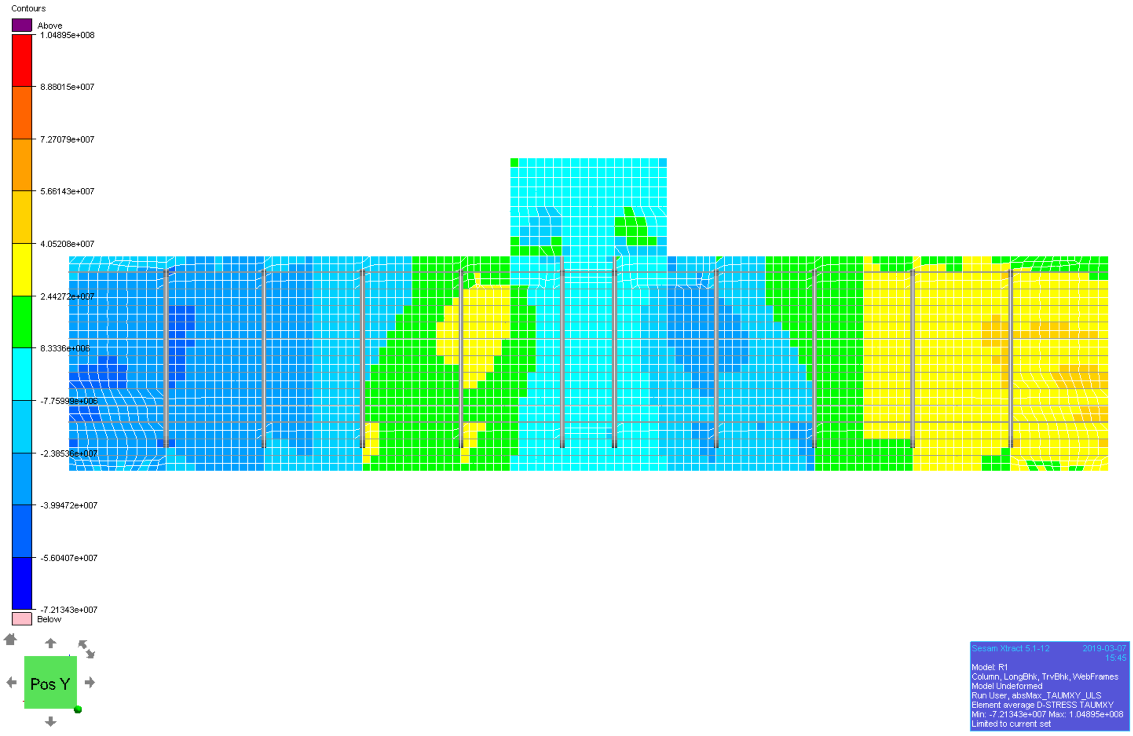

Sesam Xtract 5.1-12 2019-03-07 15:45
Model: R1
Column, LongBhk, TrvBhk, WebFrames
Model Undeformed
Run User, absMax_TAUMXY_ULS
Element average D-STRESS TAUMXY
Min: -7.21343e+007 Max: 1.04895e+008
Limited to current set

Figure 5-64 TAUMXY stresses for ULS load combinations [N/m^2] for centreline bulkhead

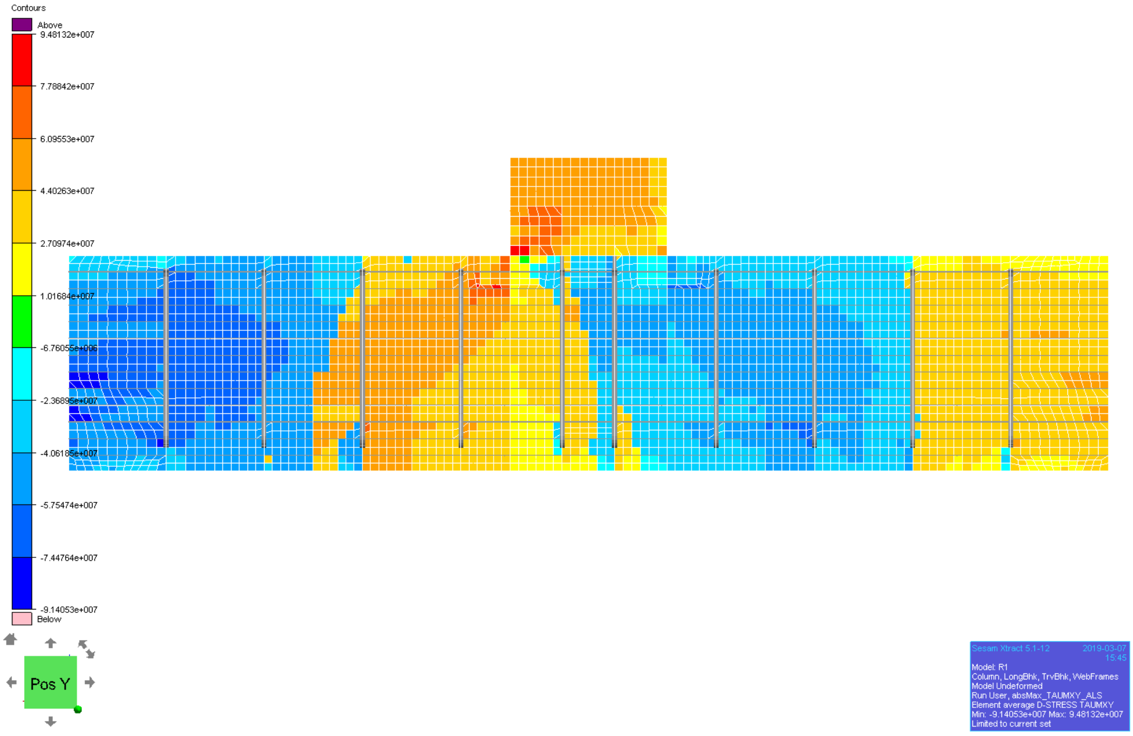

Figure 5-65 TAUMXY stresses for ALS load combinations [N/m²] for centreline bulkhead

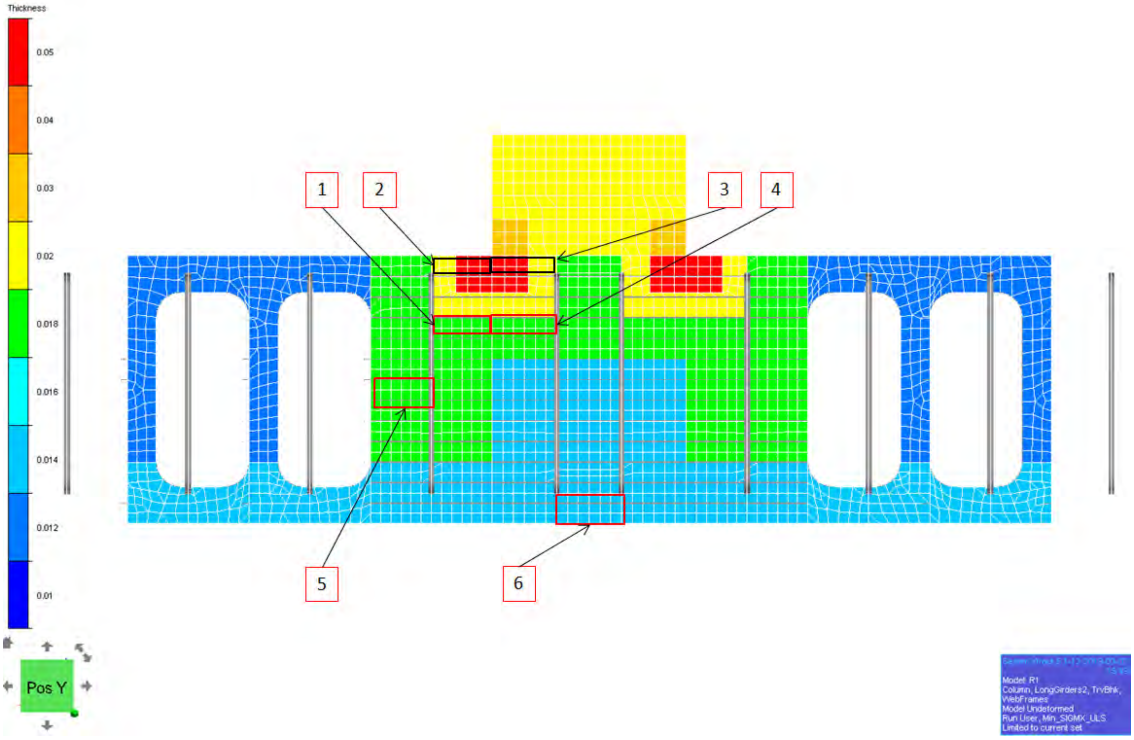

Figure 5-66 Identification of areas considered for buckling & scantling check for bulkhead 4.0 m of centreline

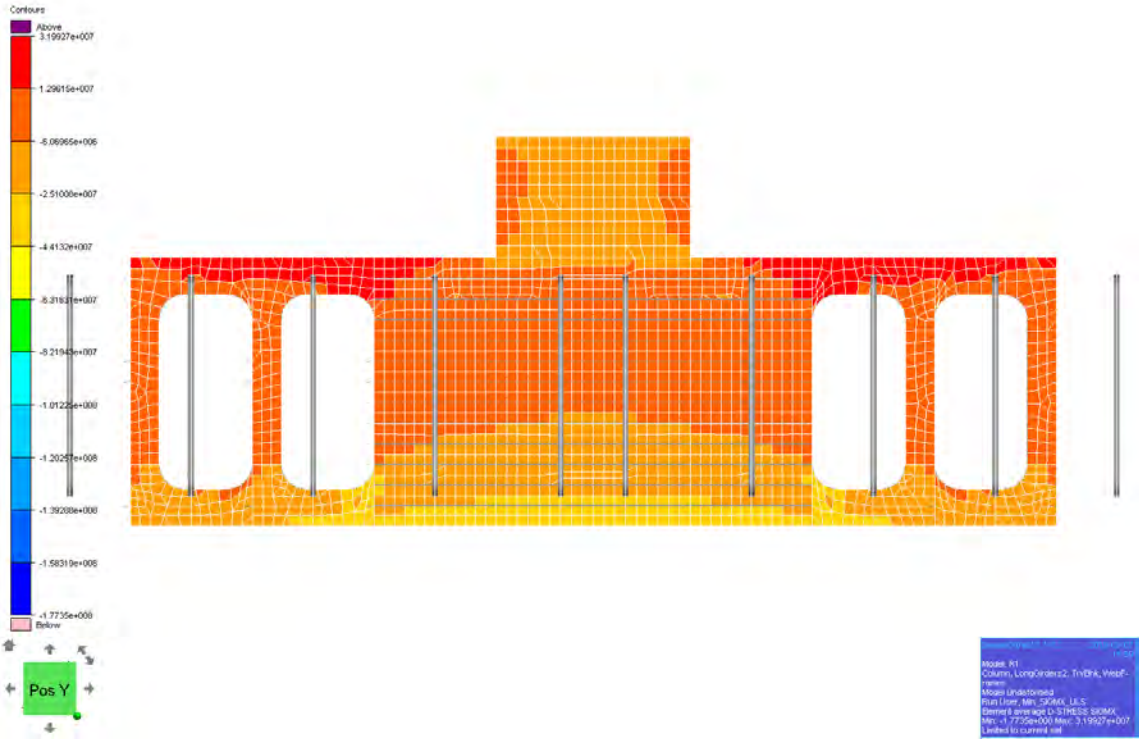

Figure 5-67 SIGMX stresses for ULS load combinations [N/m^2] for bulkhead 4.0 m of centreline

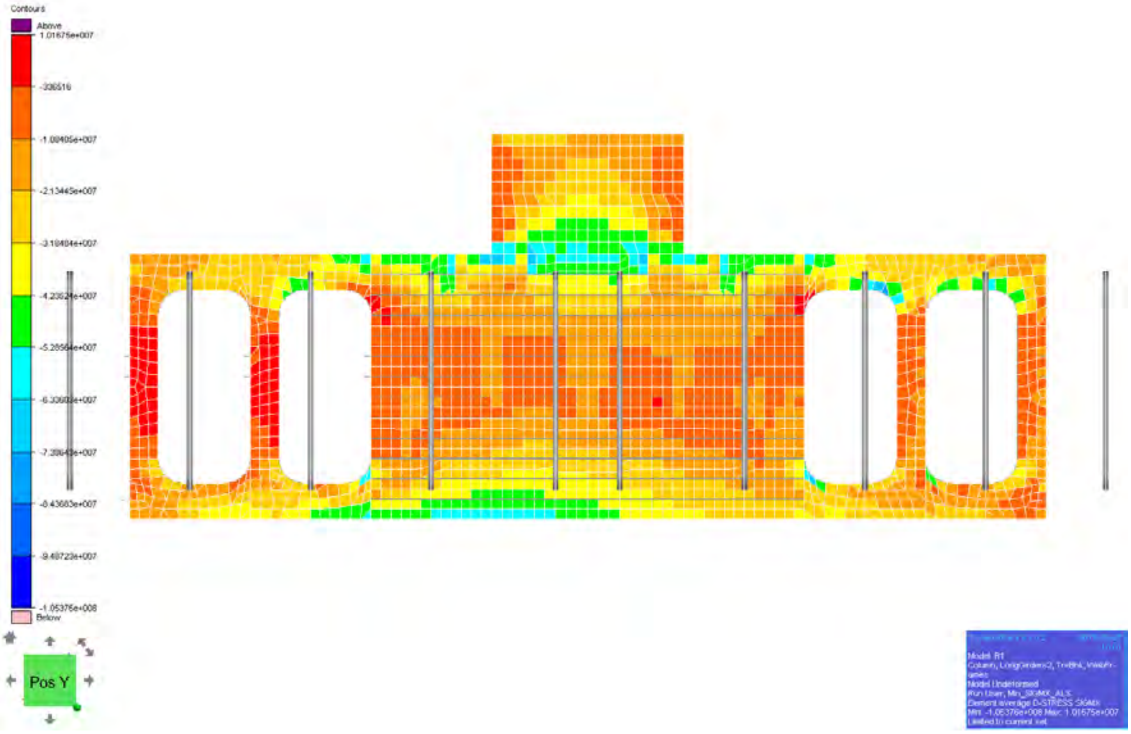

Figure 5-68 SIGMX stresses for ALS load combinations [N/m^2] for bulkhead 4.0 m of centreline

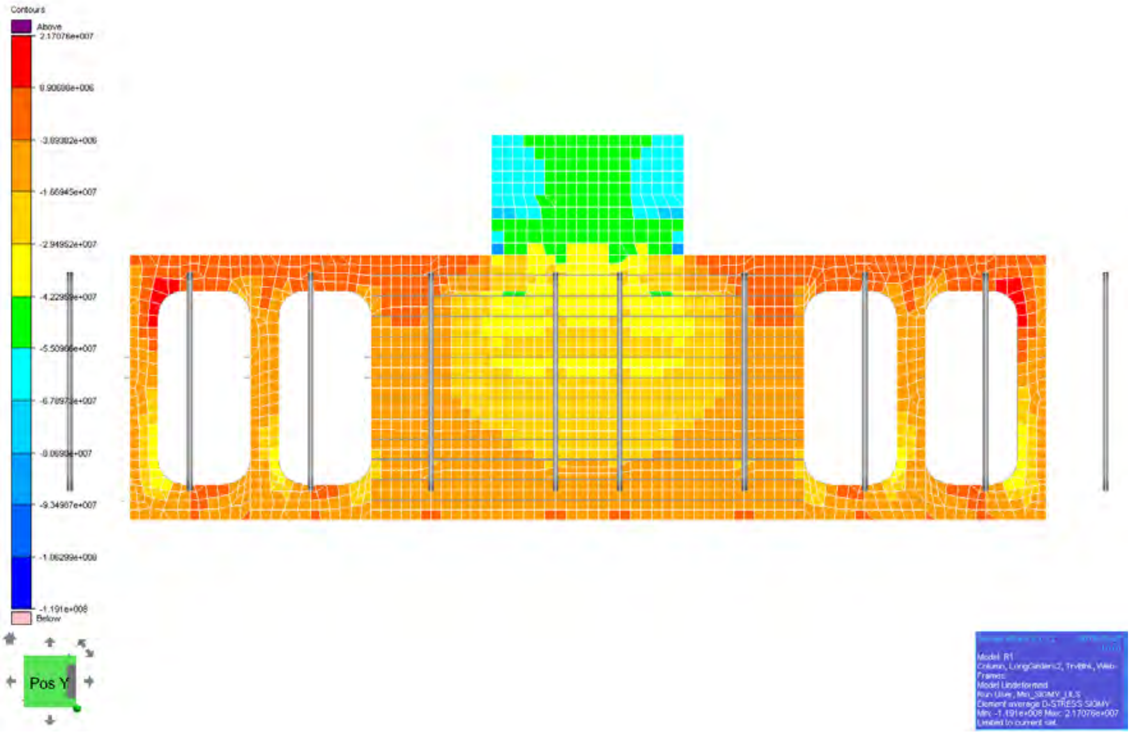

Figure 5-69 SIGMY stresses for ULS load combinations [N/m^2] for bulkhead 4.0 m of centreline

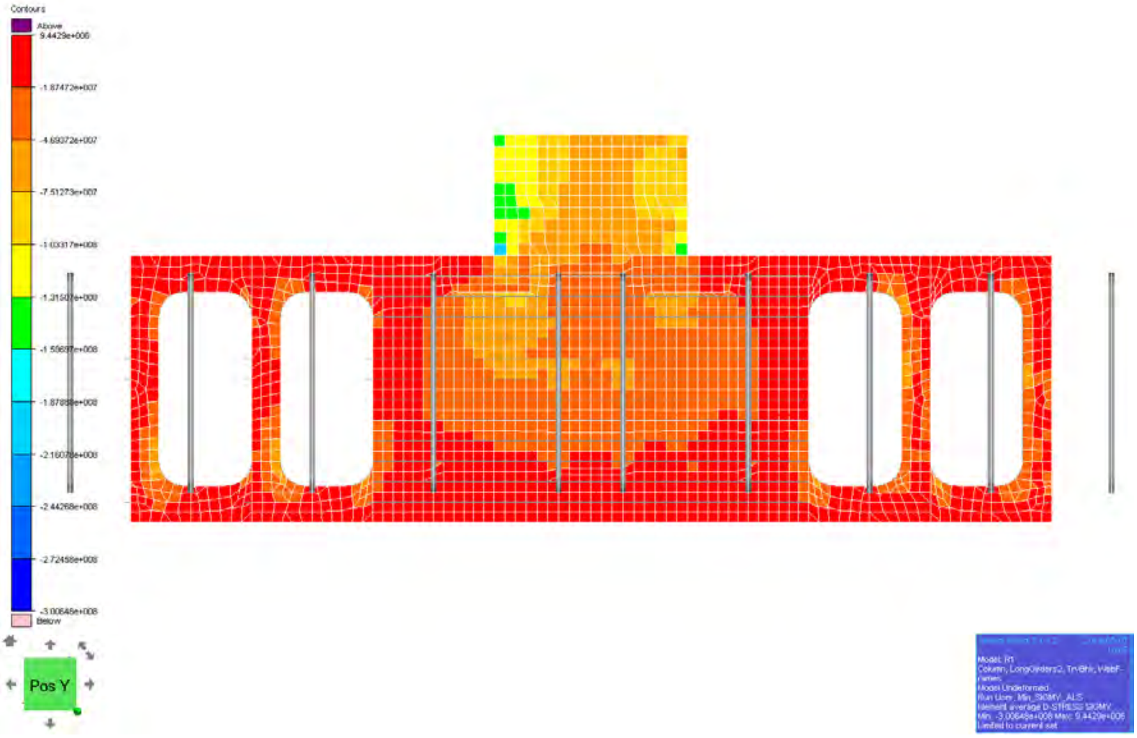

Figure 5-70 SIGMY stresses for ALS load combinations [N/m^2] for bulkhead 4.0 m of centreline

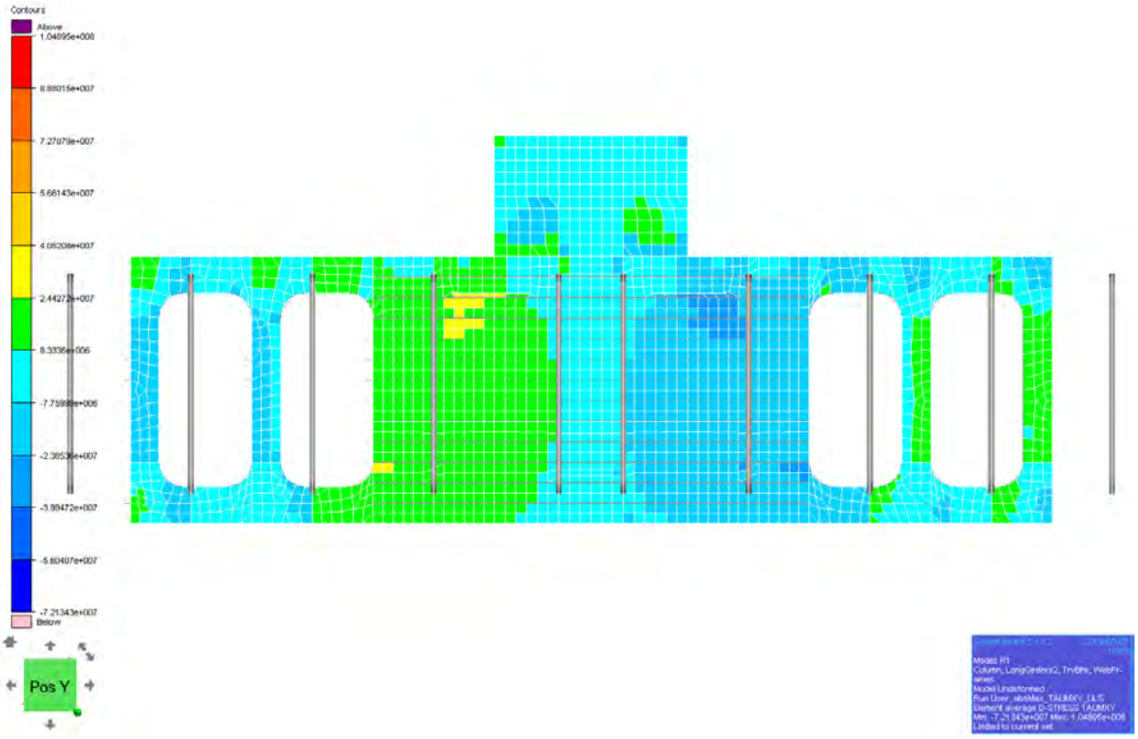

Figure 5-71 TAUMXY stresses for ULS load combinations [N/m^2] for bulkhead 4.0 m of centreline

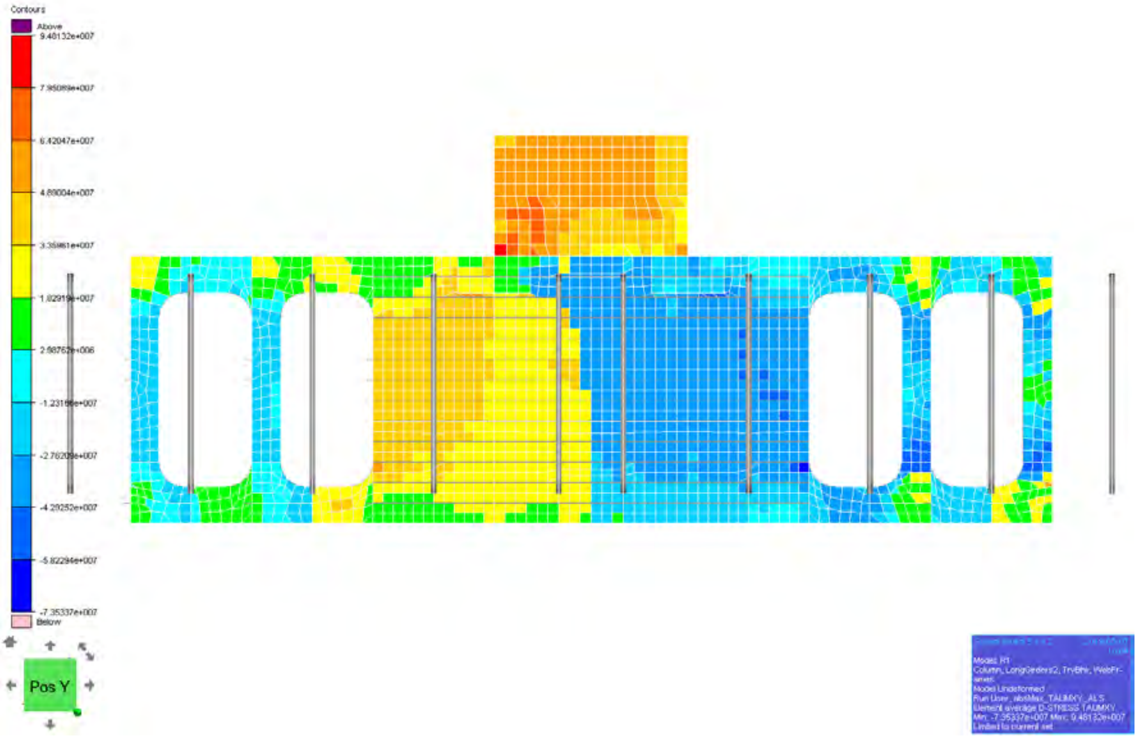

Figure 5-72 TAUMXY stresses for ALS load combinations [N/m^2] for bulkhead 4.0 m of centreline

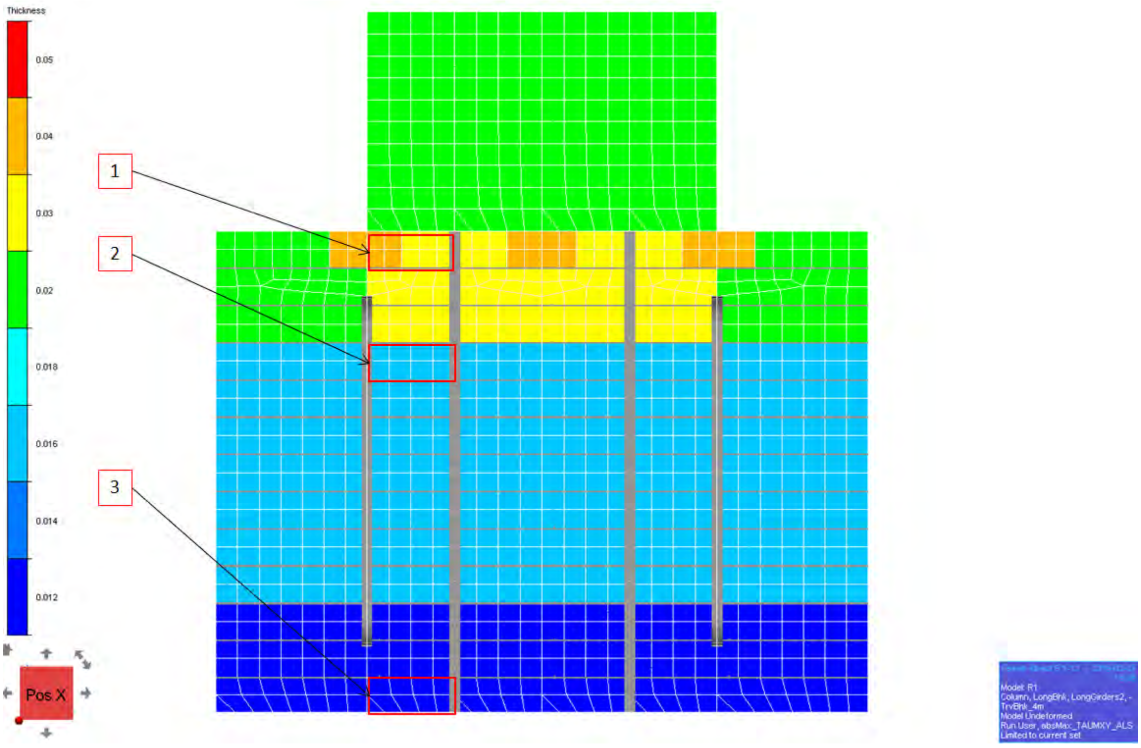

Figure 5-73 Identification of areas considered for buckling & scantling check for transverse bulkhead supporting column

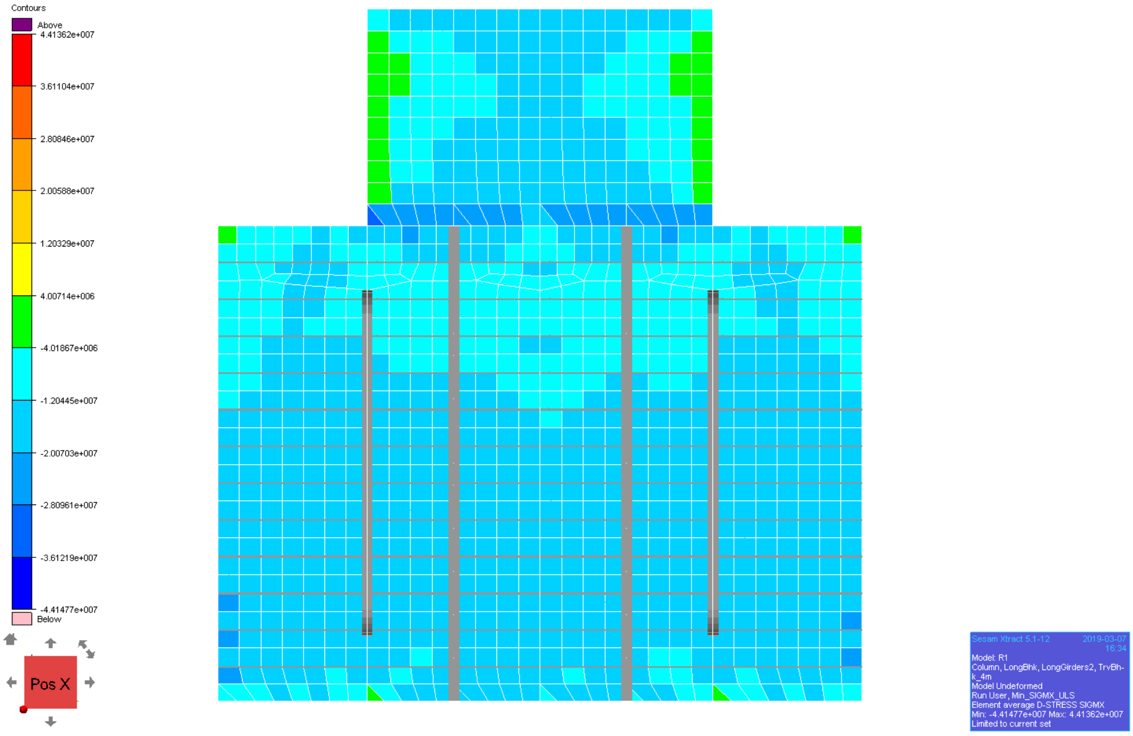

Figure 5-74 SIGMX stresses for ULS load combinations [N/m^2] for transverse bulkhead supporting column

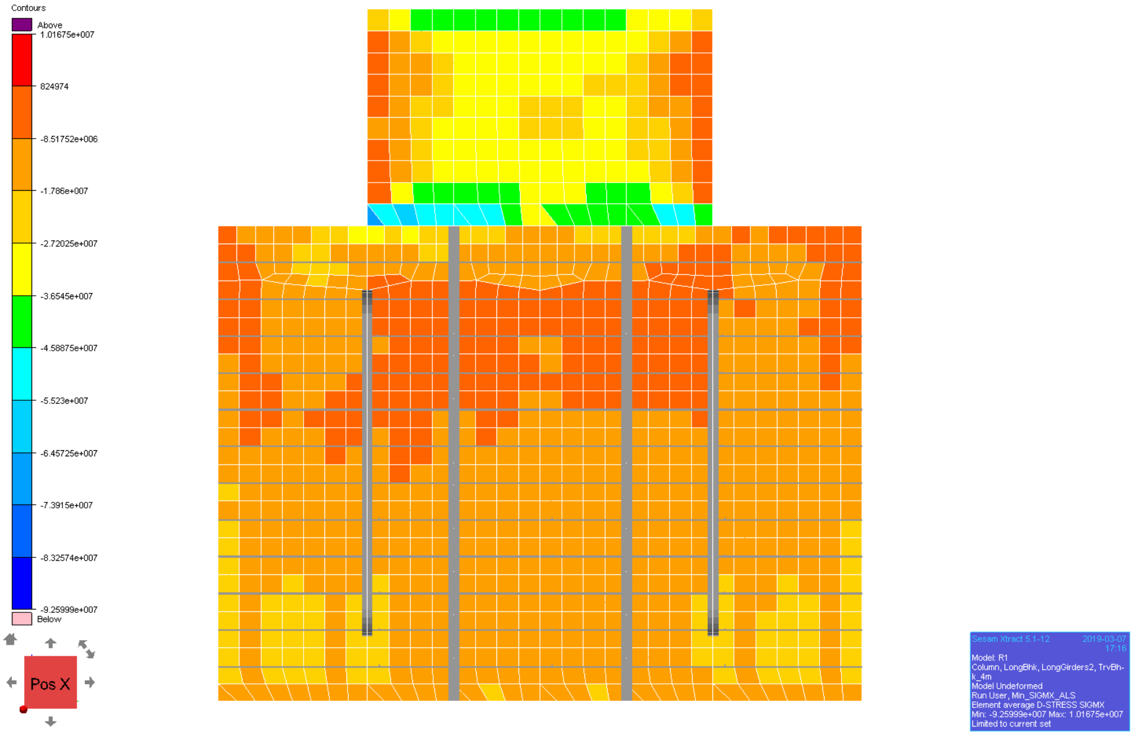

Figure 5-75 SIGMX stresses for ALS load combinations [N/m^2] for transverse bulkhead supporting column

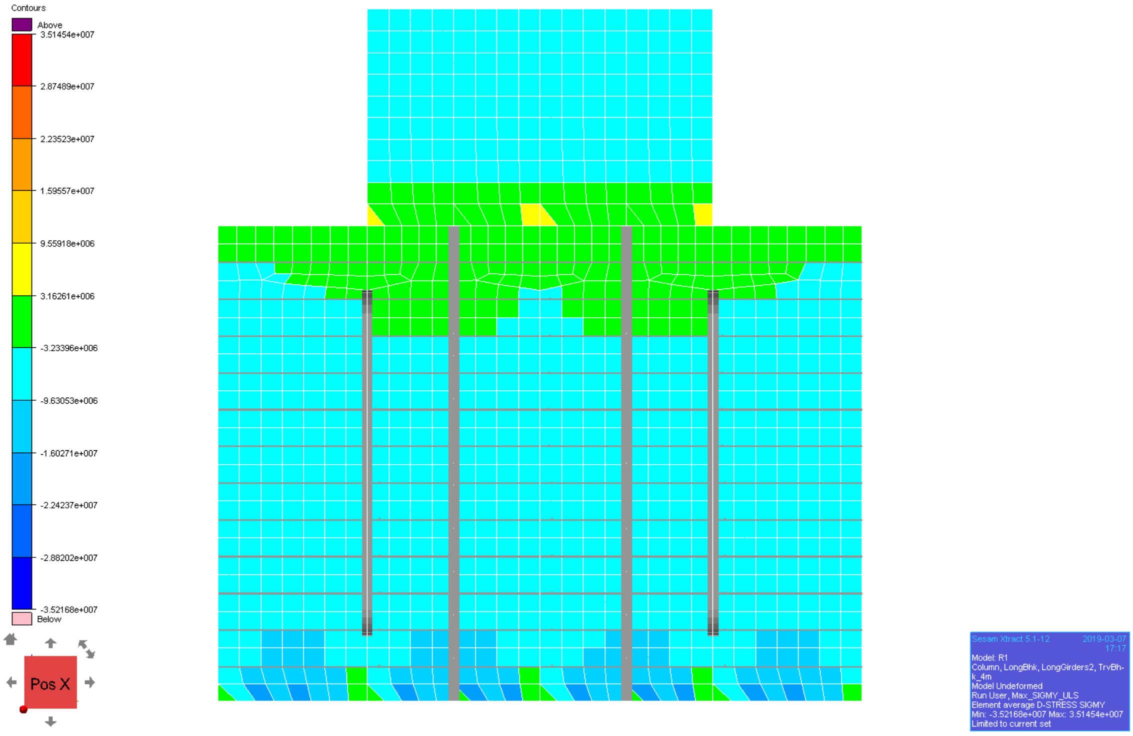

Figure 5-76 SIGMY stresses for ULS load combinations [N/m^2] for transverse bulkhead supporting column

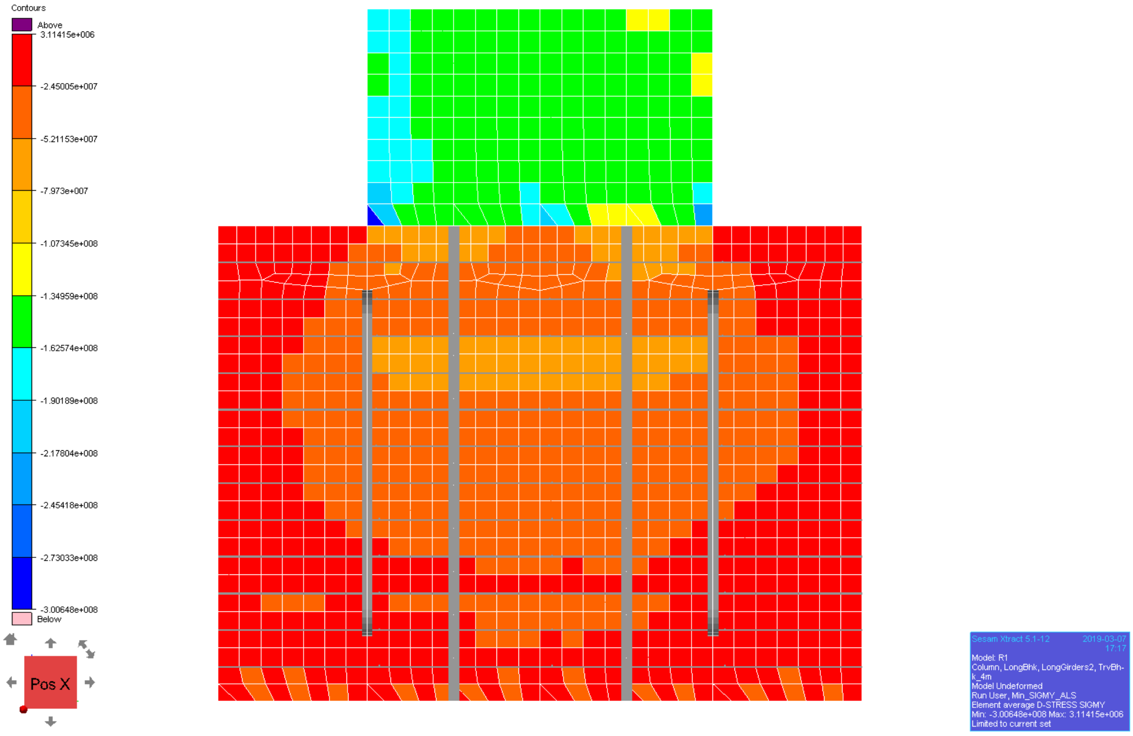

Figure 5-77 SIGMY stresses for ALS load combinations [N/m^2] for transverse bulkhead supporting column

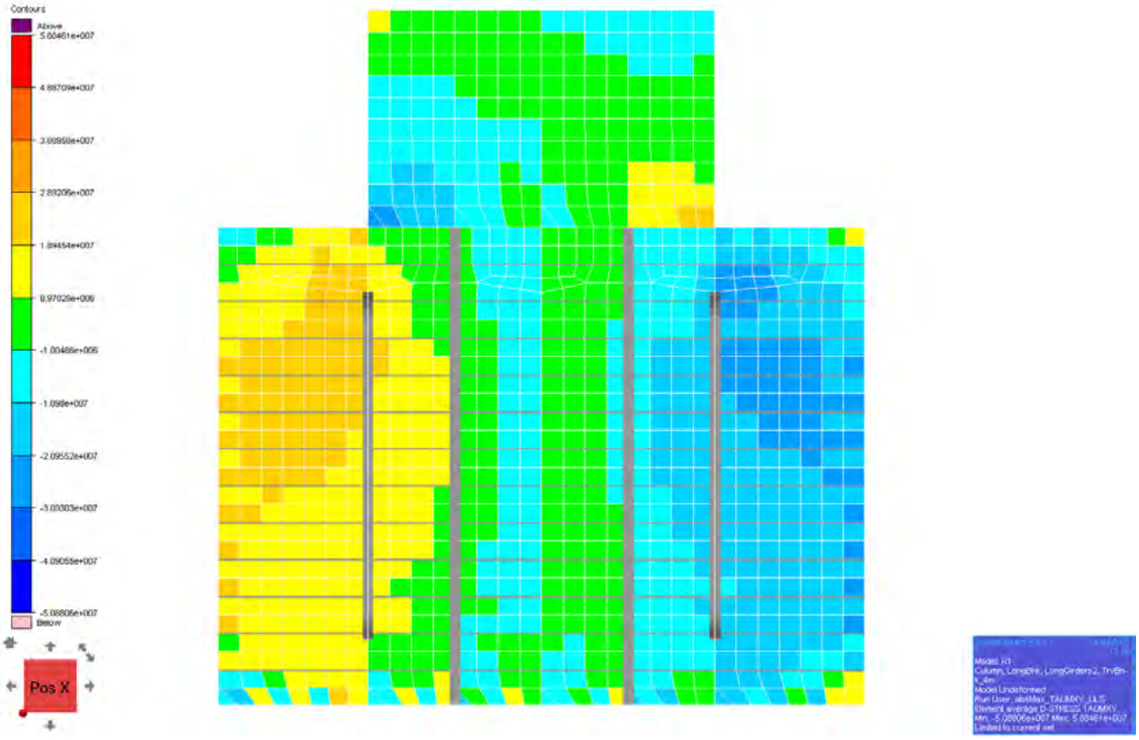

Figure 5-78 TAUMXY stresses for ULS load combinations [N/m^2] for transverse bulkhead supporting column

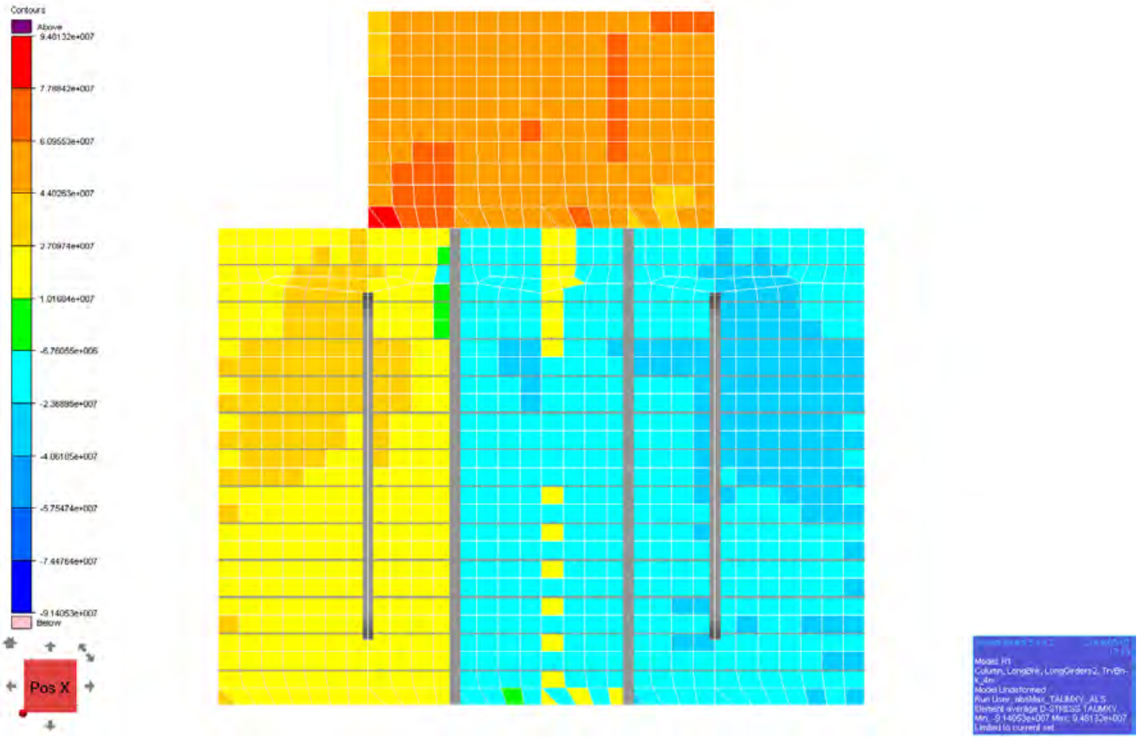

Figure 5-79 TAUMXY stresses for ALS load combinations [N/m²] for transverse bulkhead supporting column

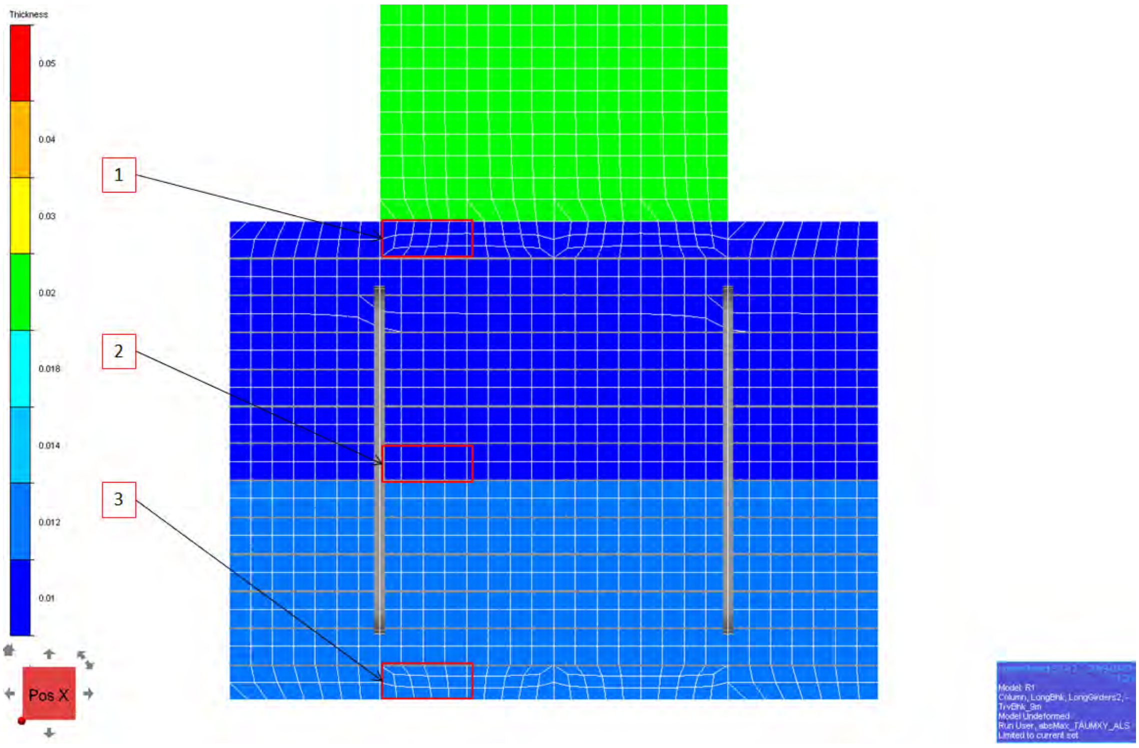

Figure 5-80 Identification of areas considered for buckling & scantling check for a typical transverse bulkhead

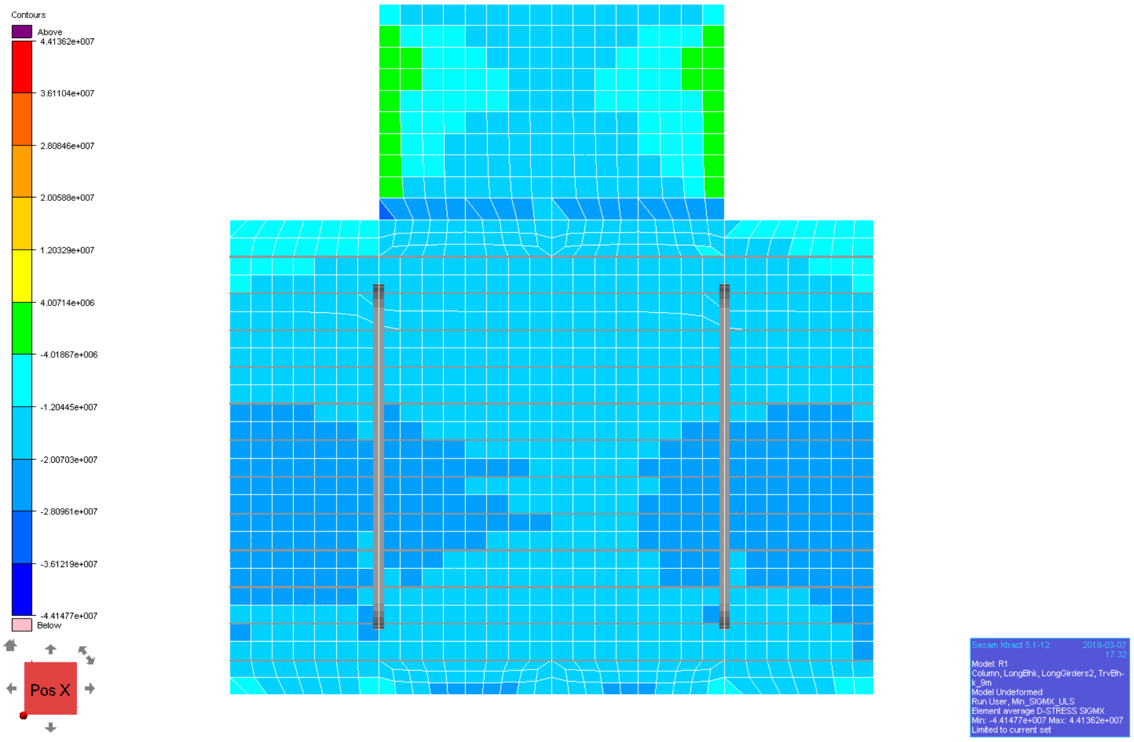

Figure 5-81 SIGMX stresses for ULS load combinations [N/m^2] for a typical transverse bulkhead

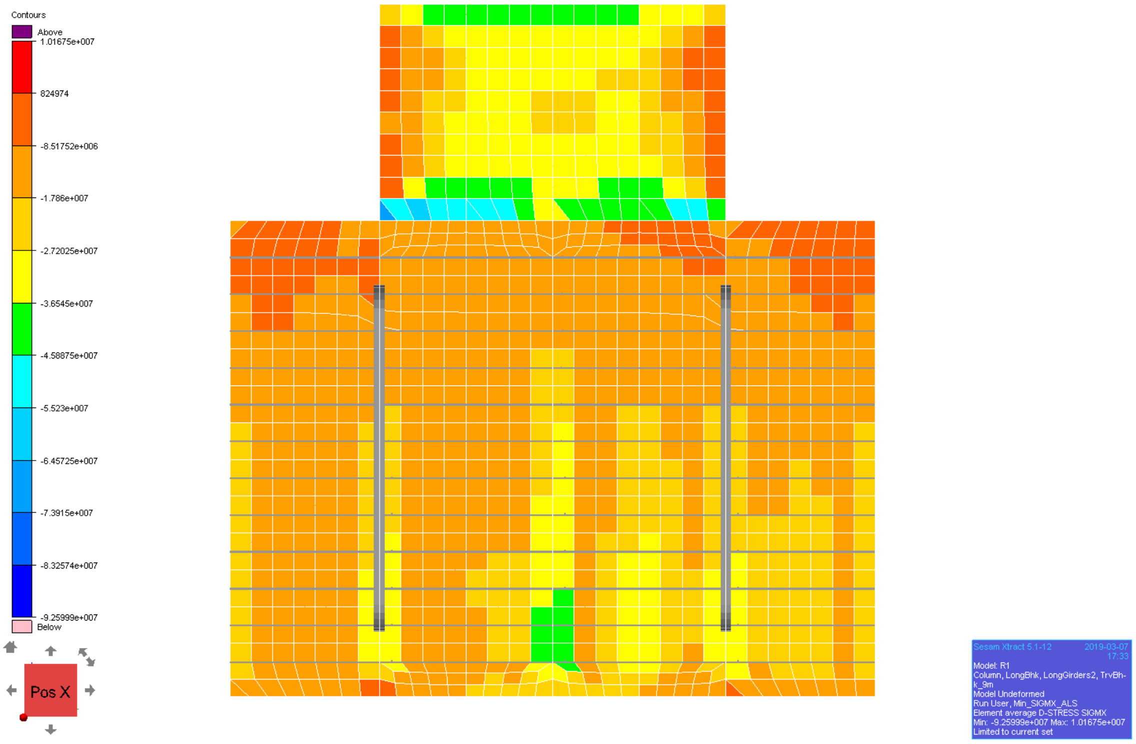

Figure 5-82 SIGMX stresses for ALS load combinations [N/m^2] for a typical transverse bulkhead

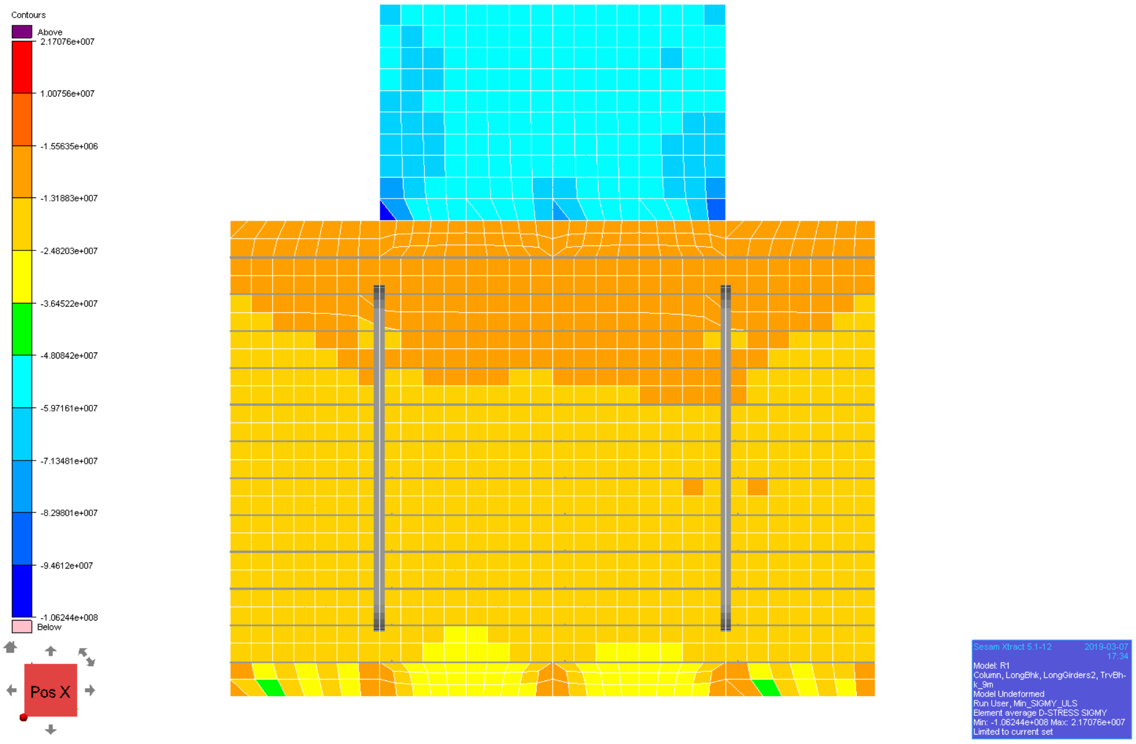

Sesam Xtract 5.1-12 2019-03-07 17:34
Model: R1
Column, LongBhk, LongGirders2, TrvBh-k_9m
Model Undeformed
Run User, Min_SIGMY_ULS
Element average D-STRESS SIGMY
Min: -1.06244e+008 Max: 2.17076e+007
Limited to current set

Figure 5-83 SIGMY stresses for ULS load combinations [N/m^2] for a typical transverse bulkhead

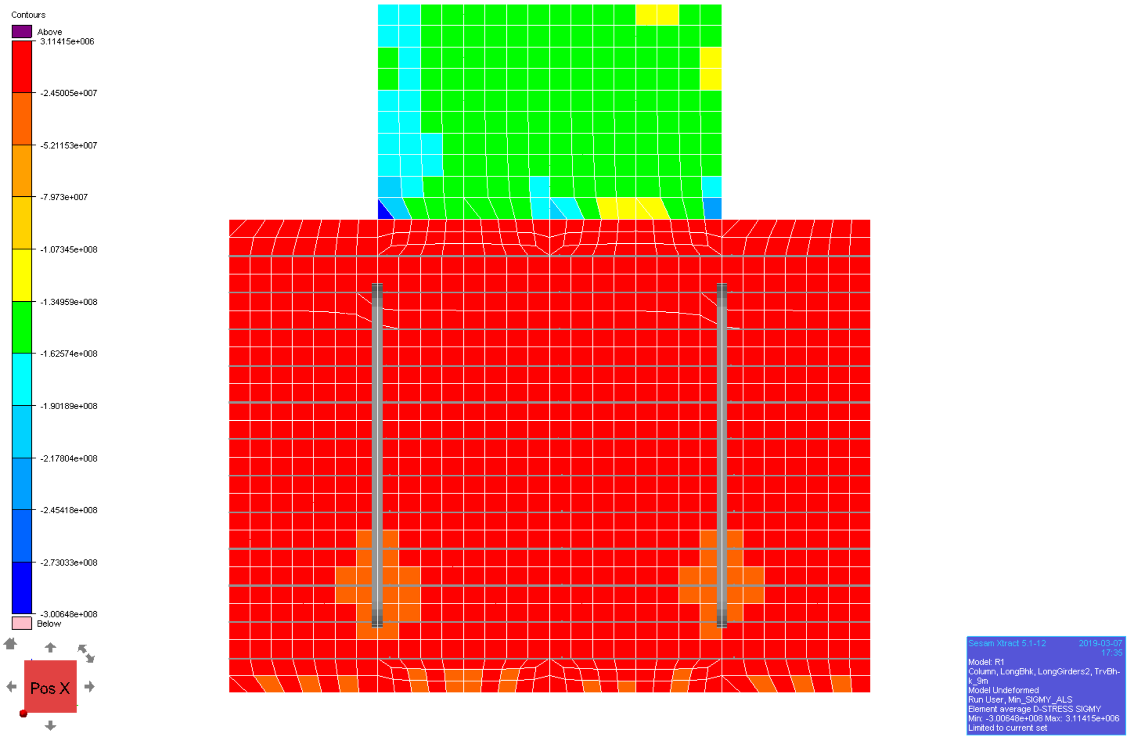

Sesam Xtract 5.1-12 2019-03-07 17:35
Model: R1
Column, LongBhk, LongGirders2, TrvBh-k_9m
Model Undeformed
Run User, Min_SIGMY_ALS
Element average D-STRESS SIGMY
Min: -3.00648e+008 Max: 3.11415e+006
Limited to current set

Figure 5-84 SIGMY stresses for ALS load combinations [N/m^2] for a typical transverse bulkhead

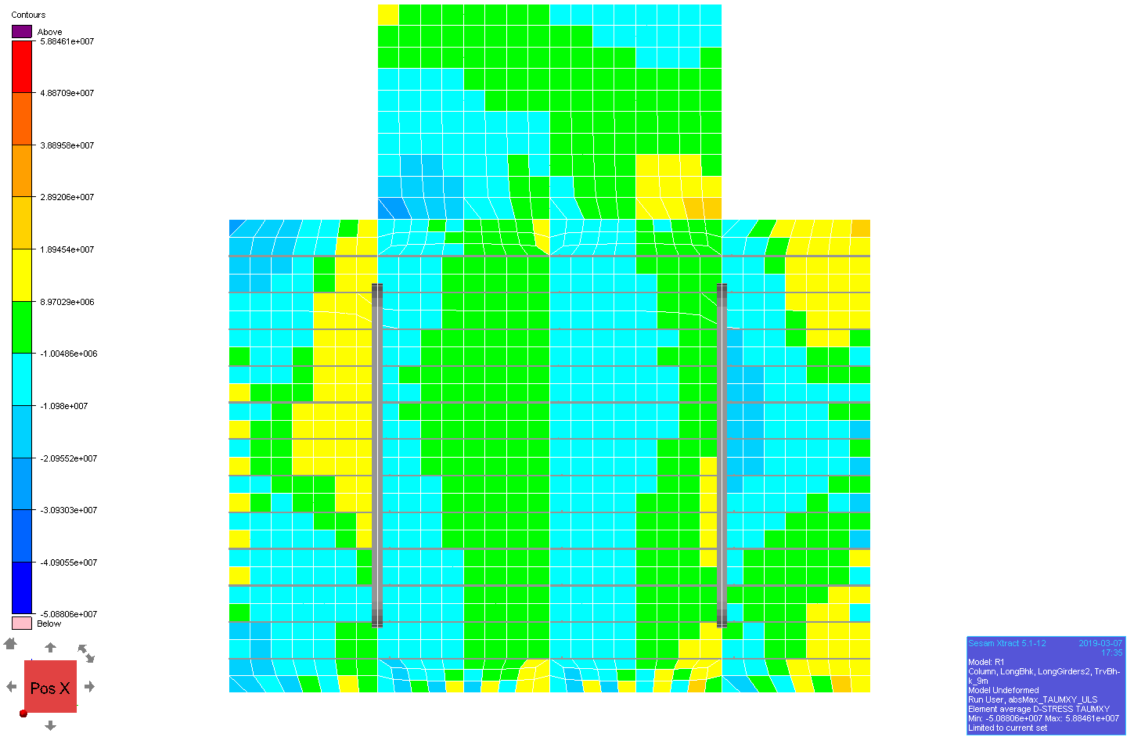

```
Sesam Xtract 5.1-12          2019-03-07
                                  17:35
Model: R1
Column, LongBhk, LongGirders2, TrvBh-
k_9m
Model Undeformed
Run User, absMax_TAUMXY_ULS
Element average D-STRESS TAUMXY
Min: -5.08806e+007 Max: 5.88461e+007
Limited to current set
```

Figure 5-85 TAUMXY stresses for ULS load combinations [N/m^2] for a typical transverse bulkhead

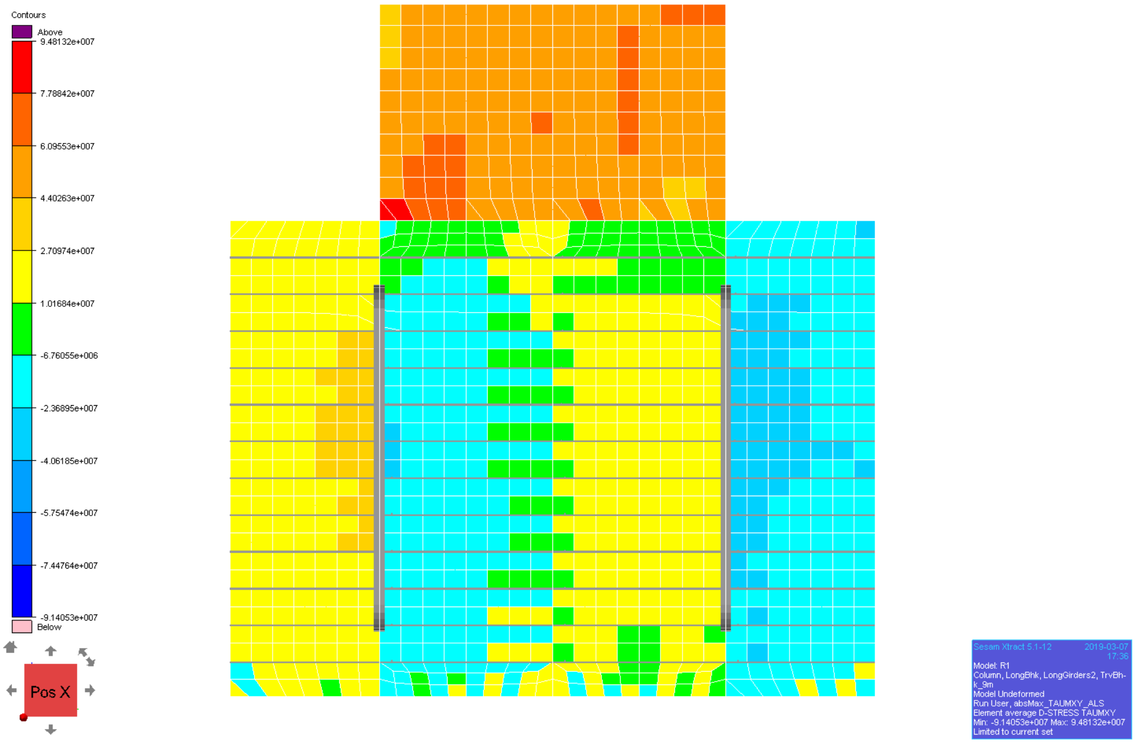

```
Sesam Xtract 5.1-12          2019-03-07
                                  17:36
Model: R1
Column, LongBhk, LongGirders2, TrvBh-
k_9m
Model Undeformed
Run User, absMax_TAUMXY_ALS
Element average D-STRESS TAUMXY
Min: -9.14053e+007 Max: 9.48132e+007
Limited to current set
```

Figure 5-86 TAUMXY stresses for ALS load combinations [N/m^2] for a typical transverse bulkhead

Table 5-1 Buckling and scantling results for ULS and ALS load combinations. Pontoon with mooring lines

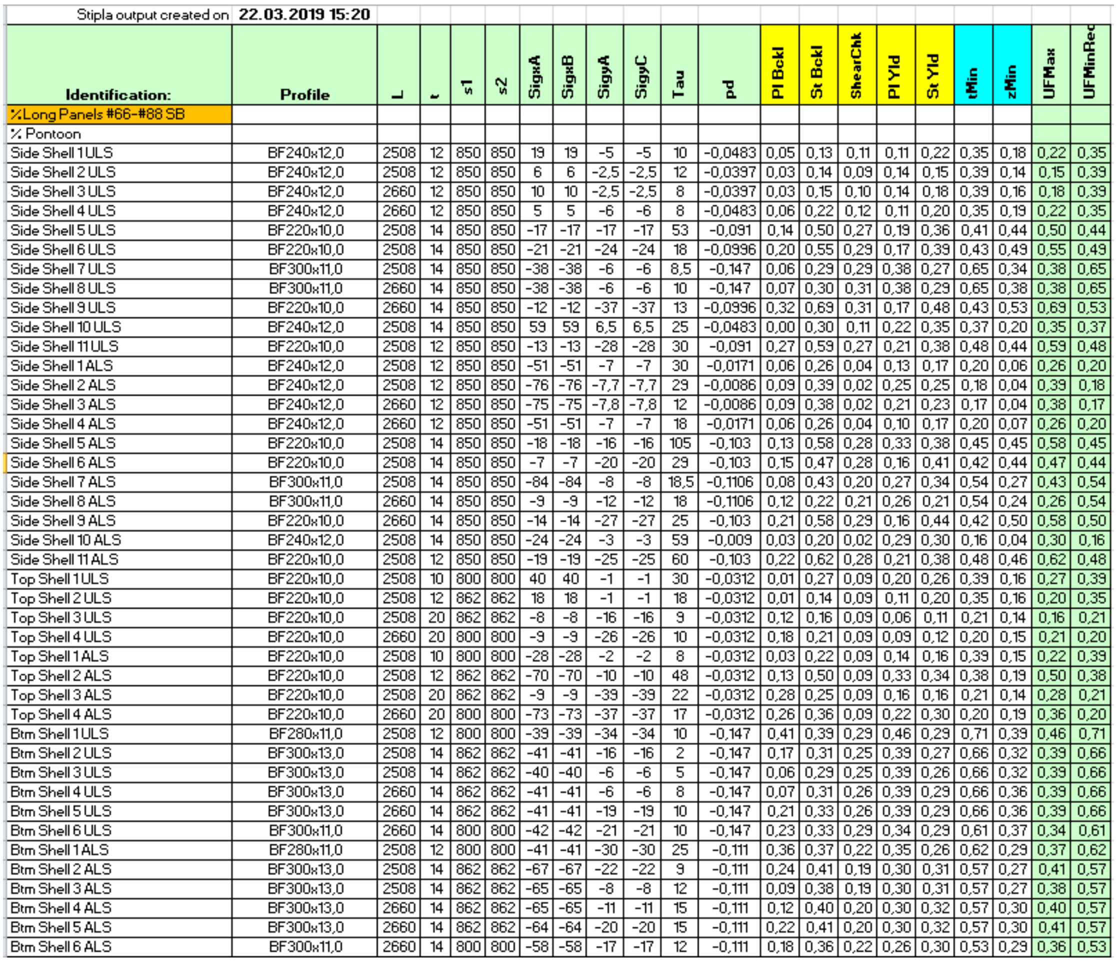

Stipla output created on **22.03.2019 15:20**

Identification:	**Profile**	**L**	**t**	**s1**	**s2**	**SigxA**	**SigxB**	**SigyA**	**SigyC**	**Tau**	**pd**	**Pl Bckl**	**St Bckl**	**ShearChk**	**Pl Yld**	**St Yld**	**tMin**	**zMin**	**UFMax**	**UFMinRec**
%Long Panels #66-#88 SB																				
% Pontoon																				
Side Shell 1 ULS	BF240x12,0	2508	12	850	850	19	19	-5	-5	10	-0,0483	0,05	0,13	0,11	0,11	0,22	0,35	0,18	0,22	0,35
Side Shell 2 ULS	BF240x12,0	2508	12	850	850	6	6	-2,5	-2,5	12	-0,0397	0,03	0,14	0,09	0,14	0,15	0,39	0,14	0,15	0,39
Side Shell 3 ULS	BF240x12,0	2660	12	850	850	10	10	-2,5	-2,5	8	-0,0397	0,03	0,15	0,10	0,14	0,18	0,39	0,16	0,18	0,39
Side Shell 4 ULS	BF240x12,0	2660	12	850	850	5	5	-6	-6	8	-0,0483	0,06	0,22	0,12	0,11	0,20	0,35	0,19	0,22	0,35
Side Shell 5 ULS	BF220x10,0	2508	14	850	850	-17	-17	-17	-17	53	-0,091	0,14	0,50	0,27	0,19	0,36	0,41	0,44	0,50	0,44
Side Shell 6 ULS	BF220x10,0	2508	14	850	850	-21	-21	-24	-24	18	-0,0996	0,20	0,55	0,29	0,17	0,39	0,43	0,49	0,55	0,49
Side Shell 7 ULS	BF300x11,0	2508	14	850	850	-38	-38	-6	-6	8,5	-0,147	0,06	0,29	0,29	0,38	0,27	0,65	0,34	0,38	0,65
Side Shell 8 ULS	BF300x11,0	2660	14	850	850	-38	-38	-6	-6	10	-0,147	0,07	0,30	0,31	0,38	0,29	0,65	0,38	0,38	0,65
Side Shell 9 ULS	BF220x10,0	2660	14	850	850	-12	-12	-37	-37	13	-0,0996	0,32	0,69	0,31	0,17	0,48	0,43	0,53	0,69	0,53
Side Shell 10 ULS	BF240x12,0	2508	14	850	850	59	59	6,5	6,5	25	-0,0483	0,00	0,30	0,11	0,22	0,35	0,37	0,20	0,35	0,37
Side Shell 11 ULS	BF220x10,0	2508	12	850	850	-13	-13	-28	-28	30	-0,091	0,27	0,59	0,27	0,21	0,38	0,48	0,44	0,59	0,48
Side Shell 1 ALS	BF240x12,0	2508	12	850	850	-51	-51	-7	-7	30	-0,0171	0,06	0,26	0,04	0,13	0,17	0,20	0,06	0,26	0,20
Side Shell 2 ALS	BF240x12,0	2508	12	850	850	-76	-76	-7,7	-7,7	29	-0,0086	0,09	0,39	0,02	0,25	0,25	0,18	0,04	0,39	0,18
Side Shell 3 ALS	BF240x12,0	2660	12	850	850	-75	-75	-7,8	-7,8	12	-0,0086	0,09	0,38	0,02	0,21	0,23	0,17	0,04	0,38	0,17
Side Shell 4 ALS	BF240x12,0	2660	12	850	850	-51	-51	-7	-7	18	-0,0171	0,06	0,26	0,04	0,10	0,17	0,20	0,07	0,26	0,20
Side Shell 5 ALS	BF220x10,0	2508	14	850	850	-18	-18	-16	-16	105	-0,103	0,13	0,58	0,28	0,33	0,38	0,45	0,45	0,58	0,45
Side Shell 6 ALS	BF220x10,0	2508	14	850	850	-7	-7	-20	-20	29	-0,103	0,15	0,47	0,28	0,16	0,41	0,42	0,44	0,47	0,44
Side Shell 7 ALS	BF300x11,0	2508	14	850	850	-84	-84	-8	-8	18,5	-0,1106	0,08	0,43	0,20	0,27	0,34	0,54	0,27	0,43	0,54
Side Shell 8 ALS	BF300x11,0	2660	14	850	850	-9	-9	-12	-12	18	-0,1106	0,12	0,22	0,21	0,26	0,21	0,54	0,24	0,26	0,54
Side Shell 9 ALS	BF220x10,0	2660	14	850	850	-14	-14	-27	-27	25	-0,103	0,21	0,58	0,29	0,16	0,44	0,42	0,50	0,58	0,50
Side Shell 10 ALS	BF240x12,0	2508	14	850	850	-24	-24	-3	-3	59	-0,009	0,03	0,20	0,02	0,29	0,30	0,16	0,04	0,30	0,16
Side Shell 11 ALS	BF220x10,0	2508	12	850	850	-19	-19	-25	-25	60	-0,103	0,22	0,62	0,28	0,21	0,38	0,48	0,46	0,62	0,48
Top Shell 1 ULS	BF220x10,0	2508	10	800	800	40	40	-1	-1	30	-0,0312	0,01	0,27	0,09	0,20	0,26	0,39	0,16	0,27	0,39
Top Shell 2 ULS	BF220x10,0	2508	12	862	862	18	18	-1	-1	18	-0,0312	0,01	0,14	0,09	0,11	0,20	0,35	0,16	0,20	0,35
Top Shell 3 ULS	BF220x10,0	2508	20	862	862	-8	-8	-16	-16	9	-0,0312	0,12	0,16	0,09	0,06	0,11	0,21	0,14	0,16	0,21
Top Shell 4 ULS	BF220x10,0	2660	20	800	800	-9	-9	-26	-26	10	-0,0312	0,18	0,21	0,09	0,09	0,12	0,20	0,15	0,21	0,20
Top Shell 1 ALS	BF220x10,0	2508	10	800	800	-28	-28	-2	-2	8	-0,0312	0,03	0,22	0,09	0,14	0,16	0,39	0,15	0,22	0,39
Top Shell 2 ALS	BF220x10,0	2508	12	862	862	-70	-70	-10	-10	48	-0,0312	0,13	0,50	0,09	0,33	0,34	0,38	0,19	0,50	0,38
Top Shell 3 ALS	BF220x10,0	2508	20	862	862	-9	-9	-39	-39	22	-0,0312	0,28	0,25	0,09	0,16	0,16	0,21	0,14	0,28	0,21
Top Shell 4 ALS	BF220x10,0	2660	20	800	800	-73	-73	-37	-37	17	-0,0312	0,26	0,36	0,09	0,22	0,30	0,20	0,19	0,36	0,20
Btm Shell 1 ULS	BF280x11,0	2508	12	800	800	-39	-39	-34	-34	10	-0,147	0,41	0,39	0,29	0,46	0,29	0,71	0,39	0,46	0,71
Btm Shell 2 ULS	BF300x13,0	2508	14	862	862	-41	-41	-16	-16	2	-0,147	0,17	0,31	0,25	0,39	0,27	0,66	0,32	0,39	0,66
Btm Shell 3 ULS	BF300x13,0	2508	14	862	862	-40	-40	-6	-6	5	-0,147	0,06	0,29	0,25	0,39	0,26	0,66	0,32	0,39	0,66
Btm Shell 4 ULS	BF300x13,0	2660	14	862	862	-41	-41	-6	-6	8	-0,147	0,07	0,31	0,26	0,39	0,29	0,66	0,36	0,39	0,66
Btm Shell 5 ULS	BF300x13,0	2660	14	862	862	-41	-41	-19	-19	10	-0,147	0,21	0,33	0,26	0,39	0,29	0,66	0,36	0,39	0,66
Btm Shell 6 ULS	BF300x11,0	2660	14	800	800	-42	-42	-21	-21	10	-0,147	0,23	0,33	0,29	0,34	0,29	0,61	0,37	0,34	0,61
Btm Shell 1 ALS	BF280x11,0	2508	12	800	800	-41	-41	-30	-30	25	-0,111	0,36	0,37	0,22	0,35	0,26	0,62	0,29	0,37	0,62
Btm Shell 2 ALS	BF300x13,0	2508	14	862	862	-67	-67	-22	-22	9	-0,111	0,24	0,41	0,19	0,30	0,31	0,57	0,27	0,41	0,57
Btm Shell 3 ALS	BF300x13,0	2508	14	862	862	-65	-65	-8	-8	12	-0,111	0,09	0,38	0,19	0,30	0,31	0,57	0,27	0,38	0,57
Btm Shell 4 ALS	BF300x13,0	2660	14	862	862	-65	-65	-11	-11	15	-0,111	0,12	0,40	0,20	0,30	0,32	0,57	0,30	0,40	0,57
Btm Shell 5 ALS	BF300x13,0	2660	14	862	862	-64	-64	-20	-20	15	-0,111	0,22	0,41	0,20	0,30	0,32	0,57	0,30	0,41	0,57
Btm Shell 6 ALS	BF300x11,0	2660	14	800	800	-58	-58	-17	-17	12	-0,111	0,18	0,36	0,22	0,26	0,30	0,53	0,29	0,36	0,53

Table 5-2 Buckling and scantling results for ULS and ALS load combinations. Pontoon with mooring lines

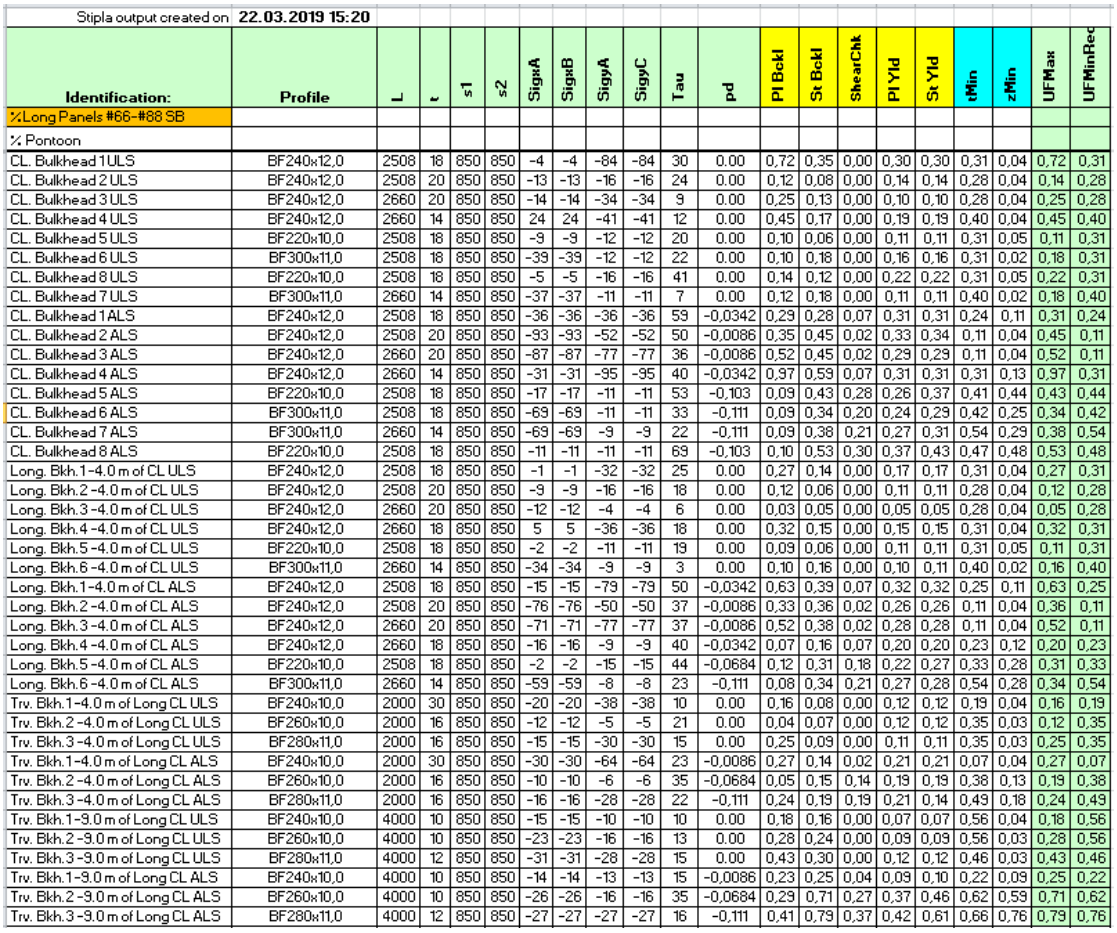

Stipla output created on **22.03.2019 15:20**

Identification:	**Profile**	**L**	**t**	**s1**	**s2**	**SigxA**	**SigxB**	**SigyA**	**SigyC**	**Tau**	**pd**	**Pl Bckl**	**St Bckl**	**ShearChk**	**Pl Yld**	**St Yld**	**tMin**	**zMin**	**UFMax**	**UFMinRec**
%Long Panels #66-#88 SB																				
% Pontoon																				
CL. Bulkhead 1 ULS	BF240x12,0	2508	18	850	850	-4	-4	-84	-84	30	0.00	0,72	0,35	0,00	0,30	0,30	0,31	0,04	0,72	0,31
CL. Bulkhead 2 ULS	BF240x12,0	2508	20	850	850	-13	-13	-16	-16	24	0.00	0,12	0,08	0,00	0,14	0,14	0,28	0,04	0,14	0,28
CL. Bulkhead 3 ULS	BF240x12,0	2660	20	850	850	-14	-14	-34	-34	9	0.00	0,25	0,13	0,00	0,10	0,10	0,28	0,04	0,25	0,28
CL. Bulkhead 4 ULS	BF240x12,0	2660	14	850	850	24	24	-41	-41	12	0.00	0,45	0,17	0,00	0,19	0,19	0,40	0,04	0,45	0,40
CL. Bulkhead 5 ULS	BF220x10,0	2508	18	850	850	-9	-9	-12	-12	20	0.00	0,10	0,06	0,00	0,11	0,11	0,31	0,05	0,11	0,31
CL. Bulkhead 6 ULS	BF300x11,0	2508	18	850	850	-39	-39	-12	-12	22	0.00	0,10	0,18	0,00	0,16	0,16	0,31	0,02	0,18	0,31
CL. Bulkhead 8 ULS	BF220x10,0	2508	18	850	850	-5	-5	-16	-16	41	0.00	0,14	0,12	0,00	0,22	0,22	0,31	0,05	0,22	0,31
CL. Bulkhead 7 ULS	BF300x11,0	2660	14	850	850	-37	-37	-11	-11	7	0.00	0,12	0,18	0,00	0,11	0,11	0,40	0,02	0,18	0,40
CL. Bulkhead 1 ALS	BF240x12,0	2508	18	850	850	-36	-36	-36	-36	59	-0,0342	0,29	0,28	0,07	0,31	0,31	0,24	0,11	0,31	0,24
CL. Bulkhead 2 ALS	BF240x12,0	2508	20	850	850	-93	-93	-52	-52	50	-0,0086	0,35	0,45	0,02	0,33	0,34	0,11	0,04	0,45	0,11
CL. Bulkhead 3 ALS	BF240x12,0	2660	20	850	850	-87	-87	-77	-77	36	-0,0086	0,52	0,45	0,02	0,29	0,29	0,11	0,04	0,52	0,11
CL. Bulkhead 4 ALS	BF240x12,0	2660	14	850	850	-31	-31	-95	-95	40	-0,0342	0,97	0,59	0,07	0,31	0,31	0,31	0,13	0,97	0,31
CL. Bulkhead 5 ALS	BF220x10,0	2508	18	850	850	-17	-17	-11	-11	53	-0,103	0,09	0,43	0,28	0,26	0,37	0,41	0,44	0,43	0,44
CL. Bulkhead 6 ALS	BF300x11,0	2508	18	850	850	-69	-69	-11	-11	33	-0,111	0,09	0,34	0,20	0,24	0,29	0,42	0,25	0,34	0,42
CL. Bulkhead 7 ALS	BF300x11,0	2660	14	850	850	-69	-69	-9	-9	22	-0,111	0,09	0,38	0,21	0,27	0,31	0,54	0,29	0,38	0,54
CL. Bulkhead 8 ALS	BF220x10,0	2508	18	850	850	-11	-11	-11	-11	69	-0,103	0,10	0,53	0,30	0,37	0,43	0,47	0,48	0,53	0,48
Long. Bkh.1 -4.0 m of CL ULS	BF240x12,0	2508	18	850	850	-1	-1	-32	-32	25	0.00	0,27	0,14	0,00	0,17	0,17	0,31	0,04	0,27	0,31
Long. Bkh.2 -4.0 m of CL ULS	BF240x12,0	2508	20	850	850	-9	-9	-16	-16	18	0.00	0,12	0,06	0,00	0,11	0,11	0,28	0,04	0,12	0,28
Long. Bkh.3 -4.0 m of CL ULS	BF240x12,0	2660	20	850	850	-12	-12	-4	-4	6	0.00	0,03	0,05	0,00	0,05	0,05	0,28	0,04	0,05	0,28
Long. Bkh.4 -4.0 m of CL ULS	BF240x12,0	2660	18	850	850	5	5	-36	-36	18	0.00	0,32	0,15	0,00	0,15	0,15	0,31	0,04	0,32	0,31
Long. Bkh.5 -4.0 m of CL ULS	BF220x10,0	2508	18	850	850	-2	-2	-11	-11	19	0.00	0,09	0,06	0,00	0,11	0,11	0,31	0,05	0,11	0,31
Long. Bkh.6 -4.0 m of CL ULS	BF300x11,0	2660	14	850	850	-34	-34	-9	-9	3	0.00	0,10	0,16	0,00	0,10	0,11	0,40	0,02	0,16	0,40
Long. Bkh.1 -4.0 m of CL ALS	BF240x12,0	2508	18	850	850	-15	-15	-79	-79	50	-0,0342	0,63	0,39	0,07	0,32	0,32	0,25	0,11	0,63	0,25
Long. Bkh.2 -4.0 m of CL ALS	BF240x12,0	2508	20	850	850	-76	-76	-50	-50	37	-0,0086	0,33	0,36	0,02	0,26	0,26	0,11	0,04	0,36	0,11
Long. Bkh.3 -4.0 m of CL ALS	BF240x12,0	2660	20	850	850	-71	-71	-77	-77	37	-0,0086	0,52	0,38	0,02	0,28	0,28	0,11	0,04	0,52	0,11
Long. Bkh.4 -4.0 m of CL ALS	BF240x12,0	2660	18	850	850	-16	-16	-9	-9	40	-0,0342	0,07	0,16	0,07	0,20	0,20	0,23	0,12	0,20	0,23
Long. Bkh.5 -4.0 m of CL ALS	BF220x10,0	2508	18	850	850	-2	-2	-15	-15	44	-0,0684	0,12	0,31	0,18	0,22	0,27	0,33	0,28	0,31	0,33
Long. Bkh.6 -4.0 m of CL ALS	BF300x11,0	2660	14	850	850	-59	-59	-8	-8	23	-0,111	0,08	0,34	0,21	0,27	0,28	0,54	0,28	0,34	0,54
Trv. Bkh.1 -4.0 m of Long CL ULS	BF240x10,0	2000	30	850	850	-20	-20	-38	-38	10	0.00	0,16	0,08	0,00	0,12	0,12	0,19	0,04	0,16	0,19
Trv. Bkh.2 -4.0 m of Long CL ULS	BF260x10,0	2000	16	850	850	-12	-12	-5	-5	21	0.00	0,04	0,07	0,00	0,12	0,12	0,35	0,03	0,12	0,35
Trv. Bkh.3 -4.0 m of Long CL ULS	BF280x11,0	2000	16	850	850	-15	-15	-30	-30	15	0.00	0,25	0,09	0,00	0,11	0,11	0,35	0,03	0,25	0,35
Trv. Bkh.1 -4.0 m of Long CL ALS	BF240x10,0	2000	30	850	850	-30	-30	-64	-64	23	-0,0086	0,27	0,14	0,02	0,21	0,21	0,07	0,04	0,27	0,07
Trv. Bkh.2 -4.0 m of Long CL ALS	BF260x10,0	2000	16	850	850	-10	-10	-6	-6	35	-0,0684	0,05	0,15	0,14	0,19	0,19	0,38	0,13	0,19	0,38
Trv. Bkh.3 -4.0 m of Long CL ALS	BF280x11,0	2000	16	850	850	-16	-16	-28	-28	22	-0,111	0,24	0,19	0,19	0,21	0,14	0,49	0,18	0,24	0,49
Trv. Bkh.1 -9.0 m of Long CL ULS	BF240x10,0	4000	10	850	850	-15	-15	-10	-10	10	0.00	0,18	0,16	0,00	0,07	0,07	0,56	0,04	0,18	0,56
Trv. Bkh.2 -9.0 m of Long CL ULS	BF260x10,0	4000	10	850	850	-23	-23	-16	-16	13	0.00	0,28	0,24	0,00	0,09	0,09	0,56	0,03	0,28	0,56
Trv. Bkh.3 -9.0 m of Long CL ULS	BF280x11,0	4000	12	850	850	-31	-31	-28	-28	15	0.00	0,43	0,30	0,00	0,12	0,12	0,46	0,03	0,43	0,46
Trv. Bkh.1 -9.0 m of Long CL ALS	BF240x10,0	4000	10	850	850	-14	-14	-13	-13	15	-0,0086	0,23	0,25	0,04	0,09	0,10	0,22	0,09	0,25	0,22
Trv. Bkh.2 -9.0 m of Long CL ALS	BF260x10,0	4000	10	850	850	-26	-26	-16	-16	35	-0,0684	0,29	0,71	0,27	0,37	0,46	0,62	0,59	0,71	0,62
Trv. Bkh.3 -9.0 m of Long CL ALS	BF280x11,0	4000	12	850	850	-27	-27	-27	-27	16	-0,111	0,41	0,79	0,37	0,42	0,61	0,66	0,76	0,79	0,76

6 Weight and material quantities

6.1 Base case pontoon

The weight summary for the low bridge pontoon "base case" without mooring lines is seen in Table 6-1 for the plates and in Table 6-2 for the stiffeners. The total steel weight for the "base case" pontoon amount to 705 ton.

Table 6-1 Structural quantities of steel plates for "base case" pontoon

Description	Steel quality	Plate thickness [mm]	Area [m^2]	Weight [Ton]
Top shell	S420	8	174	10.9
Top shell	S420	10	150	11.7
Top shell	S420	12	224	21.1
Top shell	S420	20	194	30.4
Bottom shell	S420	12	324	30.5
Bottom shell	S420	14	418	46.0
Side shell – splash zone	SDSS	10	435	34.1
Side shell – splash zone	SDSS	12	365	34.4
Side shell	S420	12	134	12.6
Side shell	S420	14	112	12.3
Trv. Bulkheads	S420	10	532	41.8
Trv. Bulkheads	S420	12	228	21.5
Trv. Bulkheads	S420	16	177	22.3
Trv. Bulkheads	S420	18	34	4.8
Trv. Bulkheads	S420	20	32	5.1
Trv. Bulkheads	S420	30	38	9.0
Trv. Bulkheads	S420	40	6	1.8
Web frames	S420	12	613	57.8
Web frames	S420	18	29	4.1
Long. Bulkheads	S420	12	468	44.1
Long. Bulkheads	S420	14	248	27.3
Long. Bulkheads	S420	18	344	48.5
Long. Bulkheads	S420	20	52	8.2
Long. Bulkheads	S420	30	9	2.1
Long. Bulkheads	S420	50	18	7.1
Total				**549.4**

Table 6-2 Structural quantities of stiffeners for "base case" pontoon

Description	Steel quality	Stiffener Dimension	Length [m]	Weight [Ton]
Top shell	S420	BF220x10	720	16.4
Bottom shell	S420	BF300x11	437	16.0
Bottom shell	S420	BF300x13	284	11.8
Side shell	S420	BF220x10	366	8.3
Side shell	S420	BF240x12	366	10.7
Side shell	S420	BF300x11	366	13.4
Trv. Bulkheads	S420	FB250x20	34	0.7
Trv. Bulkheads	S420	BF240x10	358	9.1
Trv. Bulkheads	S420	BF260x10	358	10.1
Trv. Bulkheads	S420	BF280x11	358	12.0
Web frames	S420	FB200x18	166	4.7
Web frames	S420	FB250x20	431	16.9
Long. Bulkheads	S420	BF220x10	267	6.1
Long. Bulkheads	S420	BF240x12	267	7.8
Long. Bulkheads	S420	BF300x11	267	9.8
Long. Bulkheads	S420	FB200x18	30	0.9
Long. Bulkheads	S420	FB250x20	22	0.9
Total				**155.6**

6.2 Pontoon with mooring lines

The weight of the pontoon with mooring lines is 934 ton. The total weight is split between weight of plates and stiffeners in Table 6-3

Table 6-3 Steel weight of plates in pontoon with mooring lines

Plate thickness [mm]	Steel quality	Area [m^2]	Weight [ton]
8	S420	174	10.9
10	S420	681	53.5
12	S420	1778	167.5
14	S420	2000	219.8
16	S420	324	40.7
18	S420	517	73.1
20	S420	435	68.3
30	S420	35	8.3
40	S420	17	5.5
50	S420	29	11.3
12	SDSS	317	29.9
14	SDSS	378	41.5
Total			**730.3**

Table 6-4 Steel weight of stiffeners in pontoon with mooring lines

Stiffener profile	Steel quality	Length [m]	Weight per m [kg/m]	Weight [ton]
BF222X10	S420	1290	22.8	29.4
BF240X10	S420	358	25.4	9.1
BF240X12	S420	633	29.3	18.5
BF260X10	S420	358	28.3	10.1
BF280x11	S420	716	33.4	23.9
BF300X11	S420	1511	36.7	55.5
BD300X13	S420	326	41.4	13.5
FB200X18	S420	220	28.3	6.2
FB250X20	S420	581	39.3	22.8
FB300X25	S420	254	58.9	14.9
Total				**204.1**

7 References

/1/ SBJ-32-C4-SVV-90-BA-001-0, Design Basis, Bjørnafjorden floating bridges rev. 0 2018.

/2/ SBJ-31-C3-MUL-22-RE-109, Bjørnafjorden straight floating bridge phase 3, Analysis and design (Base case) Appendix I – Design of mooring lines

/3/ DNVGL-OS-C101, Design of offshore steel structures, general – LRFD method

/4/ NS-EN 1990, Basis of structural design

/5/ NS-EN 1993-1-1, General rules and rules for buildings

/6/ NS-EN-1993-2, Steel bridges

/7/ 10205546-13-TEG-124, AMC status 2 – Pontoon – Structural arrangement, Isometric projection

/8/ 10205546-13-TEG-125, AMC status 2 – Pontoon – Structural arrangement, Plan view – pontoon bottom deck

/9/ 10205546-13-TEG-126, AMC status 2 – Pontoon – Structural arrangement, Plan view – pontoon deck 8500 A/BL

/10/ 10205546-13-TEG-127, AMC status 2 – Pontoon – Structural arrangement, Longitudinal structure – 3200 & 4000 from CL

/11/ 10205546-13-TEG-128, AMC status 2 – Pontoon – Structural arrangement, Longitudinal structure – CL

/12/ 10205546-13-TEG-129, AMC status 2 – Pontoon – Structural arrangement, Longitudinal structure – 74150 from CL

/13/ 10205546-13-TEG-130, AMC status 2 – Pontoon – Structural arrangement, Transverse section – frame 06

/14/ 10205546-13-TEG-131, AMC status 2 – Pontoon – Structural arrangement, Transverse section – frame 07

/15/ 10205546-13-TEG-132, AMC status 2 – Pontoon – Structural arrangement, Transverse section – frame 08

/16/ 10205546-13-TEG-133, AMC status 2 – Pontoon – Structural arrangement, Transverse section – frame 09

Concept development, floating bridge
E39 Bjørnafjorden

Appendix K – Enclosure 7

10205546-13-NOT-099
FEM analysis of bridge girder and column

MEMO

PROJECT	Concept development, floating bridge E39 Bjørnafjorden	DOCUMENT CODE	10205546-13-NOT-099
CLIENT	Statens vegvesen	ACCESSIBILITY	Restricted
SUBJECT	FEM analysis of bridge girder and column	PROJECT MANAGER	Svein Erik Jakobsen
TO	Statens vegvesen	PREPARED BY	Espen Tuveng
COPY TO		RESPONSIBLE UNIT	AMC

SUMMARY

This memo summarizes several finite element analyses performed on a local model, of a 125m long bridge girder with column at the lower part of the floating bridge.

- ULS3 loads from the global analysis have been applied to the column to investigate the interface between bridge girder and column. Stress in the column and bridge girder close to the column is acceptable. The structure has sufficient capacity to carry the forces applied.
- SCF factors have been found by applying unit forces to the beam ends. Particular focus has been devoted to the interface between column and bridge girder.
- Shear lag found in the FEM have been compared to the shear lag calculated with Eurocode rules. The results show that the shear lag calculated with Eurocode rules is slightly more conservative than the shear lag found with the FEM.
- Transverse frames have been checked for traffic loads. Findings are that the transverse frames have low utilization, and that the trapezoidal stiffeners carry shear forces and distribute local loads in a very effective manner.
- Torsion from an eccentric ship impact has been applied to three different column variations. Two columns with a narrow middle part, 25 mm and 40 mm skin plate thickness has been checked. One straight column with 25 mm skin plate has been checked. Results show that increasing the skin plate thickness will significantly increase the column torsional capacity with a moderate weight increase. Removing the narrow middle part of the columns so that the column is straight will increase the column torsional capacity even more with less added weight.
- Torsion from an eccentric ship impact has been applied to the column and bridge girder. Stress in the bridge girder is overall acceptable. The column is the weak link between pontoon and bridge girder.

0	24.05.2019	Final issue	E. Tuveng	P. N. Larsen	S. E. Jakobsen
REV.	DATE	DESCRIPTION	PREPARED BY	CHECKED BY	APPROVED BY

TABLE OF CONTENTS

1 FEM model

The local model of the floating bridge low part consists of a column and a bridge girder extending 1/2 span length (125/2 m) to each side of the column. The modelled bridge girder is 125 m long. The floating bridge low part column is 10.5 m tall.

The girder has an "above column" section profile, stretching 3/16 span length (23.4 m) to each side of the column center. The remaining 5/16 span length (39.1 m) at each end of the girder is modelled as a "midspan" section. The modelled part is representative for axis 15-37. The pontoon is not included in the model.

The model is based on drawings listed in Table 1-1. Since the FEM was finished before final revision of the drawings were ready, there are small deviations between FEM and drawings. The major differences are:

- The transitional cross section that is used between "midspan" and "above column" sections is not included
- Top plate thickness for a "midspan" section is 14 mm in the FEM. Changed to 16 mm on the latest drawing.
- Inclined bottom plate and bottom plate is 14 mm in the FEM. Changed to 12 mm on the latest drawing.
- Column corners with cast part and thicker plates near corners is not included.

All major parts of the beam and column are included. Details have been omitted to simplify the FEM.

Table 1-1 Drawings

Drawing number	Revision
SBJ-32-C5-AMC-22-DR-431	0
SBJ-32-C5-AMC-22-DR-432	0
SBJ-32-C5-AMC-22-DR-433	0
SBJ-32-C5-AMC-22-DR-434	0
SBJ-32-C5-AMC-22-DR-435	0
SBJ-32-C5-AMC-22-DR-436	0
SBJ-32-C5-AMC-22-DR-437	0
SBJ-32-C5-AMC-22-DR-471	0
SBJ-32-C5-AMC-22-DR-491	0
SBJ-32-C5-AMC-22-DR-492	0

The model is shown on the following figures.

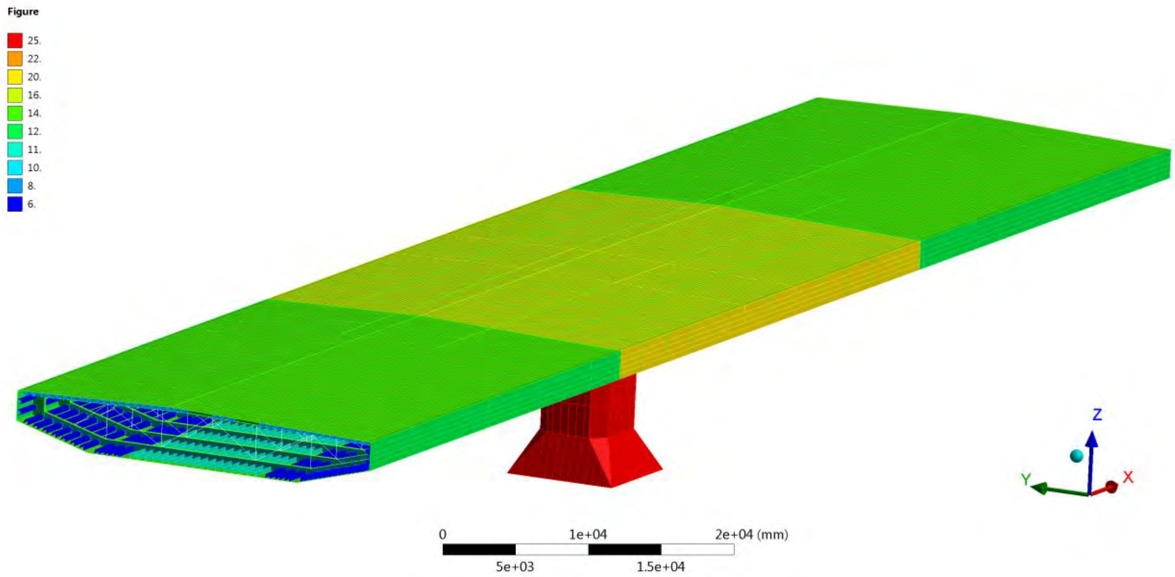

Figure 1-1 FEM geometry, iso view

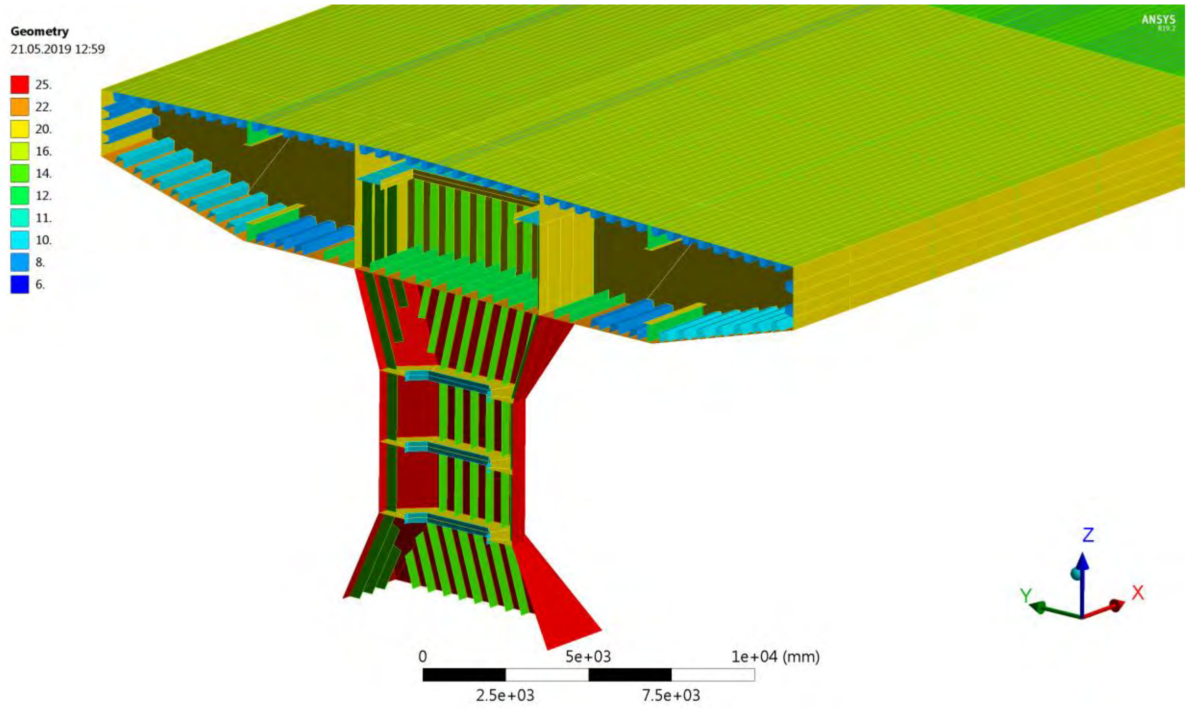

Figure 1-2 FEM geometry, cut through column and bridge girder

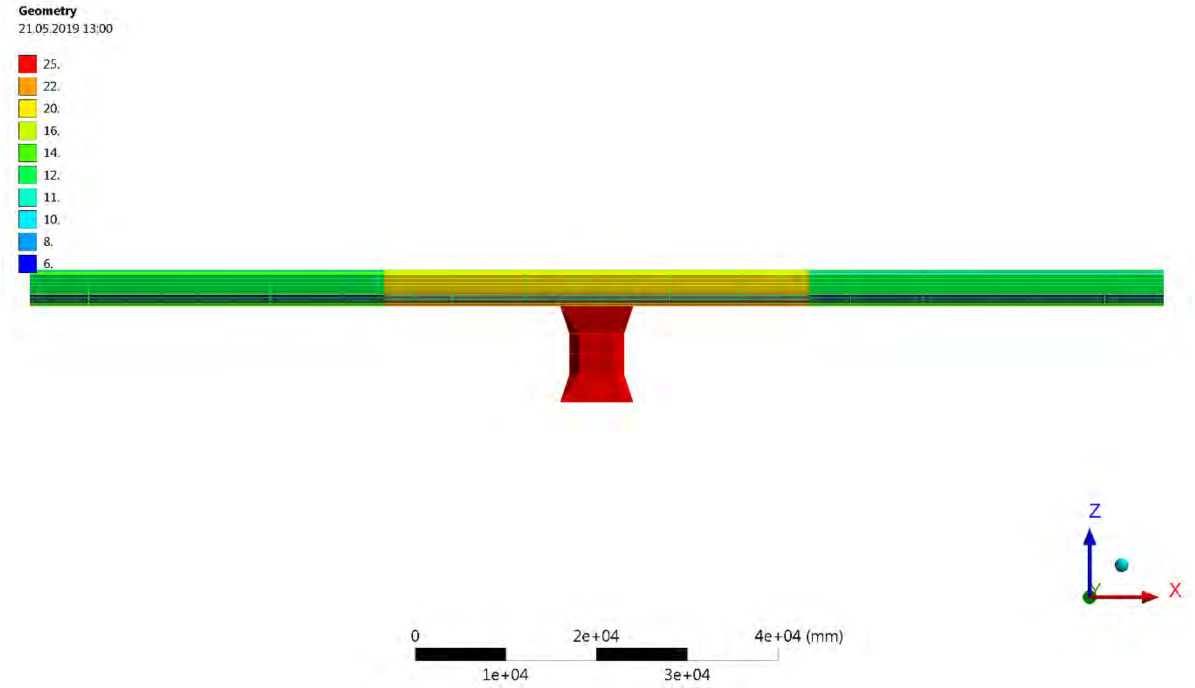

Figure 1-3 FEM geometry, side view

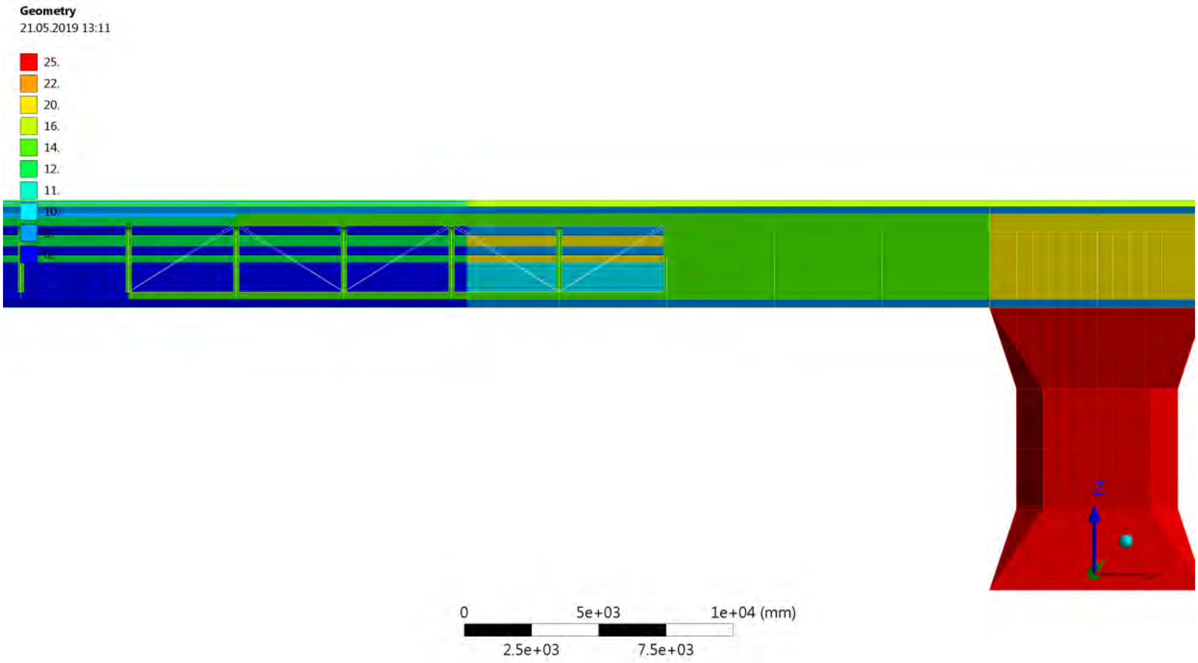

Figure 1-4 FEM geometry, side view cut

1.1 Mesh

The element mesh size is approximately 600 mm by 600 mm. This is a relatively coarse mesh, and refinements have been made to several of the analyzes. Where changes have been made, it is stated for each analysis. The FEM consists of shell (SHELL181) and beam (BEAM188) elements.

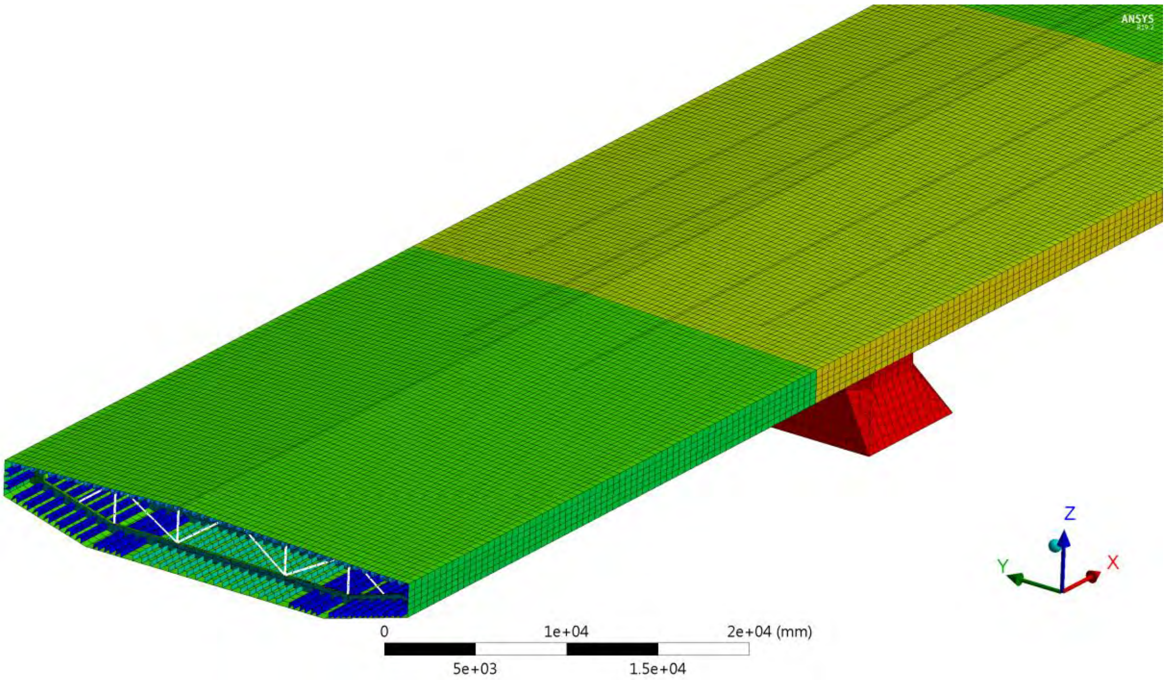

Figure 1-5 Element mesh

1.2 Material properties

As a default, linear material has been utilized. Where non-linear material properties have been used, it is stated for each analysis.

Table 1-2 Linear material properties

Property	Value
Modulus of elasticity	E = 210 000 MPa
Poison ratio	ν = 0.3
Density	ρ= 7850 kg/m^3

Table 1-3 Non-linear material properties

Property	Value
Modulus of elasticity	E = 210 000 MPa
Yield stress	f_{sy} = 420 MPa
Tangent modulus after yield	E_y = 1450 MPa
Poison ratio	ν = 0.3
Density	ρ= 7850 kg/m^3

1.3 Coordinate system

The global coordinate system is defined as follows:

Table 1-4 Coordinate system definition

Axis	Direction
X	North
Y	West
Z	Up

2 ULS forces applied to column

The purpose of this analysis is to investigate stress in the column and the interface between column and bridge girder. Since the forces from the global analysis is applied to the column only, the results are valid for the column and the bridge girder close to the column.

Modelled geometry is valid for axis 15-37. From work previously performed and documented in 13-NOT-086 Column design [1], axis 16, 24 and 32 were found to have highest utilization of axis 15-37. Therefore, forces from these axis have been tested.

2.1 Boundary conditions

Boundary conditions and axis definitions are shown on Figure 2-1 and Table 2-1.

Forces from axis 16, 24 and 32 are all applied with pinned boundary conditions. To check the sensitivity, fixed boundary conditions are also tested for axis 24 loads.

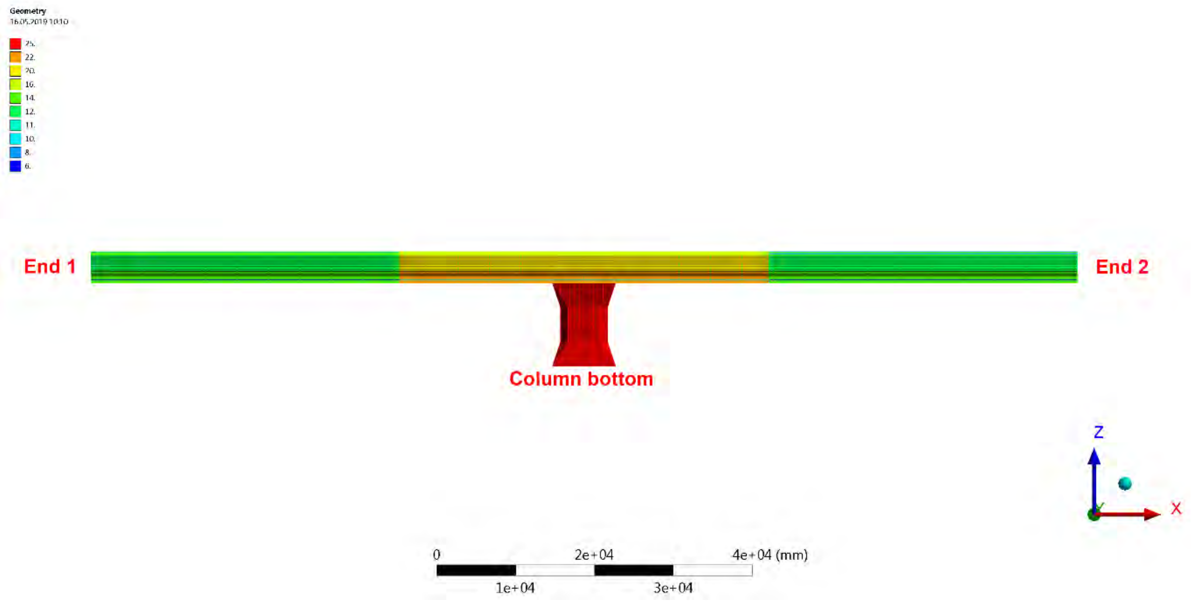

Figure 2-1 Geometry

Table 2-1 Boundary conditions

	Translation			**Rotation**		
	X	**Y**	**Z**	**X**	**Y**	**Z**
Pinned End 1 & End 2	Fixed	Fixed	Fixed	Free	Free	Free
Fixed End 1 & End 2	Fixed	Fixed	Fixed	Fixed	Fixed	Fixed

2.2 Mesh refinement

The element mesh is refined for the column and for the bridge girder near the column to get better results for relevant areas. The refined mesh has a size of approximately 150 mm by 150 mm.

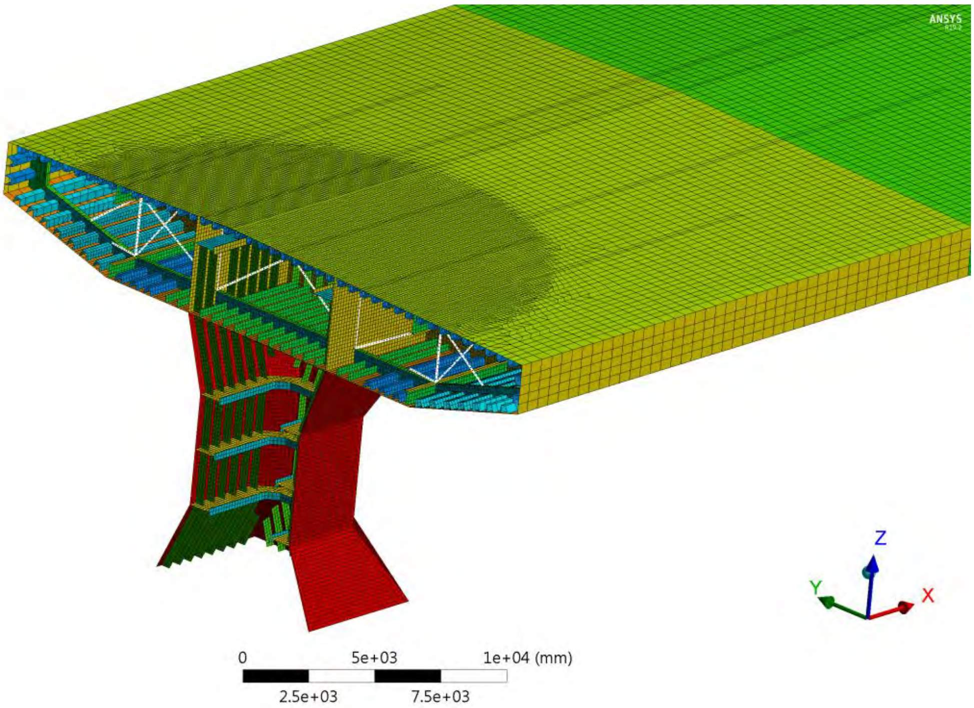

Figure 2-2 Mesh refinement

2.3 ULS3 forces

ULS3 combinations are with 100-years environmental loads without traffic.

2.3.1 Self-weight

Self-weight from steel and asphalt, railing etc. has been set to 19 tonne/m and has been included in the analysis. Self-weight from the column has been set to 83.7 tonne. Self weight for the steel is added as an acceleration. The acceleration is scaled in the analysis to match the desired self-weight. Asphalt, railing etc. is added as a pressure on the top plate.

A load factor of 1.2 has been included for self-weight.

2.3.2 Column loads

Forces are extracted from K12_06_PROD_load_combinations_columns_direct_expected_max.xlsx.

Table 2-2 Axis 16 forces

A16 bottom		V longit [MN]	V transv [MN]	N [MN]	M longit [MNm]	M transv [MNm]	T [MNm]
Ansys axis		Fx	Fy	Fz	Mx	My	Mz
Worst	Min	-5.16	-4.84	-33.02	-47.22	-24.13	-69.90
	Max	5.12	5.66	-24.48	45.19	24.36	69.90
Case 1	Min	-3.46	-4.84	-31.72	-47.22	-15.27	-69.90
	Max	3.43	5.66	-25.78	45.19	15.50	69.90
Case 2	Min	-1.63	-4.51	-31.23	-38.80	-8.52	-37.64
	Max	1.59	5.33	-26.27	36.77	8.75	37.64
Case 3	Min	-5.16	-3.67	-33.01	-30.87	-24.12	-51.00
	Max	5.12	4.49	-24.49	28.83	24.35	51.00
Case 4	Min	-2.70	-4.74	-32.09	-44.10	-13.41	-58.63
	Max	2.66	5.55	-25.41	42.07	13.64	58.63
Case 5	Min	-5.16	-3.57	-33.02	-32.37	-24.13	-51.03
	Max	5.12	4.39	-24.48	30.34	24.36	51.03
Case 6	Min	-2.70	-4.68	-32.10	-45.09	-13.42	-58.72
	Max	2.66	5.50	-25.40	43.06	13.65	58.72

Table 2-3 Axis 24 forces

A24 bottom		V longit [MN]	V transv [MN]	N [MN]	M longit [MNm]	M transv [MNm]	T [MNm]
Ansys axis		Fx	Fy	Fz	Mx	My	Mz
Worst	Min	-5.78	-5.18	-32.79	-50.32	-26.90	-61.08
	Max	5.78	5.92	-24.71	49.43	26.95	61.08
Case 1	Min	-2.44	-5.18	-31.31	-50.32	-11.46	-59.05
	Max	2.43	5.92	-26.19	49.43	11.51	59.05
Case 2	Min	-1.57	-4.88	-31.22	-43.11	-8.38	-37.16
	Max	1.56	5.62	-26.28	42.22	8.44	37.16
Case 3	Min	-5.78	-3.52	-32.76	-28.58	-26.89	-47.67
	Max	5.78	4.26	-24.74	27.69	26.94	47.67
Case 4	Min	-3.89	-4.63	-32.36	-42.91	-18.13	-61.01
	Max	3.89	5.36	-25.14	42.02	18.19	61.01
Case 5	Min	-5.78	-3.47	-32.79	-29.32	-26.90	-47.64
	Max	5.77	4.20	-24.71	28.43	26.95	47.64
Case 6	Min	-3.90	-4.60	-32.38	-43.47	-18.14	-61.08

	Max	2.66	5.50	-25.40	43.06	13.65	58.72

Table 2-4 Axis 32 forces

A32 bottom		V longit [MN]	V transv [MN]	N [MN]	M longit [MNm]	M transv [MNm]	T [MNm]
Ansys axis		Fx	Fy	Fz	Mx	My	Mz
Worst	Min	-6.58	-4.74	-33.24	-48.43	-29.02	-87.51
	Max	6.60	5.40	-24.27	47.88	28.95	87.51
Case 1	Min	-1.66	-4.39	-31.25	-44.88	-8.92	-38.85
	Max	1.68	5.06	-26.26	44.34	8.85	38.85
Case 2	Min	-2.42	-4.74	-31.36	-48.43	-11.60	-59.68
	Max	2.44	5.40	-26.15	47.88	11.53	59.68
Case 3	Min	-4.23	-3.33	-32.36	-28.20	-20.47	-47.19
	Max	4.24	4.00	-25.15	27.66	20.39	47.19
Case 4	Min	-6.56	-4.53	-33.13	-43.65	-28.97	-87.37
	Max	6.57	5.20	-24.37	43.11	28.90	87.37
Case 5	Min	-4.25	-3.32	-32.49	-28.81	-20.54	-47.21
	Max	4.26	3.99	-25.01	28.26	20.47	47.21
Case 6	Min	-6.58	-4.53	-33.24	-44.02	-29.02	-87.51
	Max	6.60	5.19	-24.27	43.48	28.95	87.51

2.4 Results

The overall stress level is acceptable. Peak stress above allowable (420 MPa/1.1 = 381.8 MPa) can be observed at the corner of the top column. This area will be reinforced with a cast part and thicker plates in the surrounding area. This reinforcement is not included in the FEM, and it is therefore expected to see high stress level in this area.

The maximum hand calculated ULS utilization for axis 9- was found to be 0.61 [1]. Stress at the top of the column when excluding the peak stress areas at the corners is in the range of 170-270 MPa. This corresponds well with the hand calculated utilizations.

Stress plots below show the maximum stress for all combinations for each axis on one plot.

2.4.1 Forces from axis 16 - pinned bridge girder ends

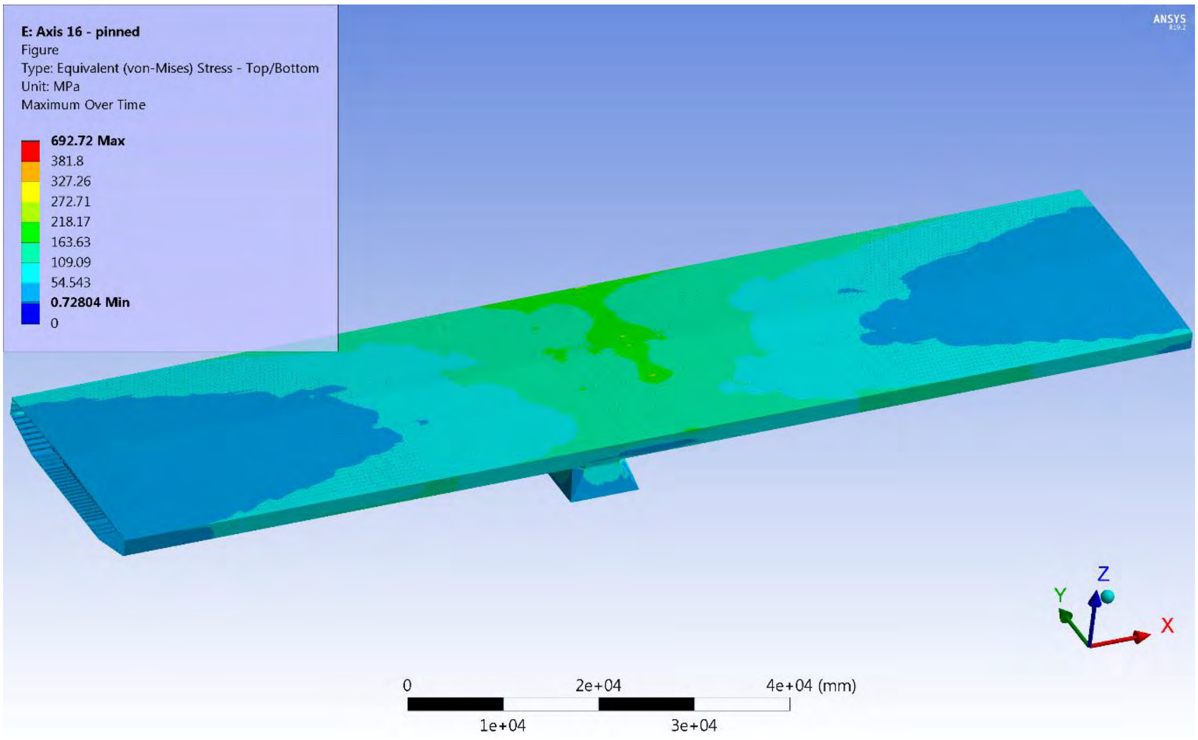

Figure 2-3 Axis 16, pinned, Von-Mises stress – top view

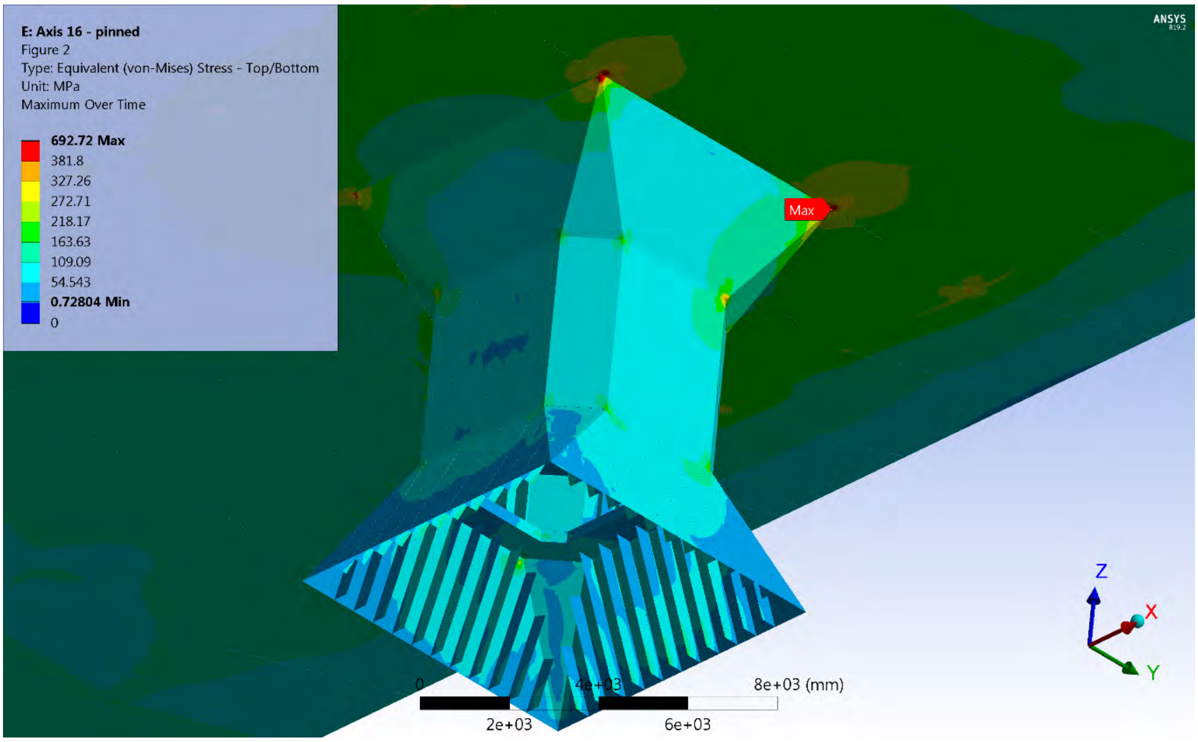

Figure 2-4 Axis 16, pinned, Von-Mises stress – bottom view

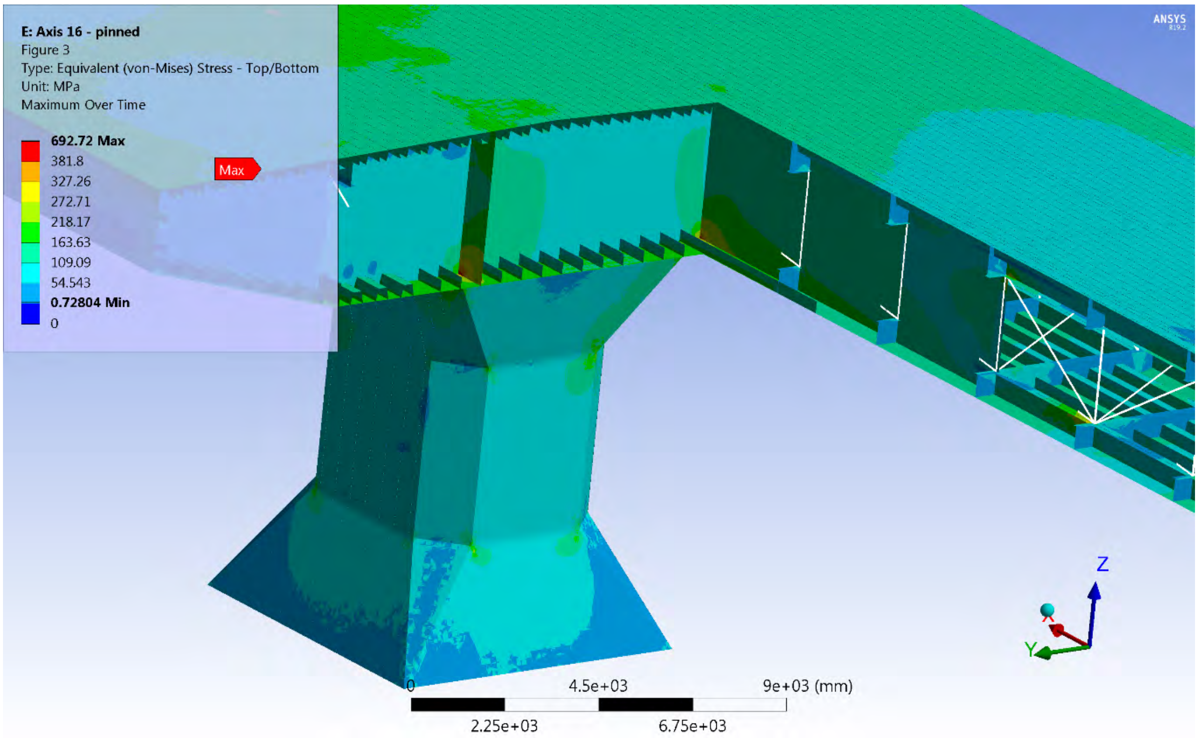

Figure 2-5 Axis 16, pinned, Von-Mises stress – cut bridge girder view

2.4.2 Forces from axis 24 - pinned bridge girder ends

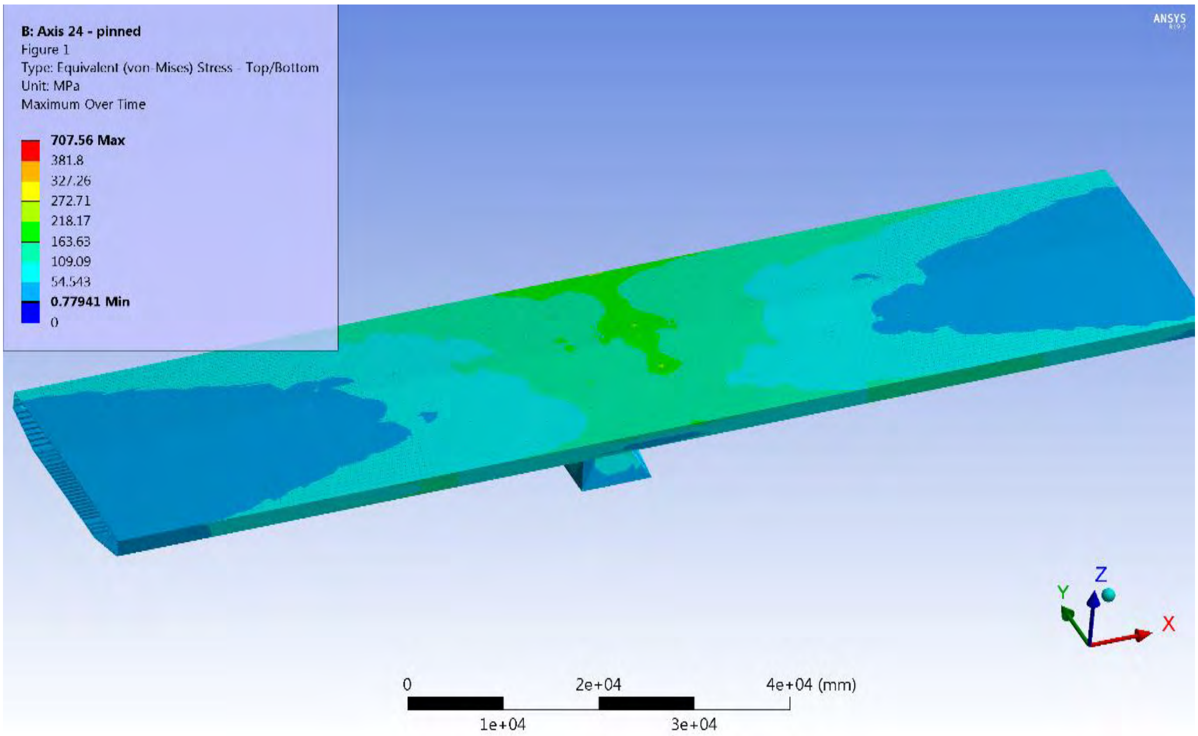

Figure 2-6 Axis 24, pinned, Von-Mises stress – top view

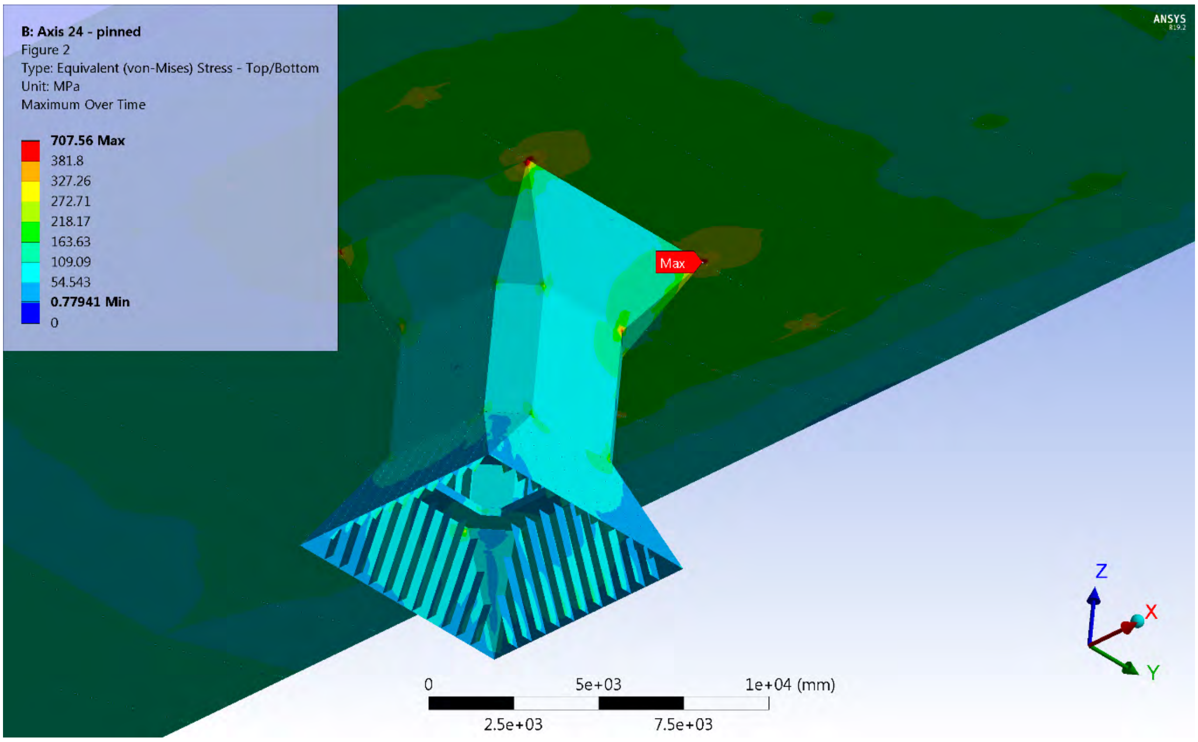

Figure 2-7 Axis 24, pinned, Von-Mises stress – bottom view

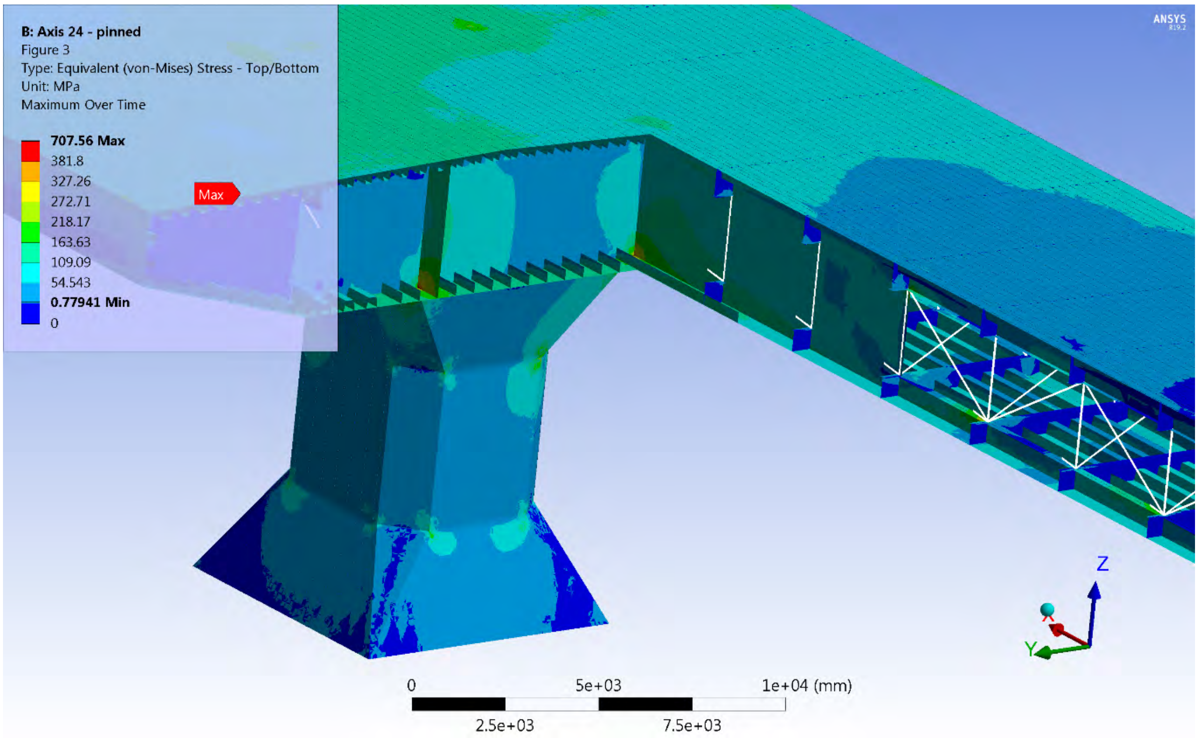

Figure 2-8 Axis 24, pinned, Von-Mises stress – cut bridge girder view

2.4.3 Forces from axis 24 – fixed bridge girder ends

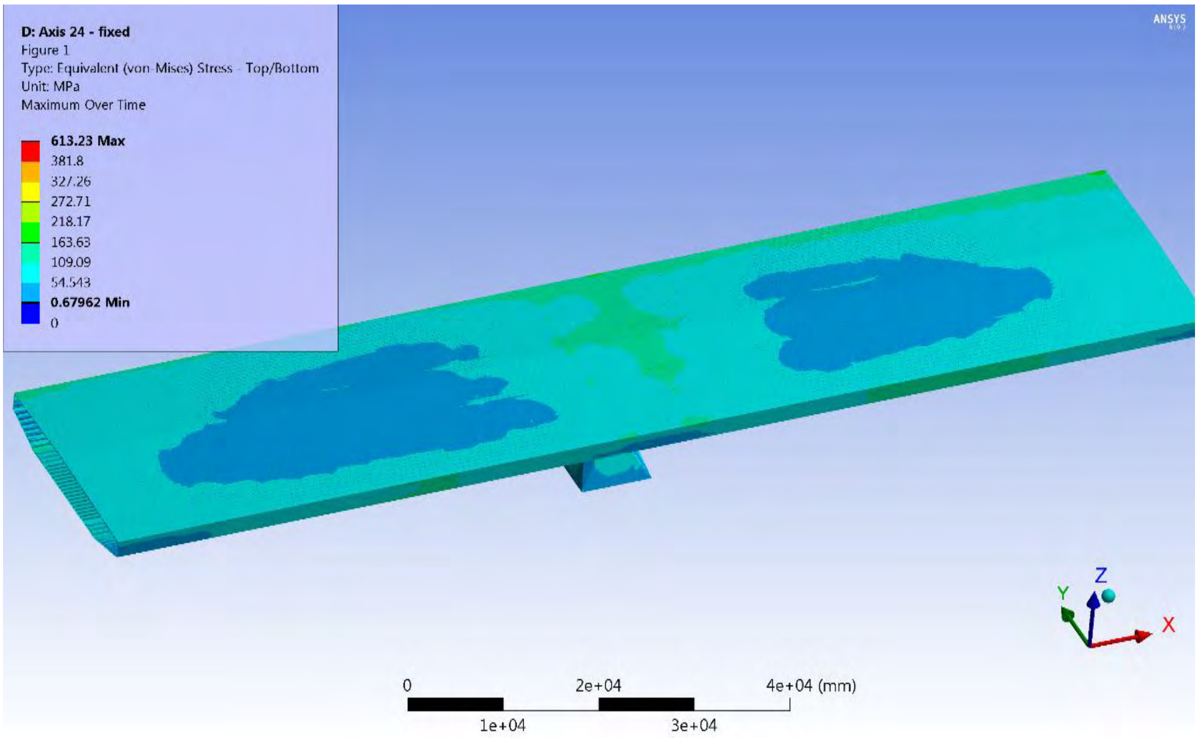

Figure 2-9 Axis 24, fixed, Von-Mises stress – top view

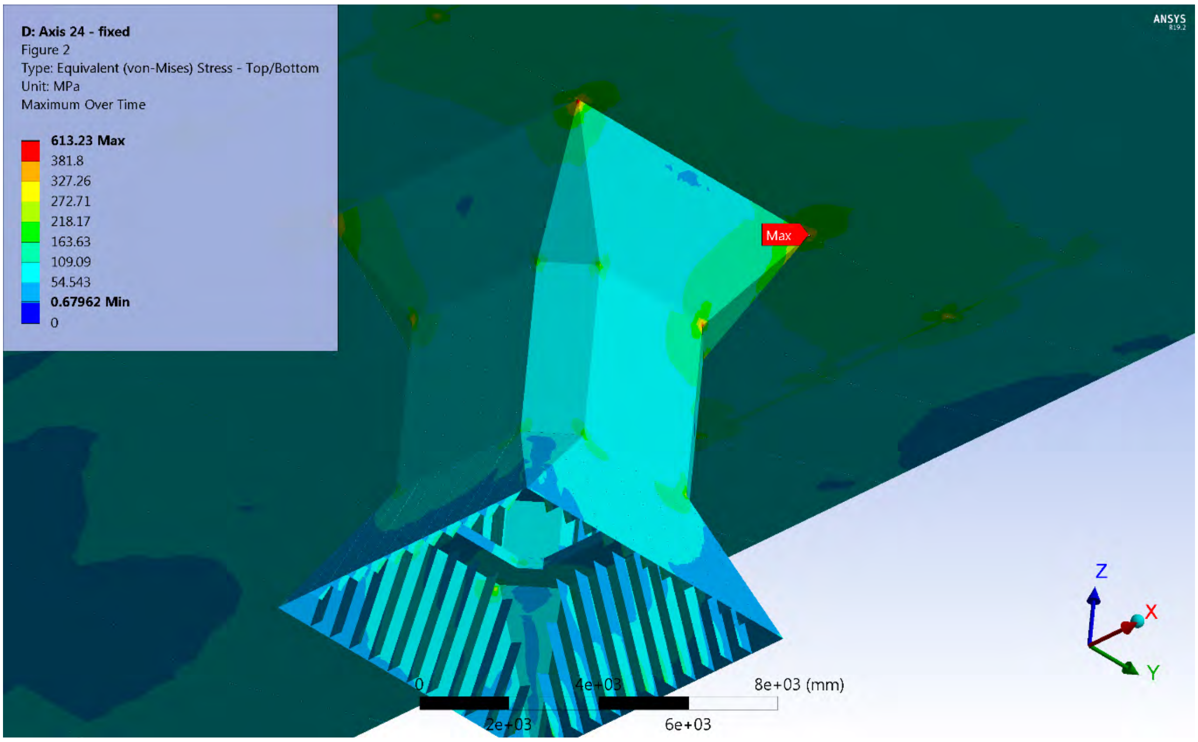

Figure 2-10 Axis 24, fixed, Von-Mises stress – bottom view

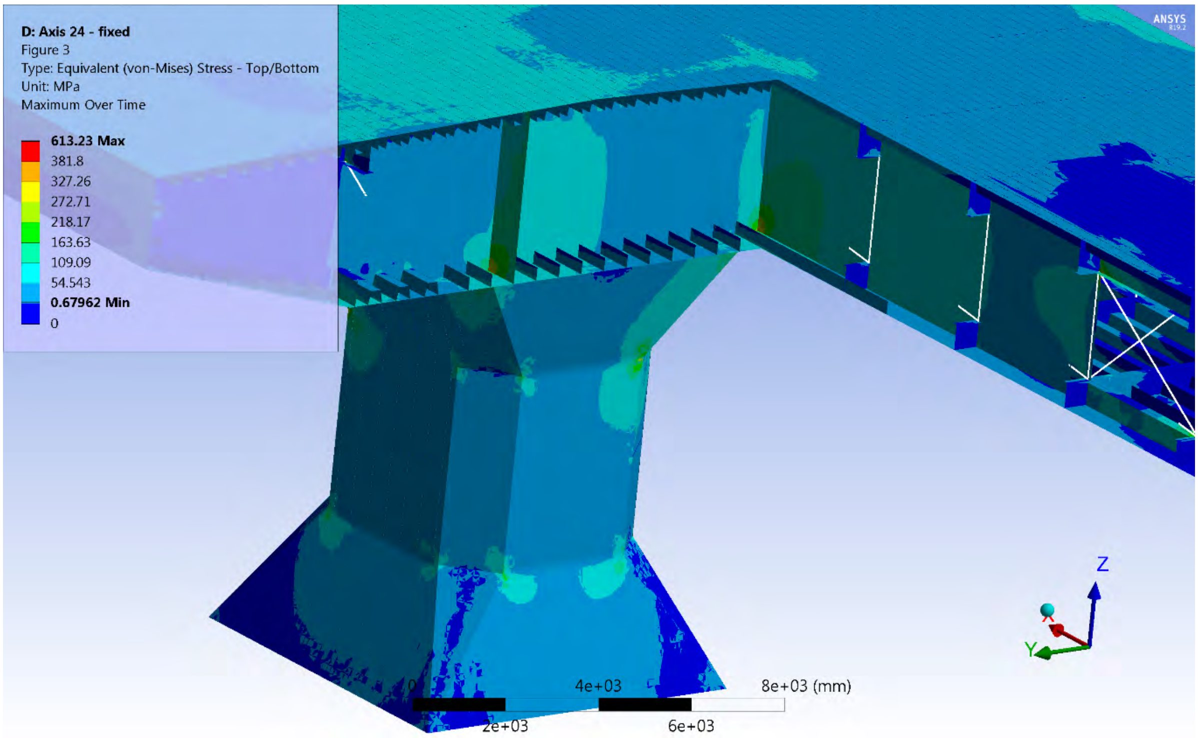

Figure 2-11 Axis 24, fixed, Von-Mises stress – cut bridge girder view

2.4.4 Forces from axis 32 - pinned bridge girder ends

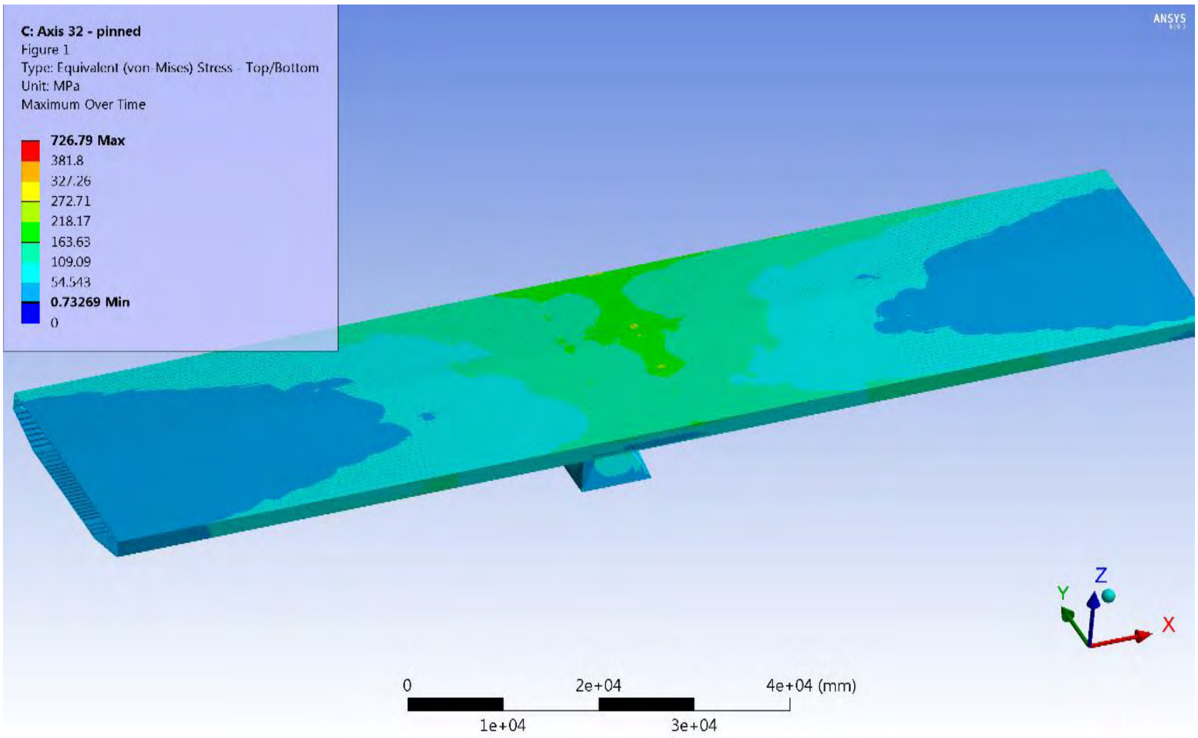

Figure 2-12 Axis 32, pinned, Von-Mises stress – top view

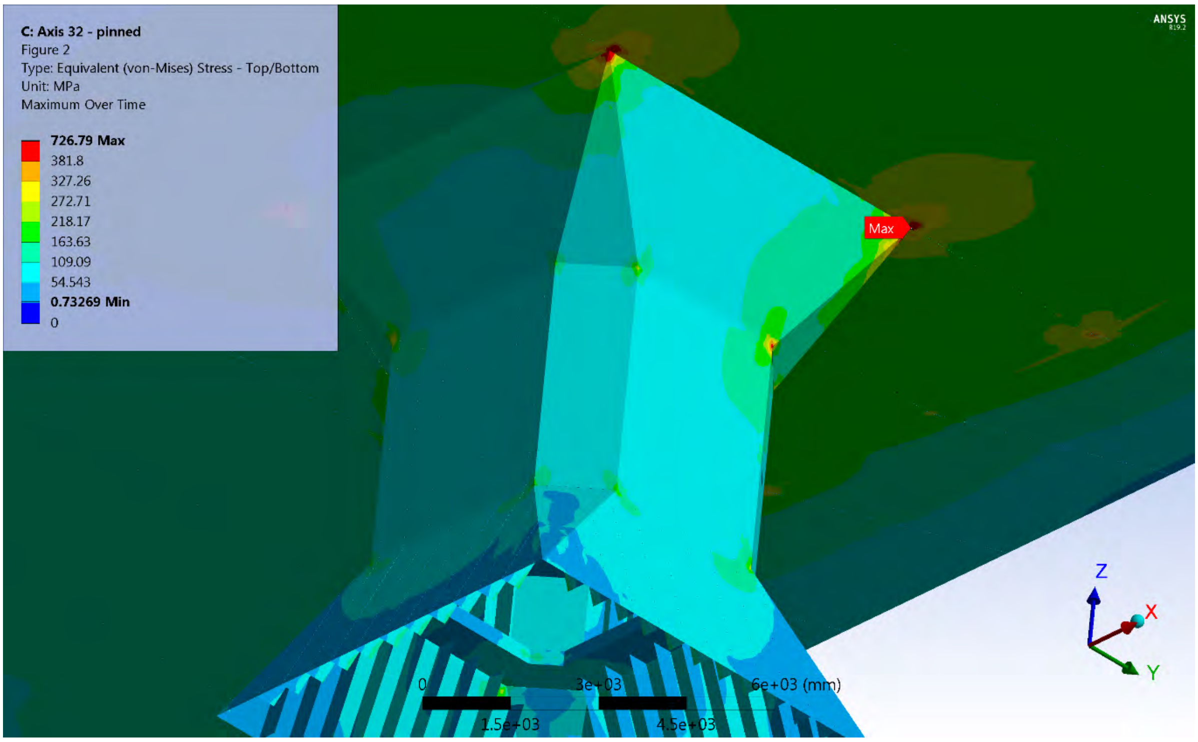

Figure 2-13 Axis 32, pinned, Von-Mises stress – bottom view

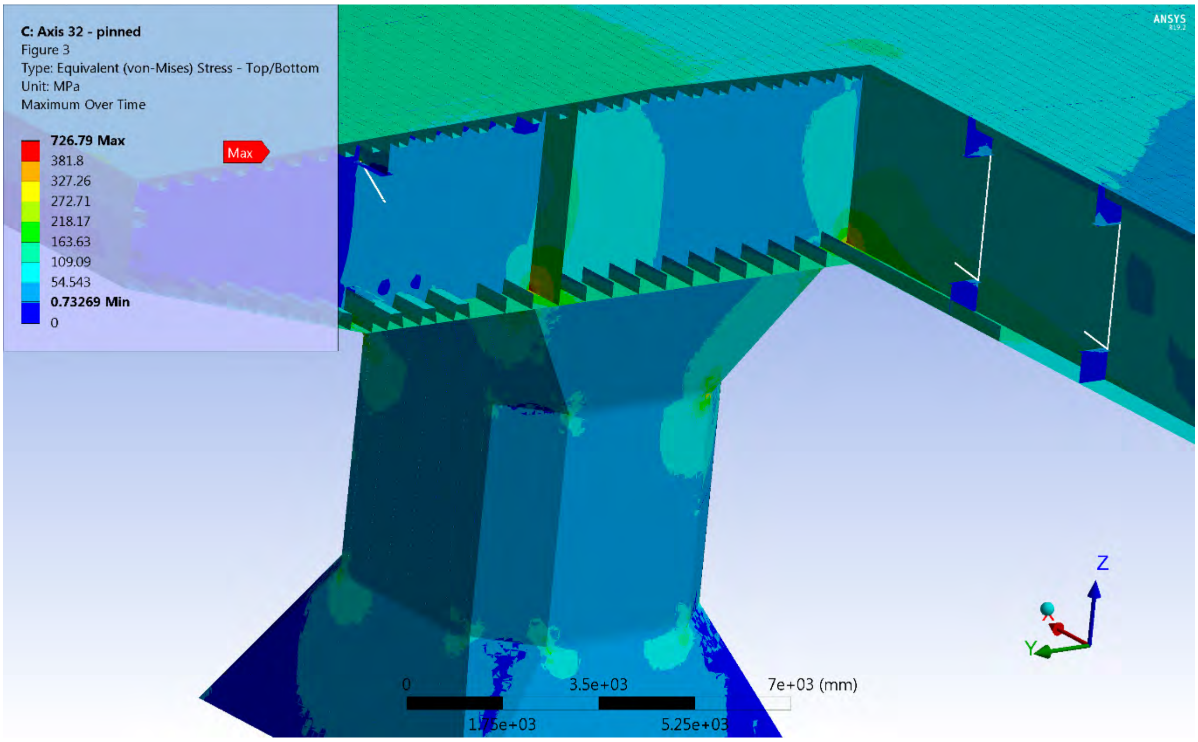

Figure 2-14 Axis 32, pinned, Von-Mises stress – cut bridge girder view

3 SCF factors

The purpose of this analysis is to find stress concentration factors (SCF) for the bridge girder near the column. The bottom plate is the focus for this analysis.

3.1 Element mesh refinement

The element mesh is refined at two areas to get better results. The refined mesh has a size of approximately 30 mm by 30 mm. Bridge girder bottom plate is 22 mm thick, and the column plate thickness is 25 mm. The element mesh size should be suitable for extracting stress to find SCF factors at relevant areas.

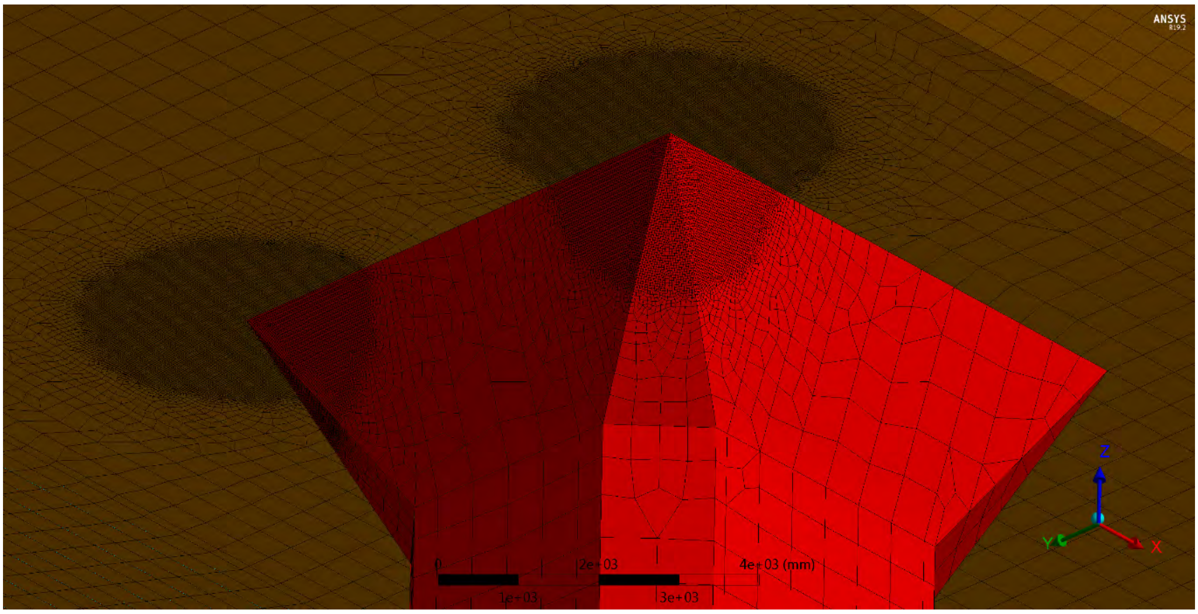

Figure 3-1 Mesh refinement

3.2 Loads

Table 3-1 Applied forces and boundary conditions - symmetric

	End 1	**End 2**	**Column bottom**
Axial	Fx = 100 MN	Fx = -100 MN	Fixed (resultant My = 0 MNm)
Weak axis bending	My = -1000 MNm	My = 1000 MNm	Fixed (resultant My = 0 MNm)
Strong axis bending	Mz = -1000 MNm	Mz = 1000 MNm	Fixed (resultant My = 0 MNm)

Table 3-2 Applied forces and boundary conditions - asymmetric

	End 1	**End 2**	**Column bottom**
Weak axis bending	My = -1000 MNm	My = 500 MNm	Fixed (resultant moment My = 500 MNm

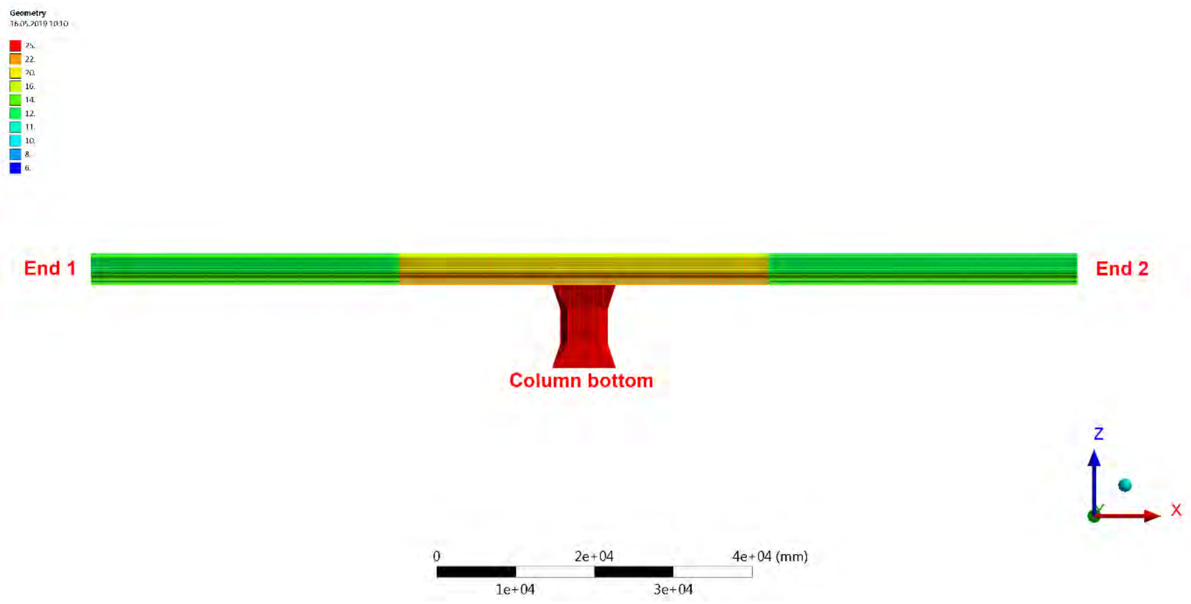

Figure 3-2 Geometry

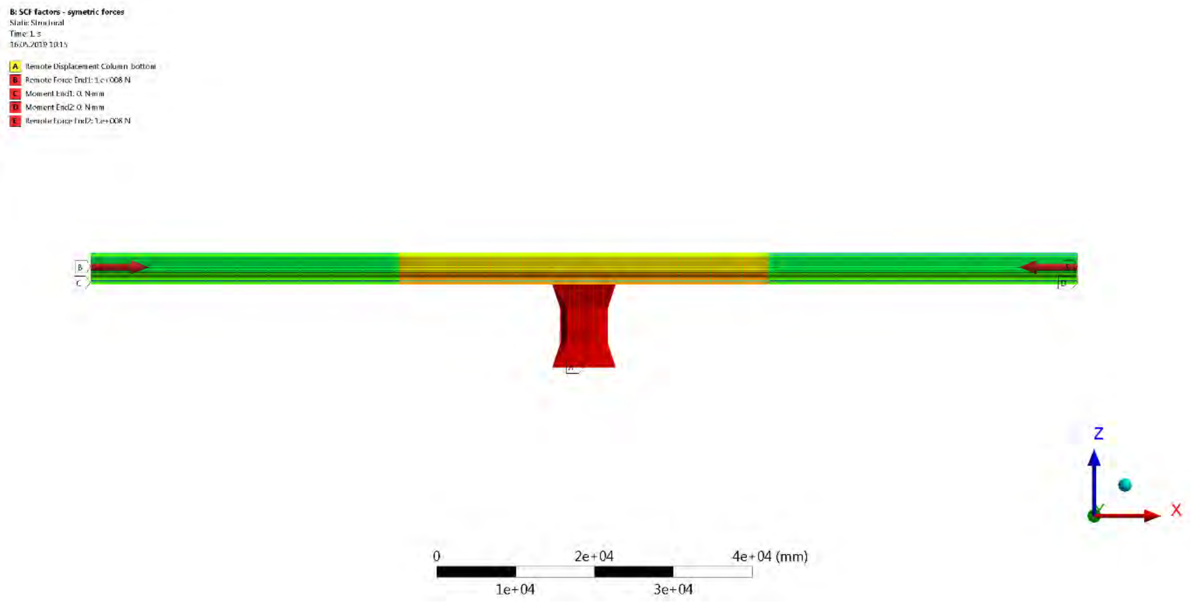

Figure 3-3 Normal force – symmetric

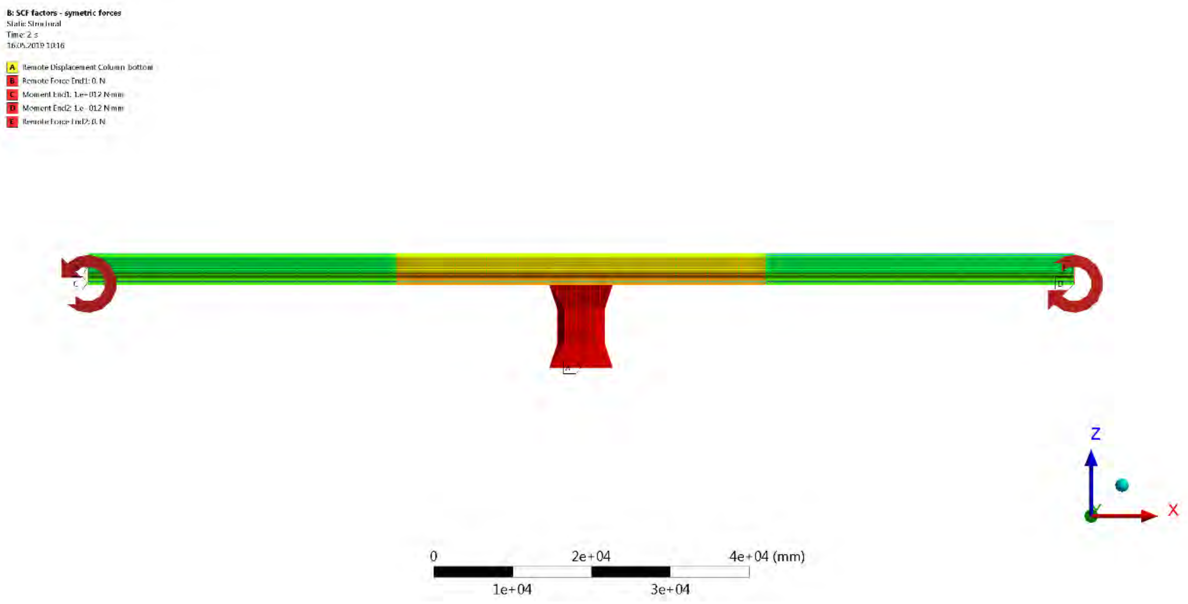

Figure 3-4 Weak axis bending moment – symmetric

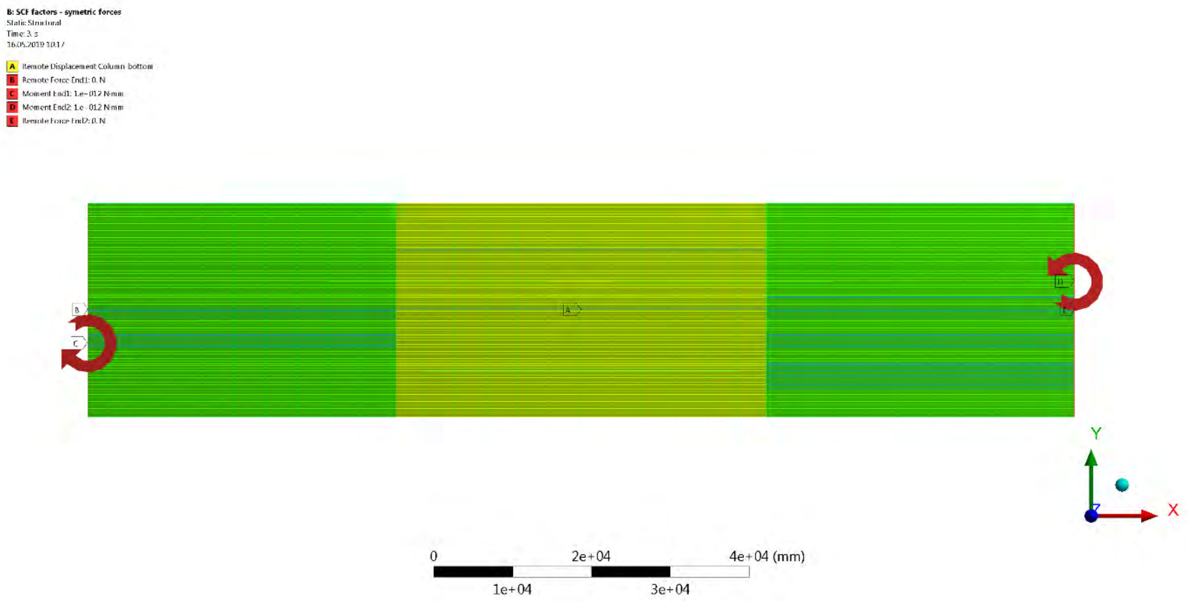

Figure 3-5 Strong axis bending moment - symmetric

3.3 Results

3.3.1 Axial force, symmetric

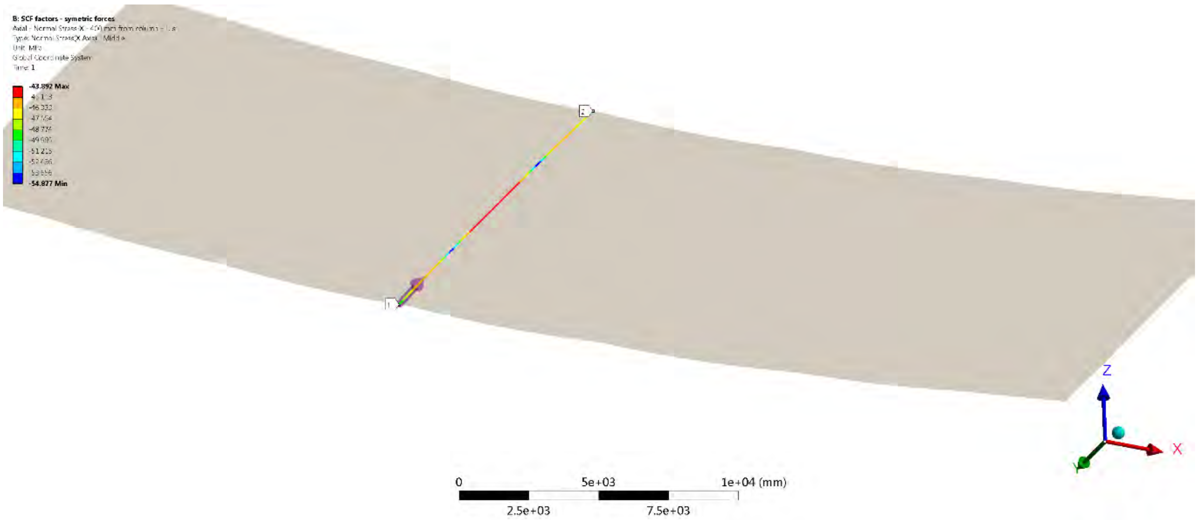

Figure 3-6 Normal stress along path – Axial force, symmetric

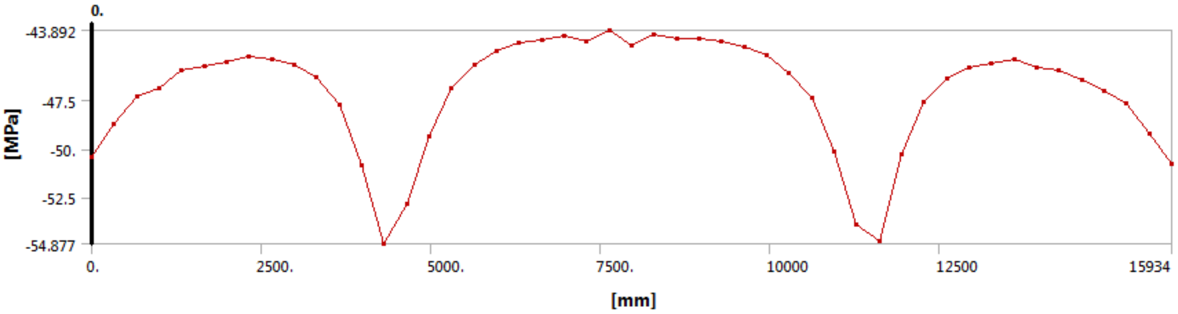

Figure 3-7 Normal stress along path, graph – Axial force, symmetric

$$SCF = \sigma_{hotspot} / \sigma_{nominal} = 54.9/43.9 = 1.25$$

3.3.2 Weak axis bending moment, symmetric

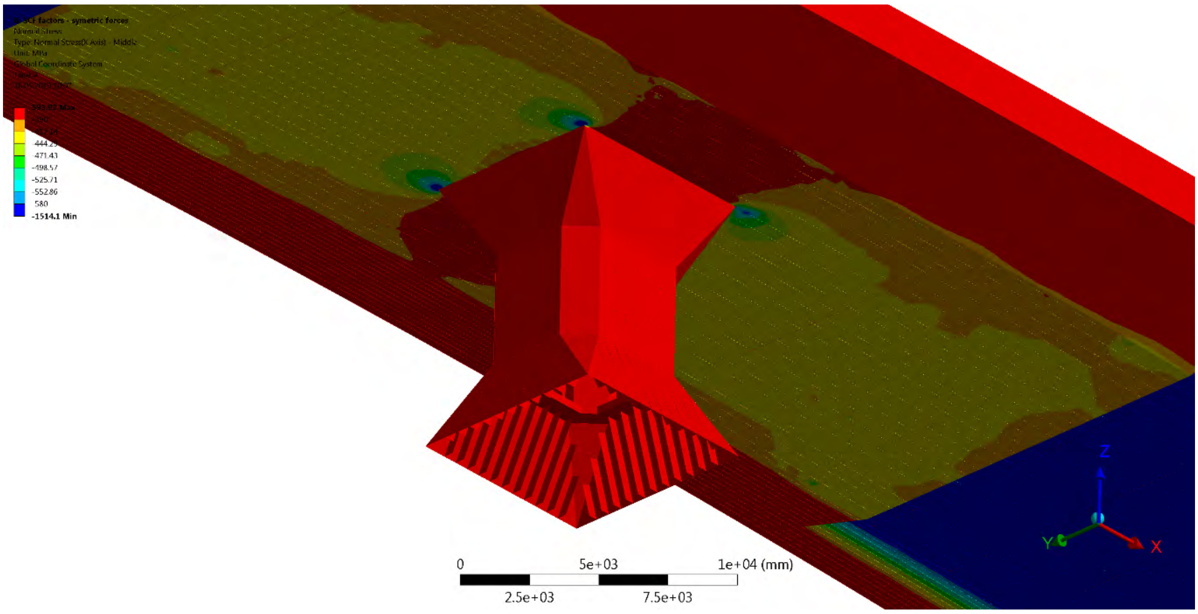

Figure 3-8 Normal stress – Weak axis bending, symmetric

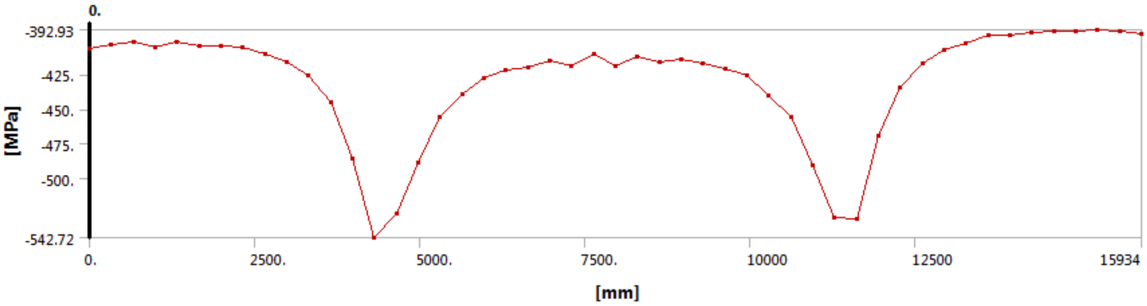

Figure 3-9 Normal stress along path, graph – Weak axis bending, symmetric

$$SCF = 542.7/392.9 = 1.38$$

3.3.3 Strong axis bending moment, symmetric

Section properties

S1 section properties:

Area moment of inertia:

$I_{y.S1} := 121.83\ m^4$

Neutral axis from UK bottom plate: $y_{0.S1} := -1.831\ m$

Distance from neutral axis:

$$\text{Point } \begin{bmatrix} 1 \\ 2 \end{bmatrix} \quad y_{S1} := \begin{bmatrix} 6.15 \\ -9.85 \end{bmatrix} m - y_{0.S1} = \begin{bmatrix} 7.981 \\ -8.019 \end{bmatrix} m$$

Calculated bending resistance (full section, no reductions):

$$W_{S1} := \frac{I_{y.S1}}{y_{S1}} = \begin{bmatrix} 15.265 \\ -15.193 \end{bmatrix} m^3$$

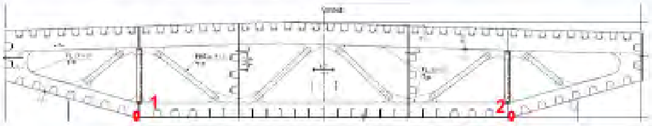

Calculated stress at investigated section - strong axis bending moment

Applied moment at beam end: $M_z := -1000\ MN \cdot m$

Calculated stress at point 1, 2 and 3:

$$\text{Point } \begin{bmatrix} 1 \\ 2 \end{bmatrix} \quad \sigma := \frac{M_z}{W_{S1}} = \begin{bmatrix} -65.509 \\ 65.821 \end{bmatrix} MPa$$

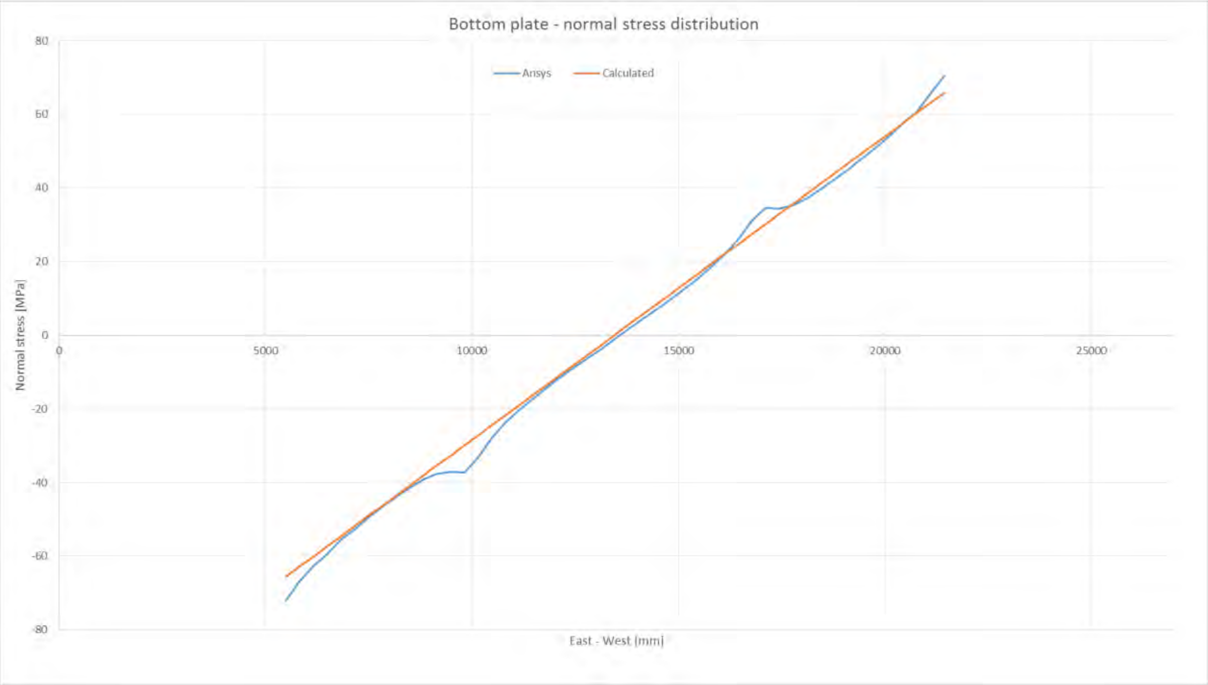

Figure 3-10 Normal stress along path, graph - Strong axis bending, symmetric

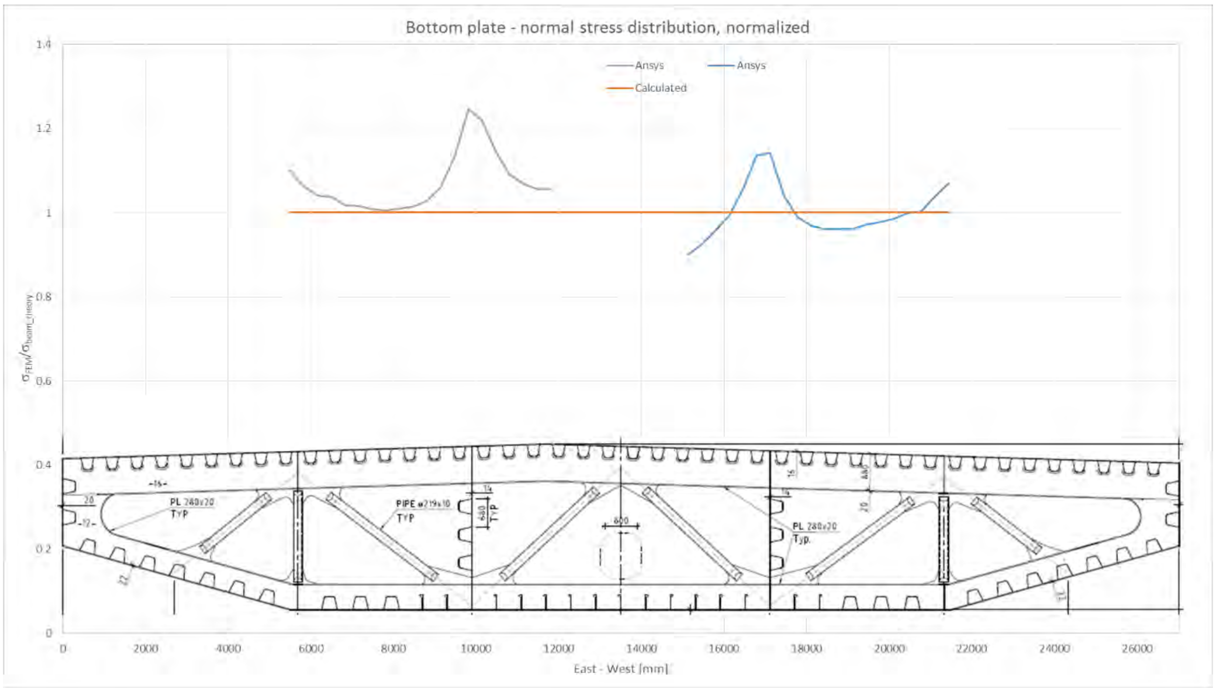

Figure 3-11 Normal stress along path, normalized - Strong axis bending, symmetric

$$SCF = 1.25$$

3.3.4 Weak axis bending moment, asymetric

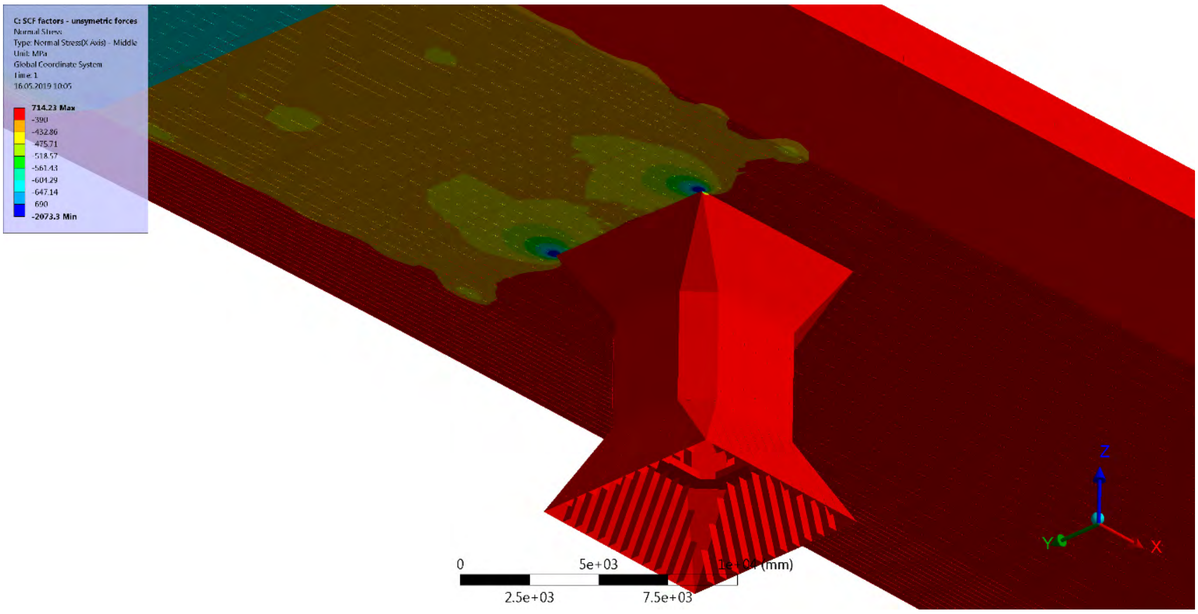

Figure 3-12 Normal stress – Weak axis bending, asymmetric

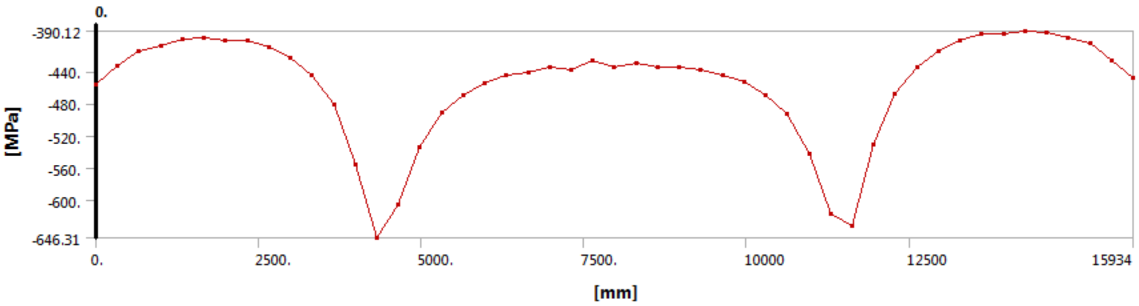

Figure 3-13 Normal stress along path, graph – Weak axis bending, asymmetric

$$SCF = 646.3/390.1 = 1.66$$

3.4 Summary of SCF factors found

Table 3-3 SCF factors

	Applied force		
Boundary condition	**N**	**M_weak**	**M_strong**
Symmetric End 1: 100% End 2: 100%	1.25	1.38	1.25
Asymmetric End 1: 100% End 2: 50% Column bottom: 50%		1.66	

4 Shear lag

The purpose of this analysis is to show how shear lag affects the bridge girder and to document that the shear lag calculated with NS-EN 1993-1-5 [2] is conservative. The part checked here is the top plate of the “above column” section. For weak axis bending, the calculated shear lag factor for SLS and FLS is 0.785. Therefore, the weak axis area moment of inertia including shear lag is 78.5% of the full area moment of inertia.

Hand calculated stress based on beam theory is compared to stress found in the FEM.

4.1 Geometry

For this analysis, the column is not included.

4.2 Boundary conditions

The bridge girder is fixed at a transverse vertical section at the center of the bridge girder. Effectively creating two cantilevers. The element model could have been halved, but the computational time is so short (1-2 min) that this optimization has not been done.

Table 4-1 Boundary conditions

	Translation			Rotation		
	X	Y	Z	X	Y	Z
End 1	Free	Free	Free	Free	Free	Fixed
End 2	Free	Free	Free	Free	Free	Fixed
Girder center	Fixed	Fixed	Fixed	Fixed	Fixed	Fixed

4.3 Loads

Two loads have been checked:

- Point load at the end of the bridge girder. P = 1000 kN. See Figure 4-1
- Distributed load over the length of the bridge girder. Q = 133.4 kN/m^2 (equivalent to steel self weight in the FEM). See Figure 4-2

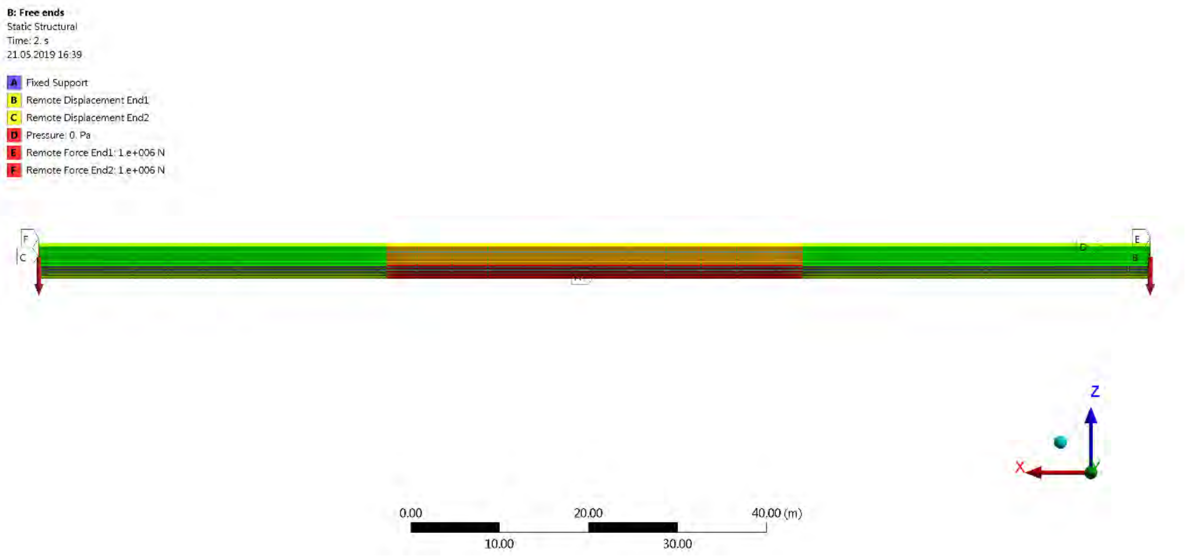

B: Free ends
Static Structural
Time: 2. s
21.05.2019 16:39

A Fixed Support
B Remote Displacement End1
C Remote Displacement End2
D Pressure: 0. Pa
E Remote Force End1: 1.e+006 N
F Remote Force End2: 1.e+006 N

Figure 4-1 Point load

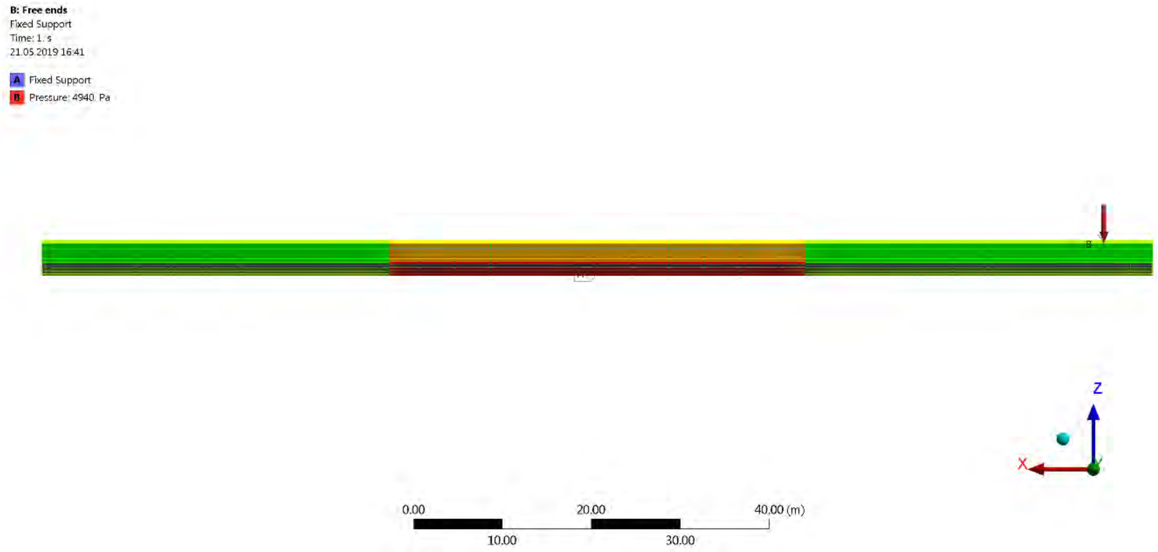

B: Free ends
Fixed Support
Time: 1. s
21.05.2019 16:41

A Fixed Support
B Pressure: 4940. Pa

Figure 4-2 Distributed load

4.4 Hand calculated stress

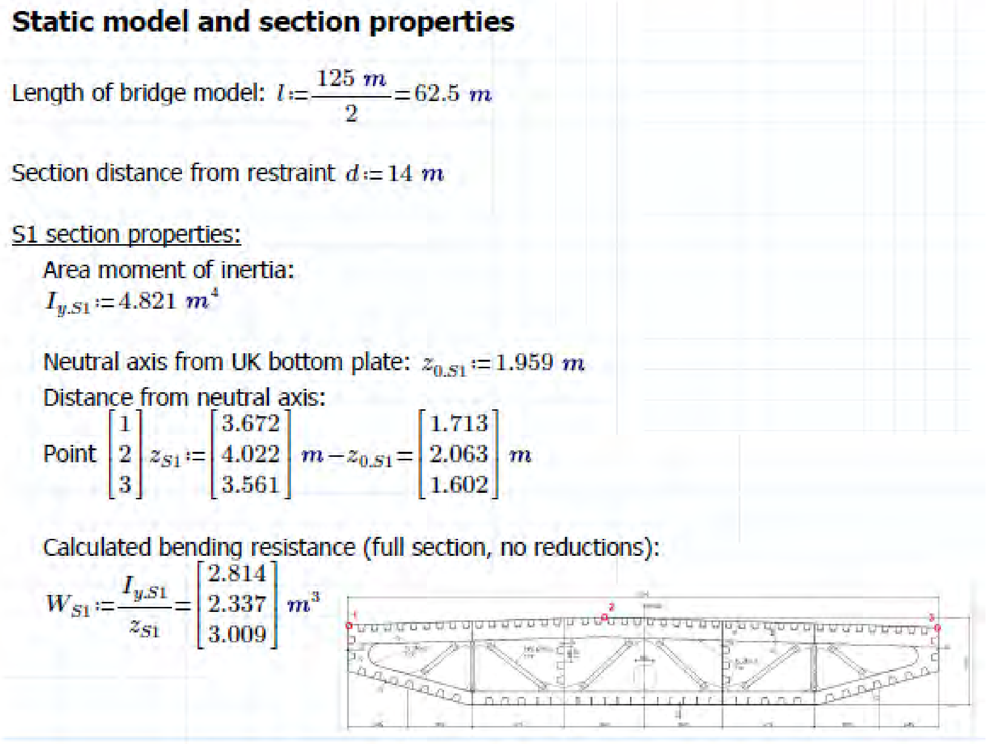

Static model and section properties

Length of bridge model: $l := \frac{125\ m}{2} = 62.5\ m$

Section distance from restraint $d := 14\ m$

S1 section properties:

Area moment of inertia:
$I_{y.S1} := 4.821\ m^4$

Neutral axis from UK bottom plate: $z_{0.S1} := 1.959\ m$

Distance from neutral axis:

Point $\begin{bmatrix} 1 \\ 2 \\ 3 \end{bmatrix}$ $z_{S1} := \begin{bmatrix} 3.672 \\ 4.022 \\ 3.561 \end{bmatrix} m - z_{0.S1} = \begin{bmatrix} 1.713 \\ 2.063 \\ 1.602 \end{bmatrix} m$

Calculated bending resistance (full section, no reductions):

$W_{S1} := \frac{I_{y.S1}}{z_{S1}} = \begin{bmatrix} 2.814 \\ 2.337 \\ 3.009 \end{bmatrix} m^3$

Calculated stress at investigated section - point load - cantilever

Point load: $P := 1000\ kN$

Section distance from restraint $d := 14\ m$

Moment at restraint: $M_p := P \cdot l = 62500\ kN \cdot m$

Moment at investigated section: $M_{p.section} := M_p \dfrac{(l-d)}{l} = 48500\ kN \cdot m$

Calculated stress at point 1, 2 and 3:

$$\text{Point} \begin{bmatrix} 1 \\ 2 \\ 3 \end{bmatrix} \sigma := \frac{M_{p.section}}{W_{S1}} = \begin{bmatrix} 17.233 \\ 20.754 \\ 16.116 \end{bmatrix} MPa$$

Calculated stress at investigated section - Distributed load - cantilever

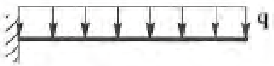

Distributed load: $q := 133.4\ \dfrac{kN}{m}$

Section distance from restraint $d := 14\ m$

Moment at restraint: $M_q := \dfrac{q \cdot l^2}{2} = 260547\ kN \cdot m$

Moment at investigated section: $M_{q.section} := \dfrac{q \cdot (l-d)^2}{2} = 156895\ kN \cdot m$

Calculated stress at point 1, 2 and 3:

$$\text{Point} \begin{bmatrix} 1 \\ 2 \\ 3 \end{bmatrix} \sigma := \frac{M_{q.section}}{W_{S1}} = \begin{bmatrix} 55.748 \\ 67.138 \\ 52.136 \end{bmatrix} MPa$$

4.6 Paths for reading stress from FEM

Normal stress for the element middle in x-direction has been extracted along paths at set distances from the fixation. An example of a path 14 m from the fixation is shown in Figure 4-3.

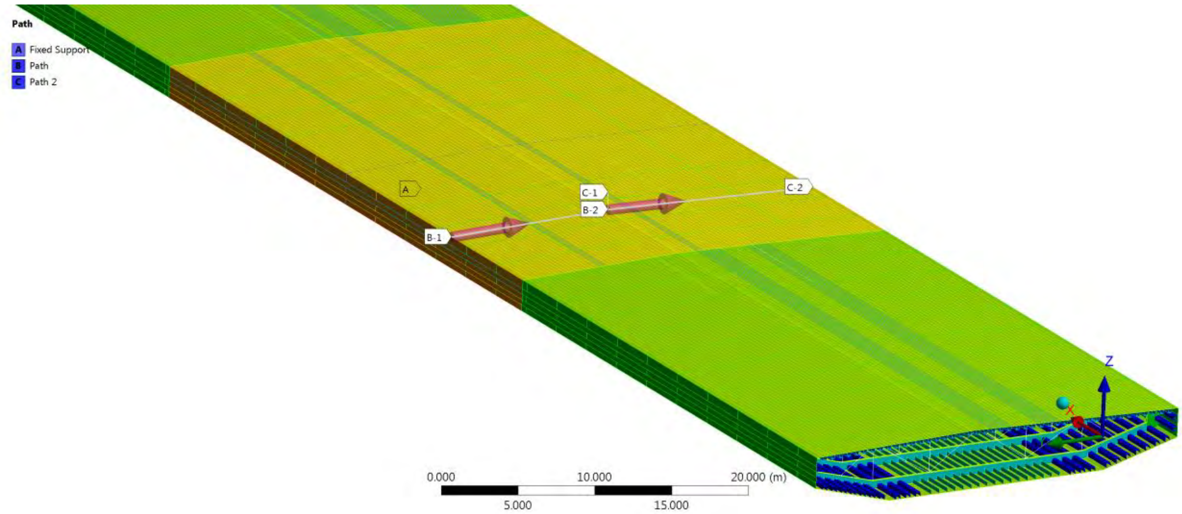

Figure 4-3 Path 14 m from fixation

4.7 Results

An example plot of normal stress in x-direction is shown in Figure 4-4. This is for the load case with point load at the end of the cantilever.

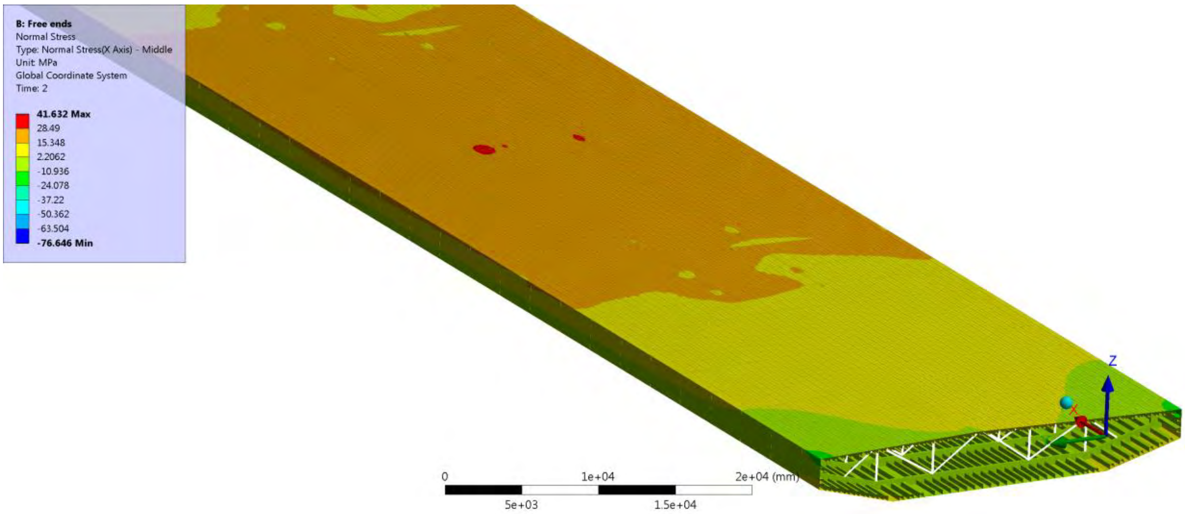

Figure 4-4 Example of normal stress

To get a better understanding, the stress along the path is extracted and plotted in Figure 4-5 along with the calculated stress based on beam theory.

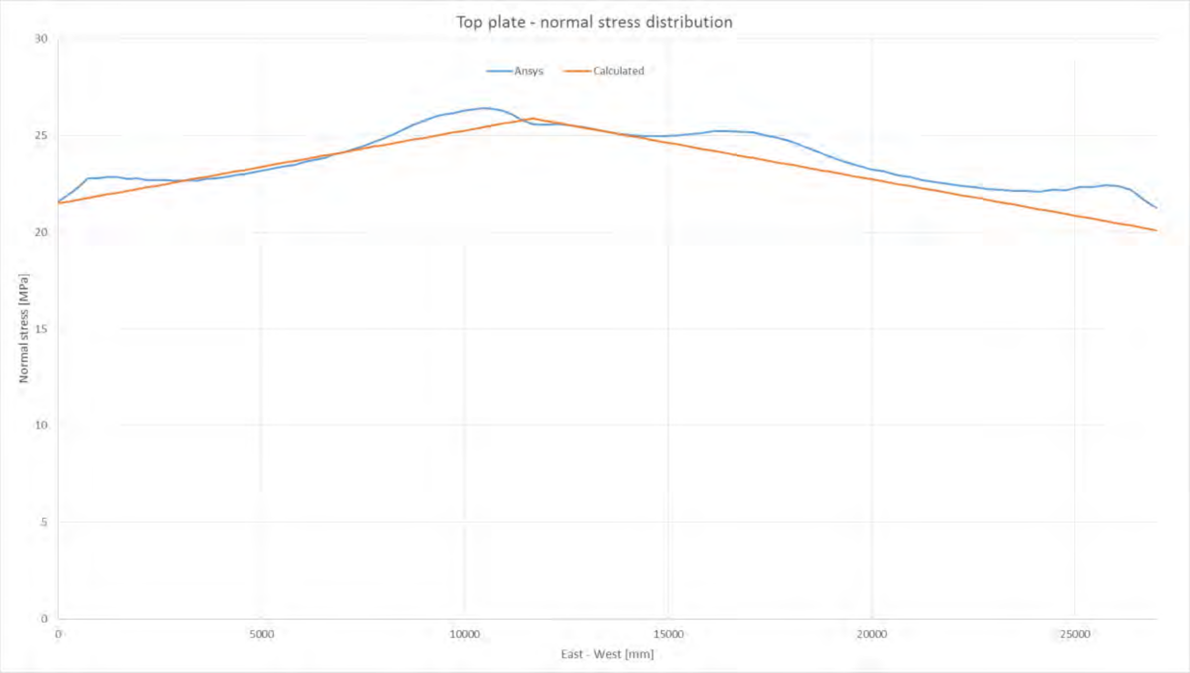

Figure 4-5 Stress along path, 2 m from the fixation.

Due to the geometric shape of the top plate, normalizing the stress gives an even better understanding of how the stress in the FEM varies from beam theory. See Figure 4-6 for the normalized plot that corresponds to the stress plotted in Figure 4-5.

$$\sigma_{Norm} = \frac{\sigma_{FEM}}{\sigma_{Beam\_theory}}$$

4.7.1 Point load

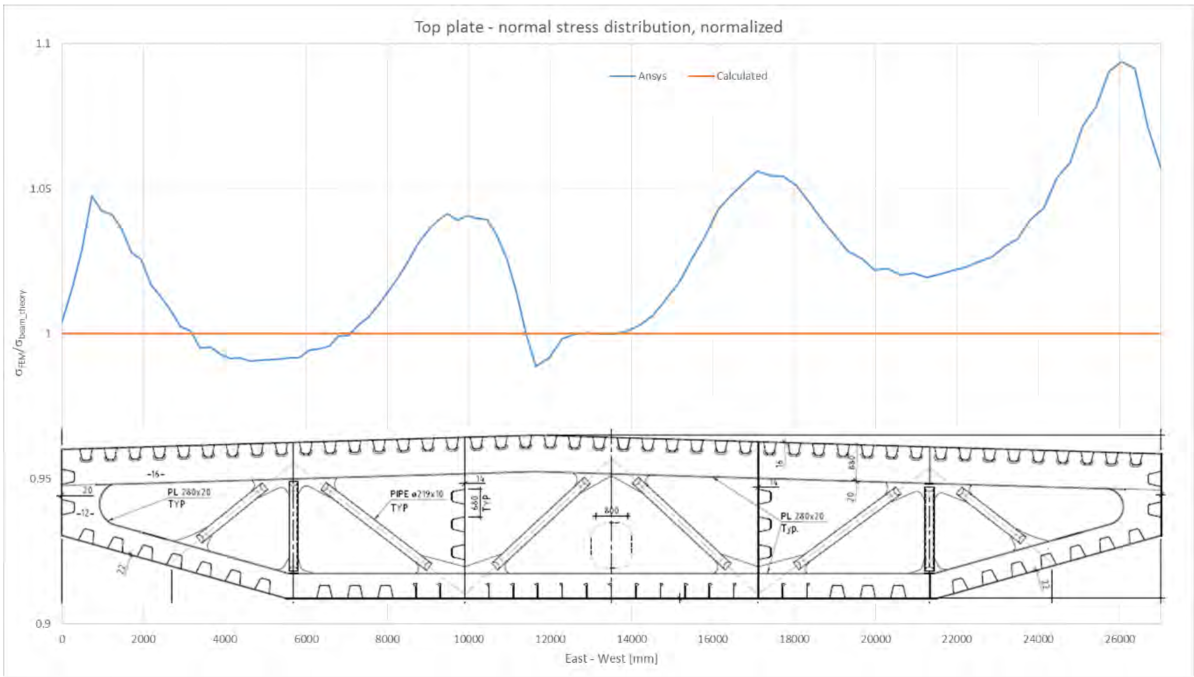

Figure 4-6 Normalized stress, 2 m from fixation

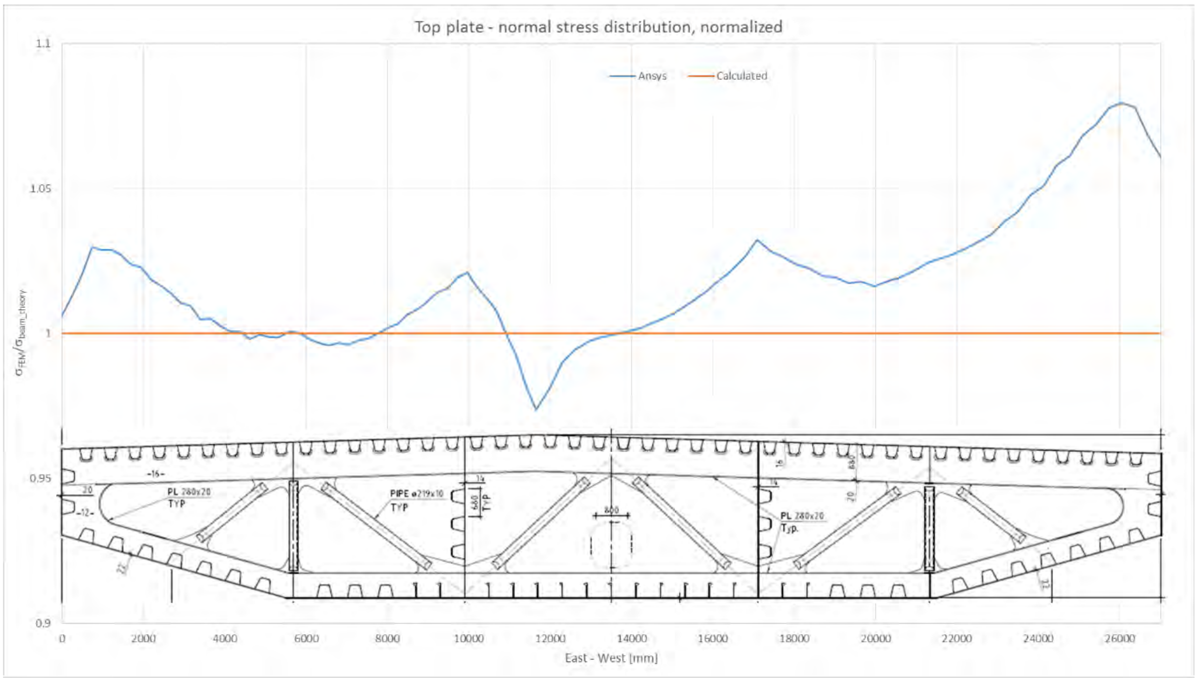

Figure 4-7 Normalized stress, 6 m from fixation

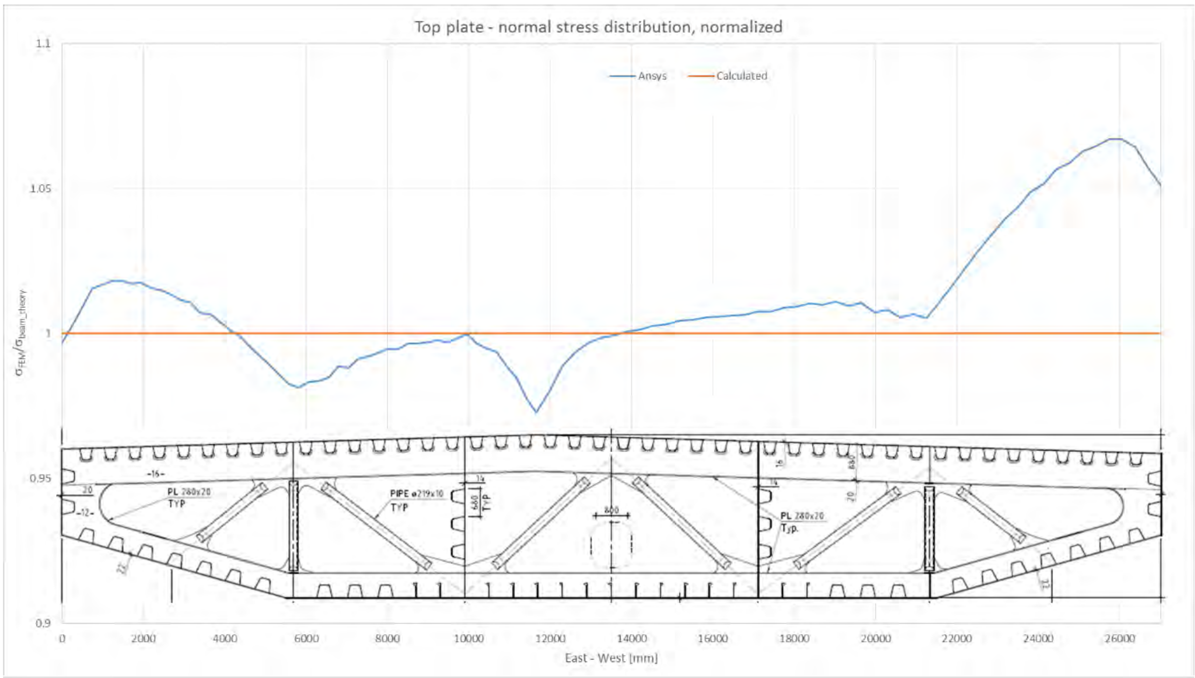

Figure 4-8 Normalized stress, 10 m from fixation

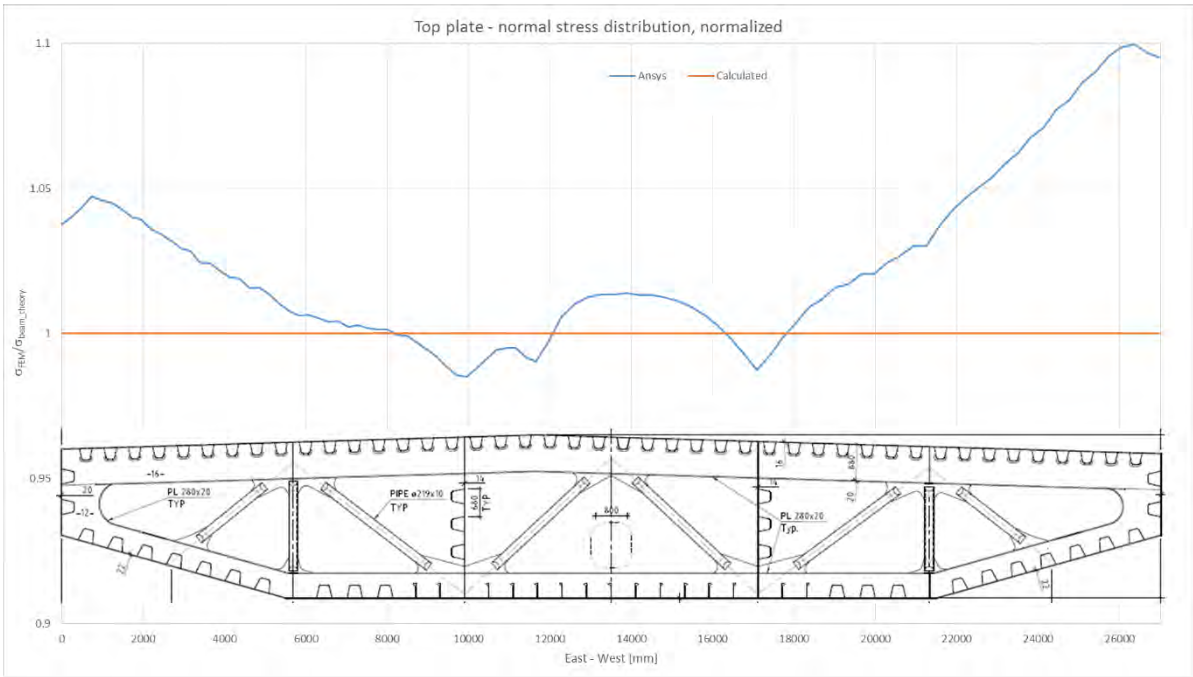

Figure 4-9 Normalized stress, 14 m from fixation

Maximum increase in stress is observed 2 m from the fixation. The stress is 10% higher than when calculated with beam theory. This corresponds to a shear lag factor of 0.91.

$$\sigma_{x_{full}} = \frac{M_y * y}{I_{z_{full}}}$$

$$\sigma_{x_{shear\_lag}} = \frac{M_y * y}{\beta * I_{z_{full}}}$$

$$\frac{\sigma_{x_{shear\_lag}}}{\sigma_{x_{full}}} = 1.1$$

$$\beta = \frac{1}{1.1} = 0.91$$

4.7.2 Distributed load

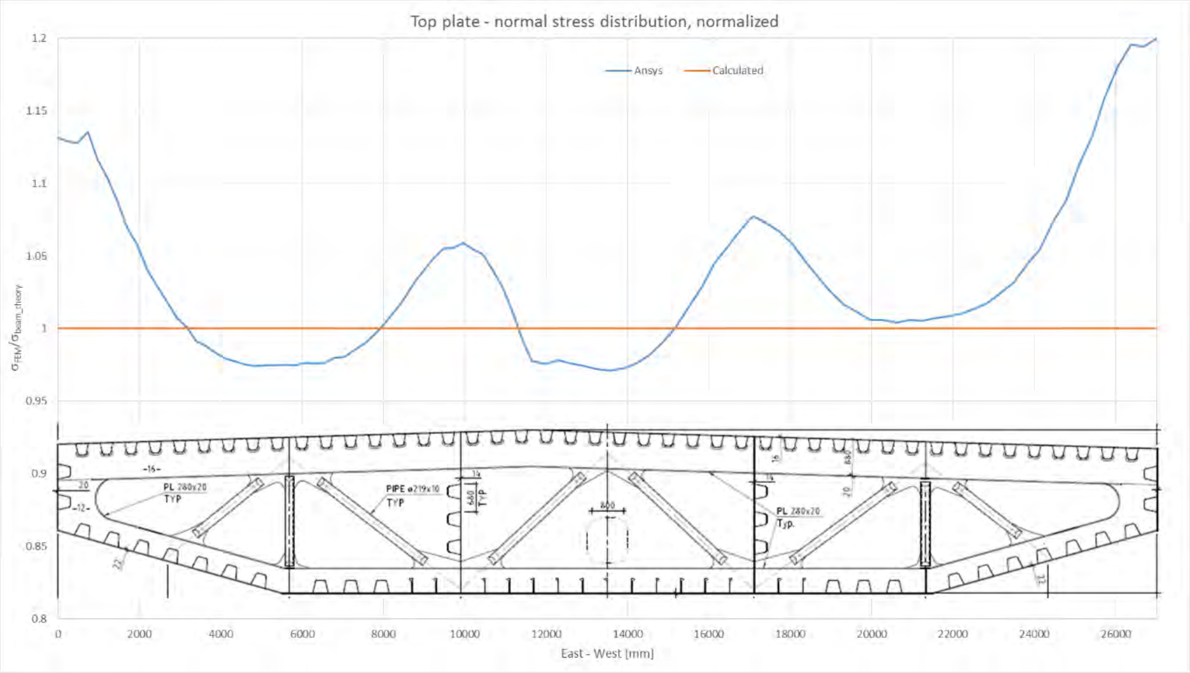

Figure 4-10 Normalized stress, 2 m from fixation

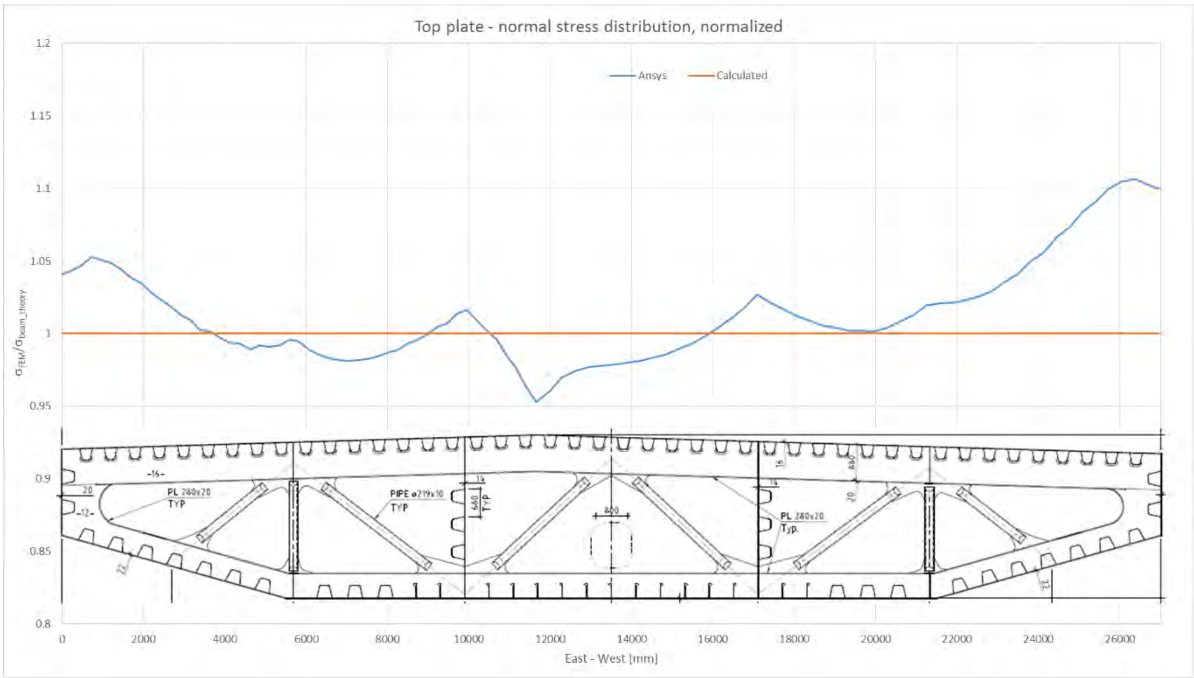

Figure 4-11 Normalized stress, 6 m from fixation

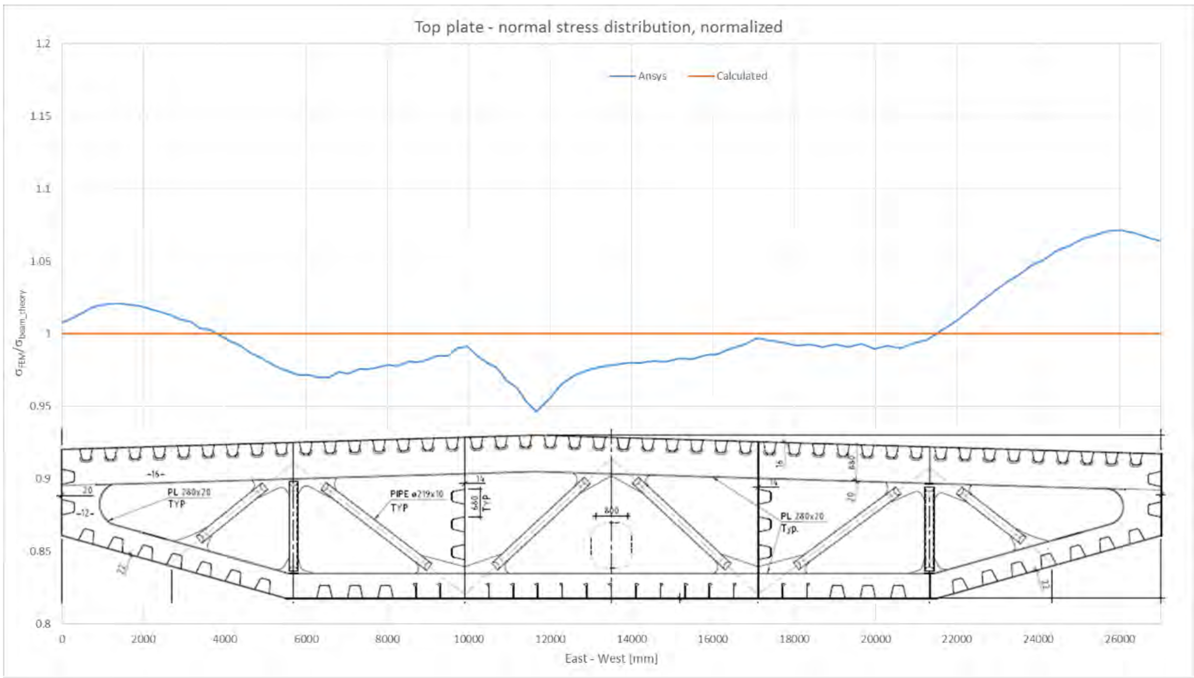

Figure 4-12 Normalized stress, 10 m from fixation

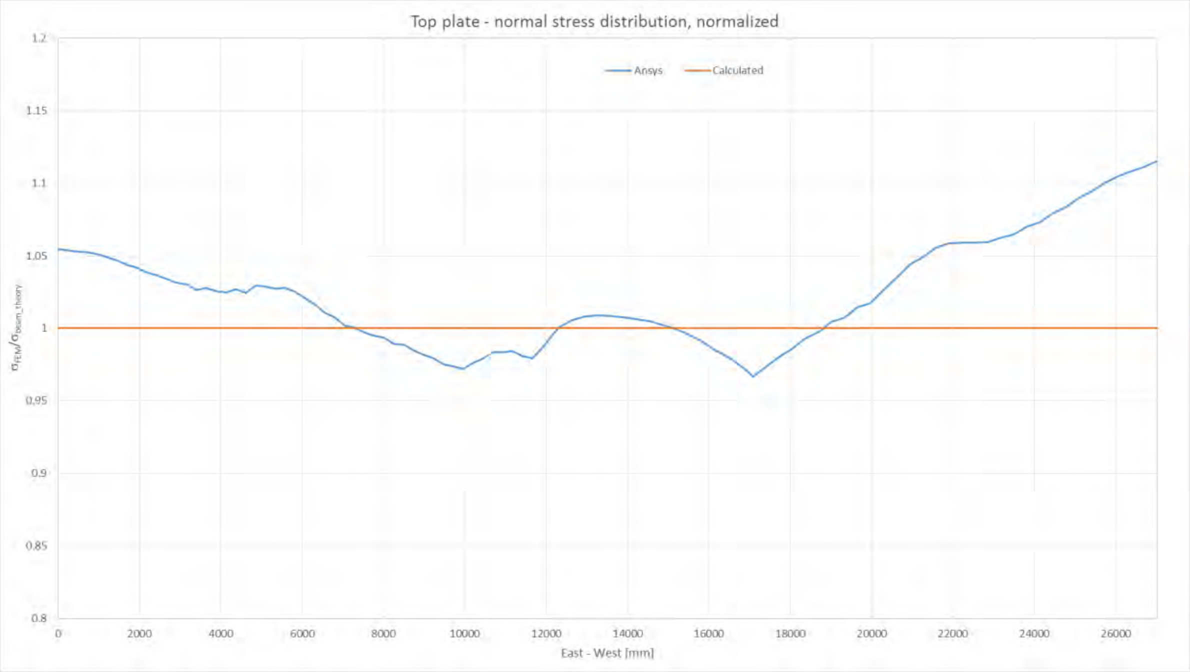

Figure 4-13 Normalized stress, 14 m from fixation

Maximum increase in stress is 2 m from the fixation. The stress is 20% higher than when calculated with beam theory. This corresponds to a shear lag factor of 0.83.

5 Transverse frames

The purpose of this model is to show how the transversal frames carry forces, and to demonstrate that the boundary conditions applied it the Staad model documented in 10205546-13-NOT-083 Transverse Trusses in Bridge Girder [3] will yield highly conservative forces and utilizations. The assumption in the Staad model is that the bridge girder webs carry the shear forces alone. This FEM show that the trapezoidal stiffeners carry a significant amount of the shear forces and distributes local forces to adjacent transverse frames. In addition, that the top plate with the trapezoidal stiffeners and transverse frames is very effective at distributing local forces to a large area.

5.1 Geometry

Two different geometrical models have been run. One that is identical to the one presented in section 1, and one where all longitudinal trapezoidal- and bulb stiffeners are removed.

5.2 Boundary conditions

Boundary conditions according to Table 5-1.

Table 5-1 Boundary conditions

	Translation			Rotation		
	X	Y	Z	X	Y	Z
End 1	Free	Free	Free	Free	Free	Free
End 2	Free	Free	Free	Free	Free	Free
Column bottom	Fixed	Fixed	Fixed	Fixed	Fixed	Fixed

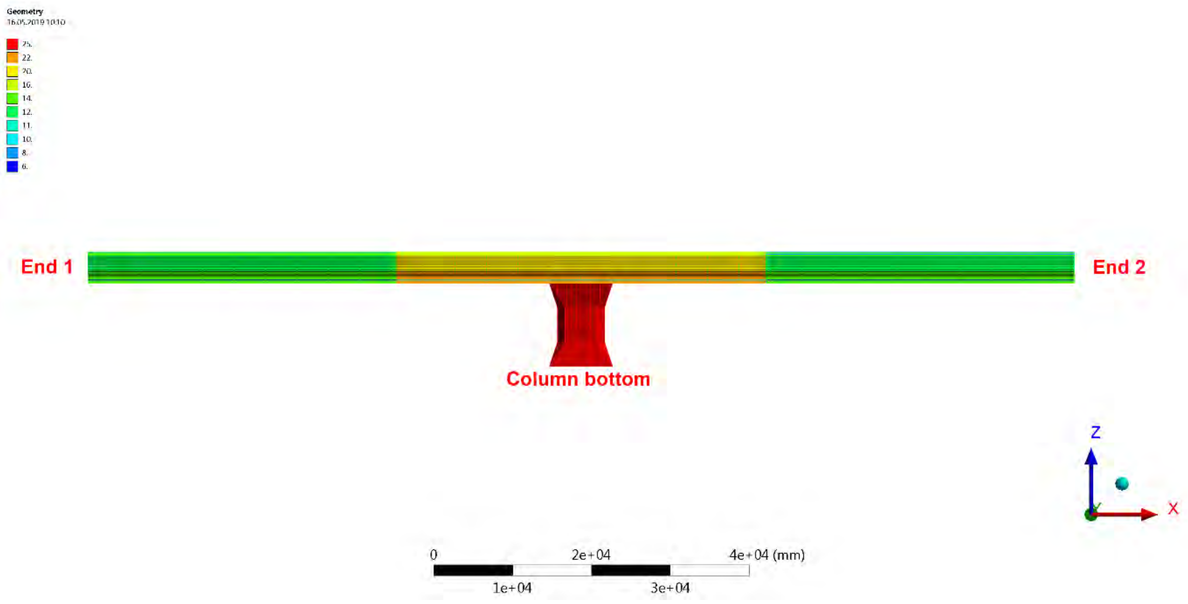

Figure 5-1 Boundary conditions

5.3 Loads

Traffic and dead loads have been applied to the bridge girder. A ULS2 combination with dominating traffic load has been chosen. Traffic loads are taken from NS-EN 1991-2 Table 4.2 [4]. 1 year environmental loads are not included. The purpose here is to investigate the load transfer between transverse frames and how the longitudinal trapezoidal stiffeners contribute.

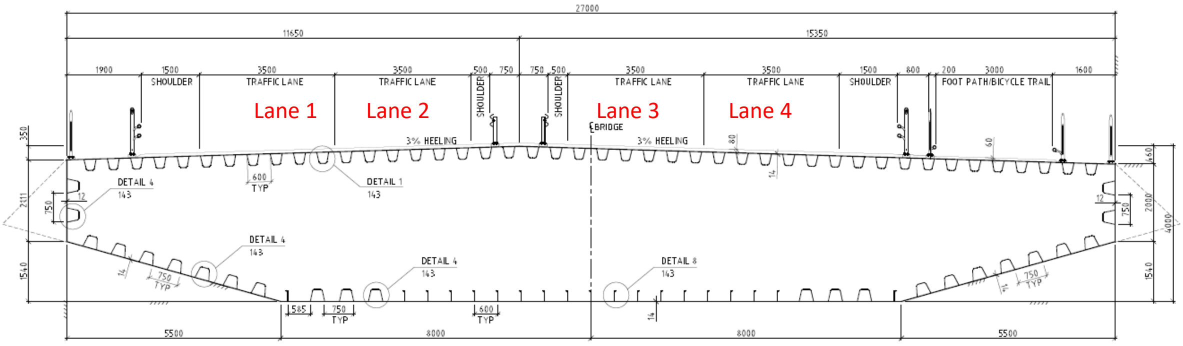

Table 5-2 Applied forces in the finite element model

Load	Description	Load	Target resultant Fz [kN]	Ansys resultant in percentage of target
1	Self-weight steel	a_z = 9.81 m/s^2	17 799.1	95.7 %
2	Self-weight asphalt, railing etc.	p = 1.817 kN/m^2	6 129.2	100.1 %
3	Traffic other areas	p = 2.5 kN/m^2	8 437.5	100.0 %
4	Traffic Lane 1	q = 9.0 kN/m^2 * 0.6	1 268.8	100.1 %
5	Traffic Lane 2	q = 9.0 kN/m^2 * 0.6	1 268.8	100.0 %
6	Traffic Lane 3	q = 9.0 kN/m^2 * 0.6	1 268.8	100.0 %
7	Traffic Lane 4	q = 9.0 kN/m^2 * 0.6	1 268.8	100.0 %
8	Axle loads Lane 1	Q = 2 * 1.0 kN (unit load)	2.0	100.0 %
9	Axle loads Lane 2	Q = 2 * 1.0 kN (unit load)	2.0	100.0 %
10	Axle loads Lane 3	Q = 2 * 1.0 kN (unit load)	2.0	100.0 %
11	Axle loads Lane 4	Q = 2 * 1.0 kN (unit load)	2.0	100.0 %

Traffic in lanes 1-4 (load 4-7) is added to traffic in other lanes (load 3).
The addition is: (9 kN/m^2 * 0.6) – 2.5 kN/m^2 = 2.9 kN/m^2

Axle loads are applied 48 m from the center of the column. This has been done to minimize the effect of the column and boundary conditions applied at the bridge girder end. The axle loads are applied as shown on Figure 5-2 with one axle 600 mm on one side of the transverse frame, and the other axle 600 mm on the other side.

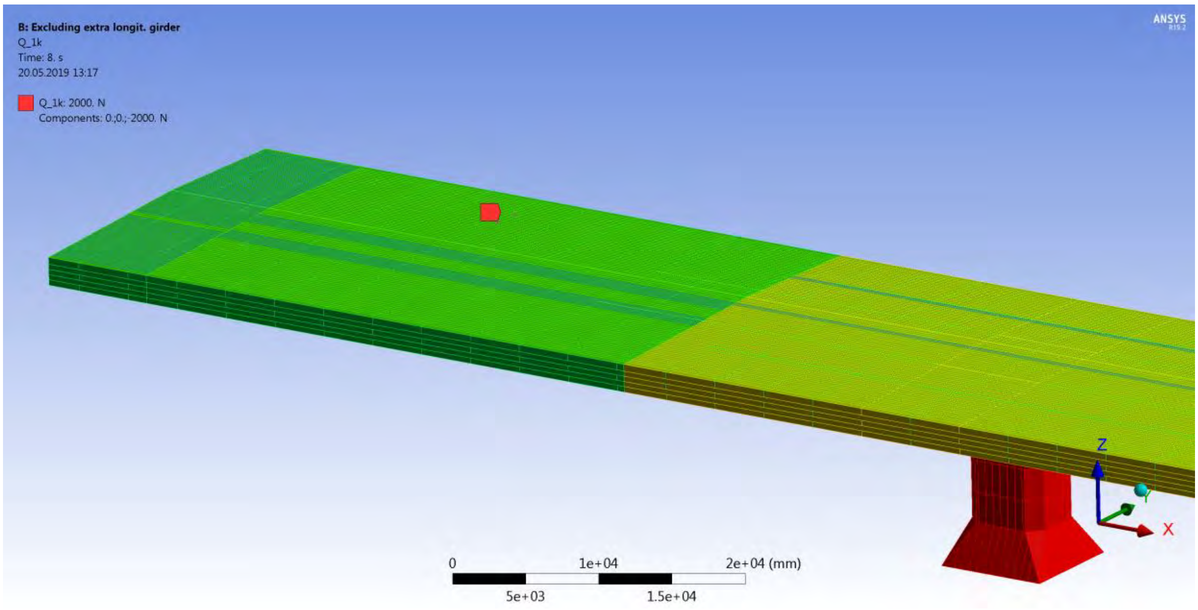

Figure 5-2 Axle load

5.4 Combinations

Four combinations have been run to evaluate the forces in the transversal frames. The combinations are listed in Table 5-3.

Table 5-3 Load combinations

Combination Load	LC 1	LC 2	LC 3	LC 4
1	1.2	1.2	1.2	1.2
2	1.2	1.2	1.2	1.2
3	1.35	1.35	1.35	1.35
4	1.35			
5		1.35		
6			1.35	
7				1.35
8	1.35 * 300			
9	1.35 * 200	1.35 * 300	1.35 * 100	1.35 * 100
10	1.35 * 100	1.35 * 200	1.35 * 300	1.35 * 200
11		1.35 * 100	1.35 * 200	1.35 * 300

5.5 Results

Results show that the longitudinal trapezoidal stiffeners in the top plate of the bridge girder are very effective at distributing point loads to adjacent transverse frames, and that the bridge girder web carry only a fraction of the shear forces. Beam forces and stress is significantly lower on the model with longitudinal trapezoidal stiffeners. Overall stress and utilization is low for transverse frames when including longitudinal trapezoidal stiffeners, leaving much capacity to take environmental forces (not included in this analysis).

For the FEM with trapezoidal stiffeners removed, the shear stress in the bridge girder webs are much higher. This analysis resembles the Staad analysis with supports at the bridge girder webs.

See summary of beam axial forces in Table 5-4 and shell stress on the following figures. On the figures below, the axle load is applied on the middle of the five transverse frames shown with results. Only LC 1 is presented with figures. Results are similar for the other load combinations.

Table 5-4 Summary beam axial stress

Combination	**Including trapezoidal stiffeners**		**Excluding trapezoidal stiffeners**	
	Max tension [kN]	**Max compression [kN]**	**Max tension [kN]**	**Max compression [kN]**
LC 1	40.7	-142.1	662.0	605.7
LC 2	58.9	-69.4	817.2	603.2
LC 3	51.9	-82.7	831.3	583.5
LC 4	65.0	-64.7	831.7	-648.6

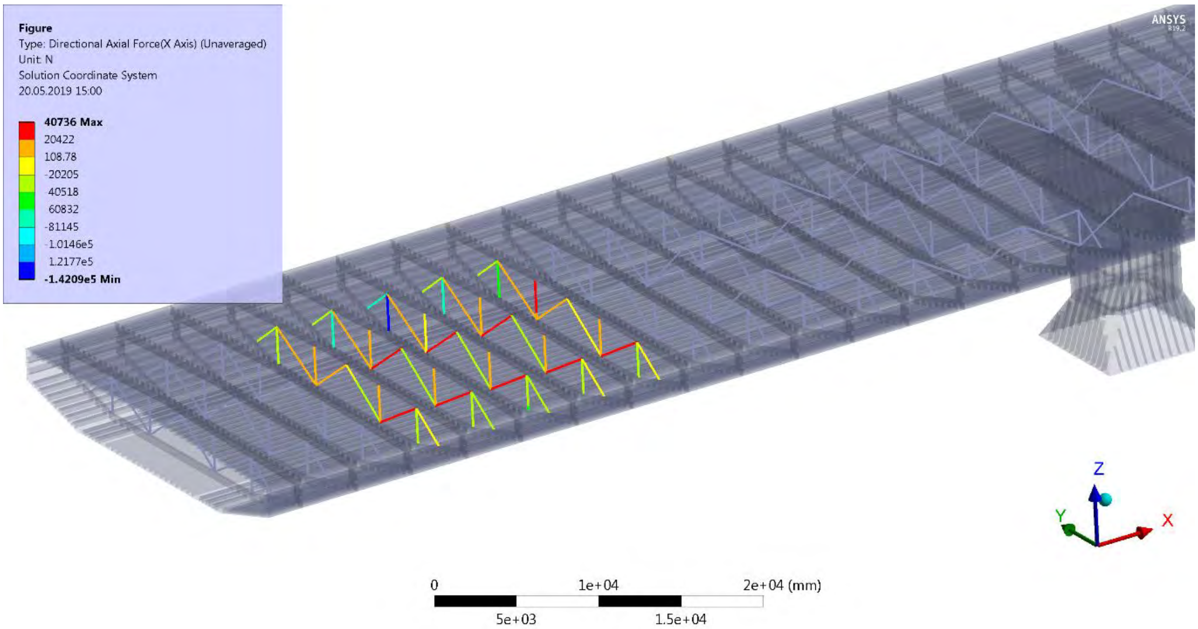

Figure 5-3 Beam axial force, LC 1

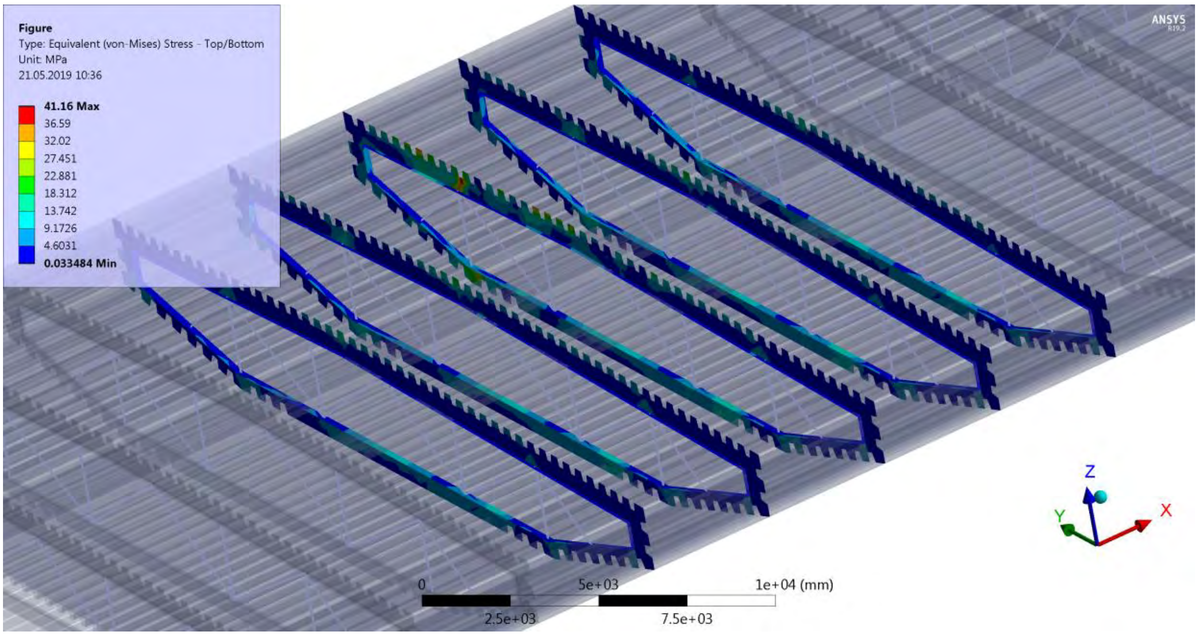

Figure 5-4 Transverse frames von-Mises stress, LC1

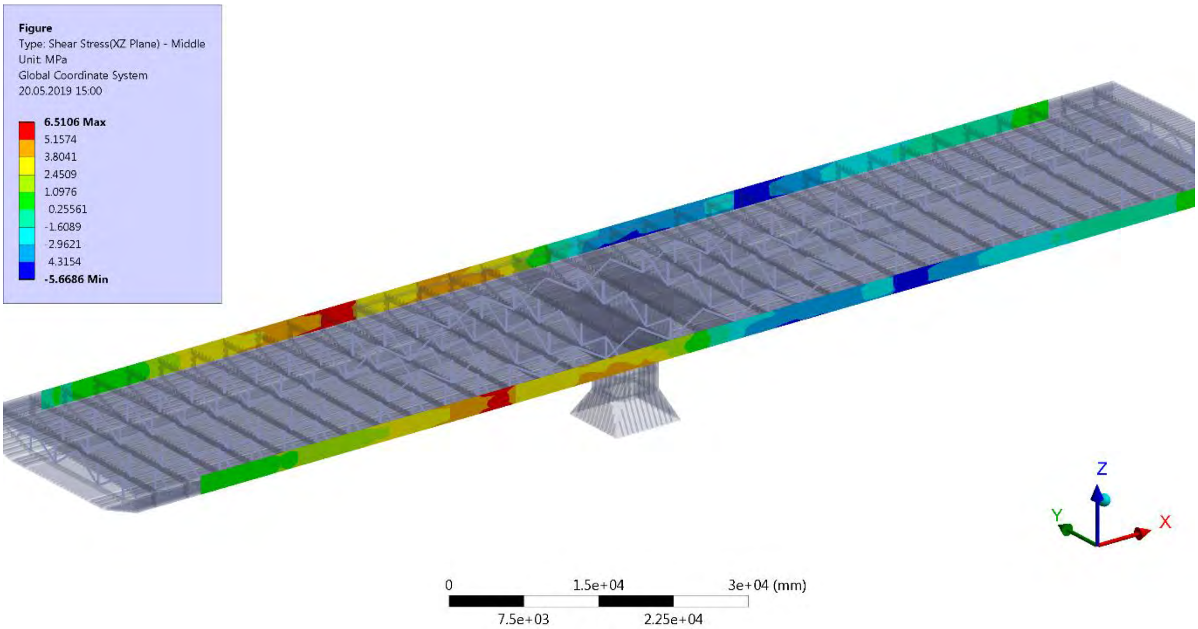

Figure 5-5 Bridge girder web shear stress, LC1

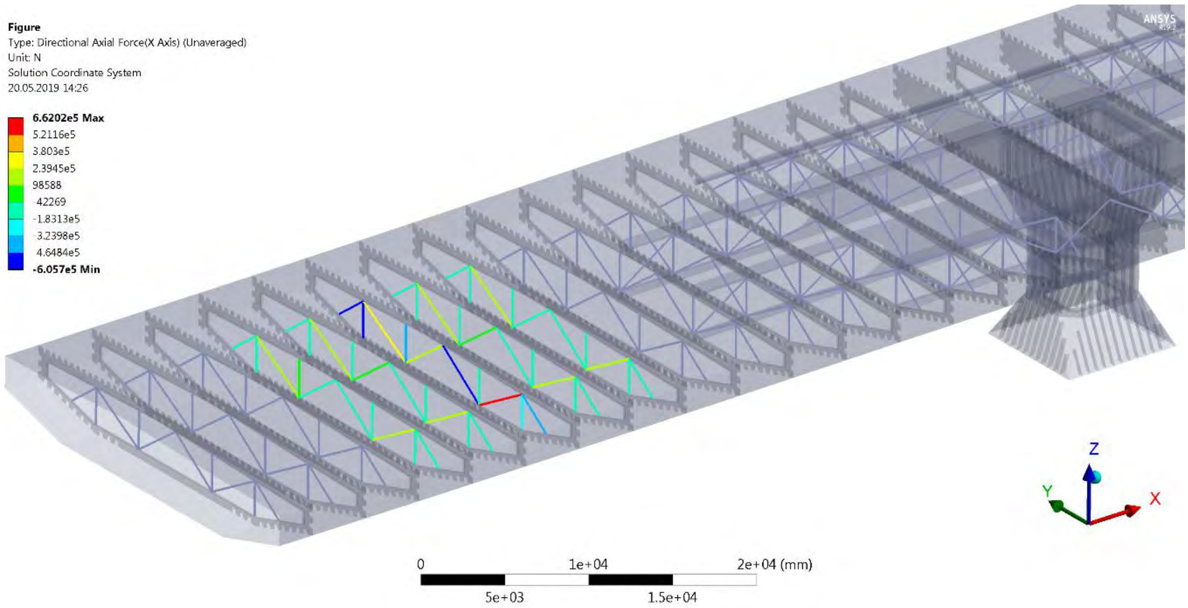

Figure 5-6 Beam axial force – trapezoidal stiffeners removed from analysis, LC 1

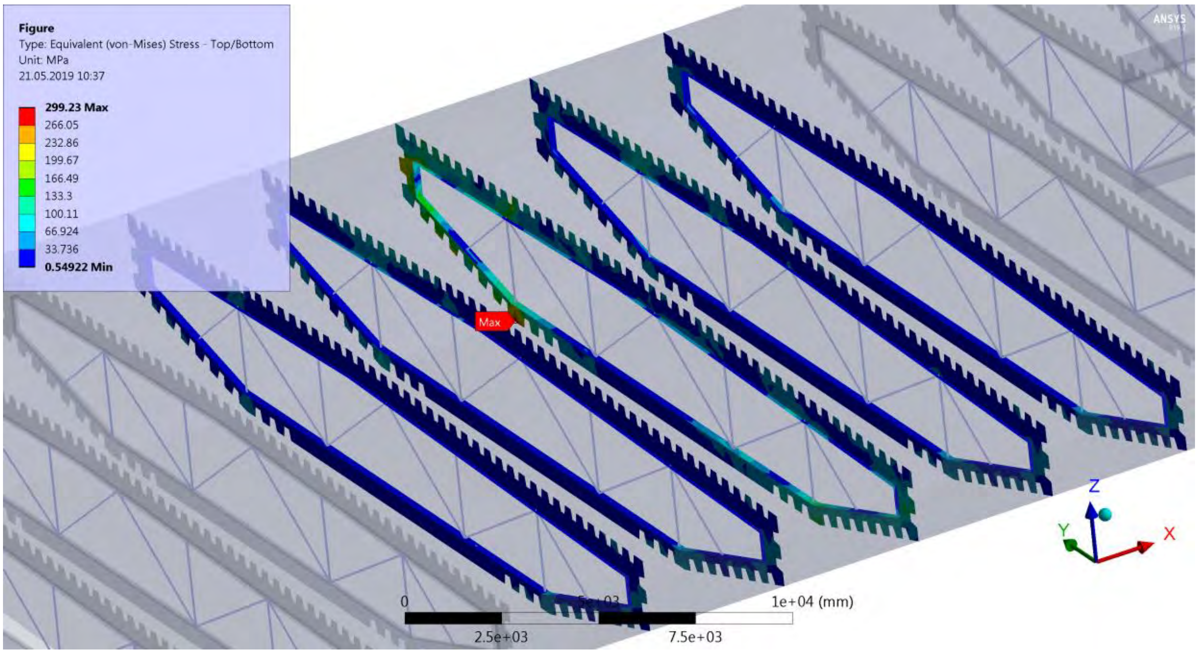

Figure 5-7 Transverse frames von-Mises stress– trapezoidal stiffeners removed from analysis, LC1

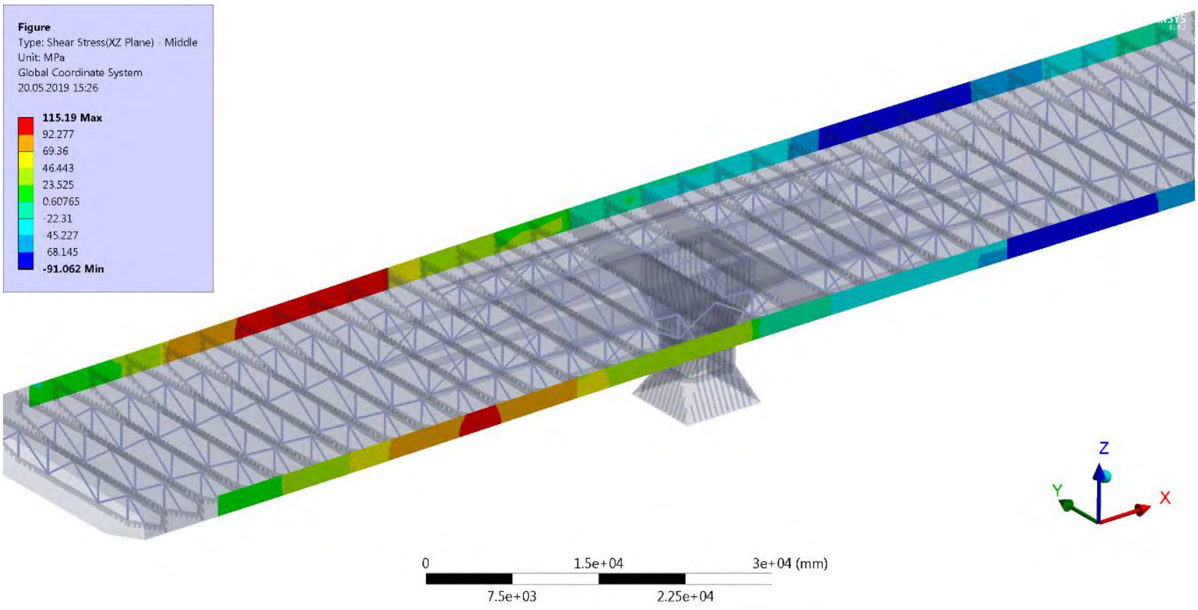

Figure 5-8 Bridge girder web shear stress – trapezoidal stiffeners removed from analysis, LC1

6 Ship impact column

To investigate the capacity of the column for an eccentric ship impact where torsion of the column is dominating the load, an analysis of the column only has been run. The analysis evaluate the capacity of the column and the effect of increasing the plate thickness, or change the column geometry. An explicit ship impact analysis of the column can be found in Appendix J [5]. The analyses presented here are implicit.

6.1 Geometry

Three variations of the column has been run. Two variations of the current low bridge column design as shown in Figure 6-1 where the skin plate thickness varies.

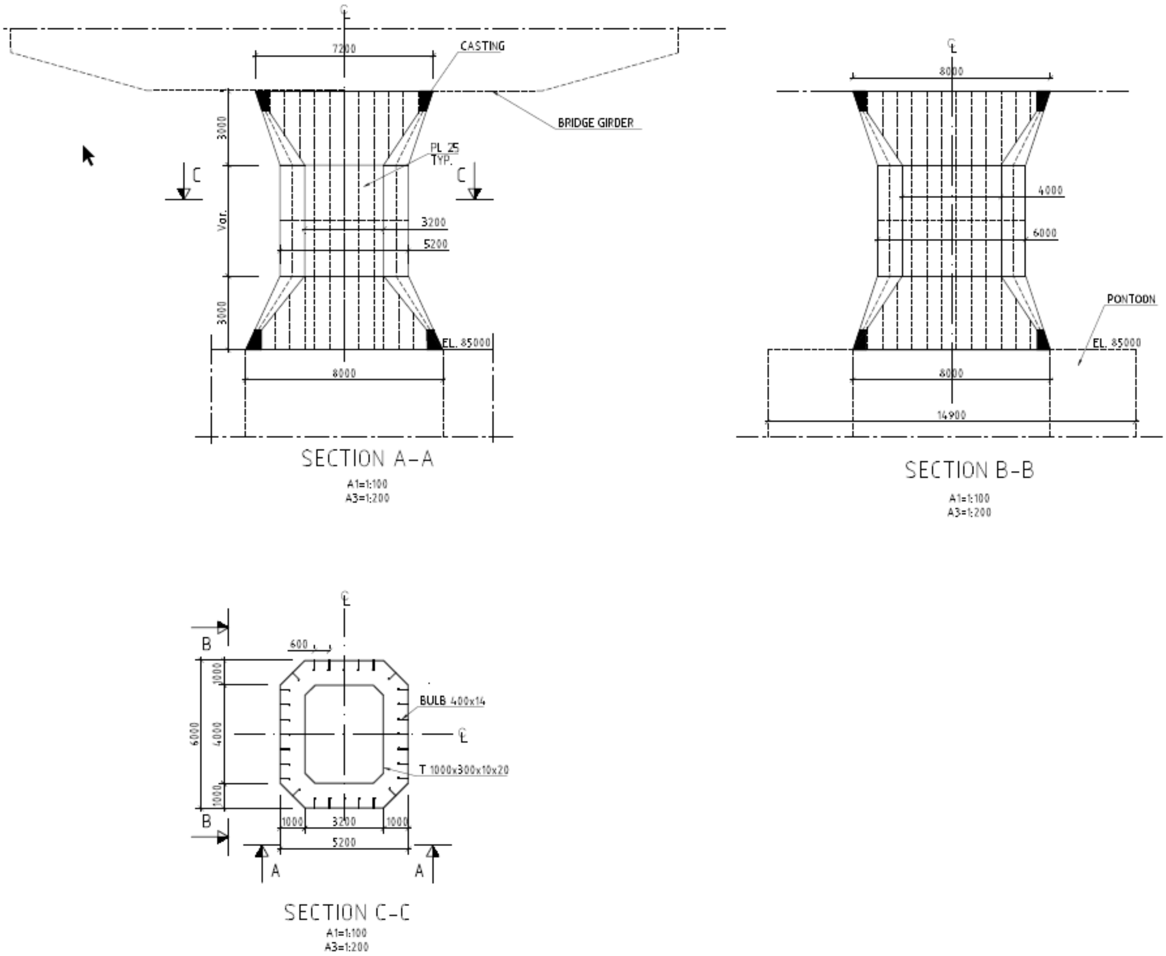

Figure 6-1 Column geometry with narrow middle part

The last variation is an 8 m X 8 m straight column. Chamfered corners are included. The geometry is shown in Figure 6-2.

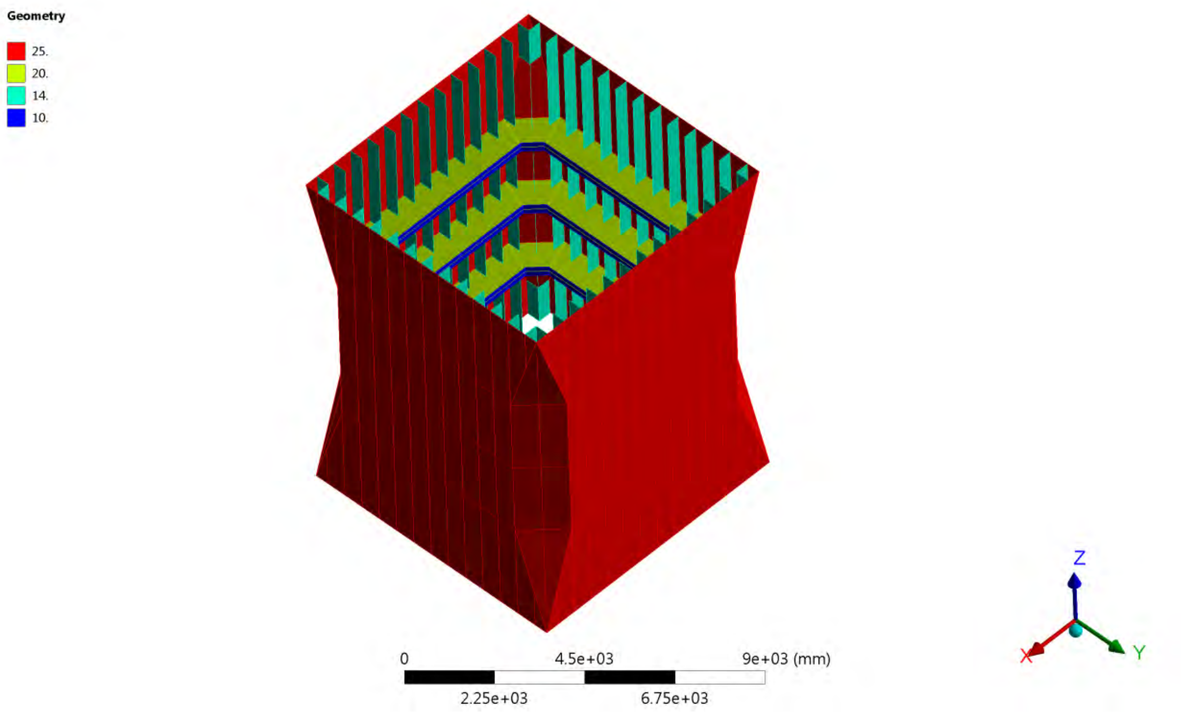

Figure 6-2 8 m X 8 m straight column geometry

A summary of geometries is shown in the table below.

Table 6-1 Column geometries

Analysis	Skin plate thickness [mm]	Outer dimensions [m]		
		Bottom	Middle	Top
1	25	8.0 X 8.0	5.2 x 6.0	7.2 x 8.0
2	40	8.0 X 8.0	5.2 x 6.0	7.2 x 8.0
3	25	8.0 X 8.0	8.0 X 8.0	8.0 X 8.0

Analysis 2 is also run as an explicit analysis to better document the dynamic behavior of the column during an impact. This is documented in Appendix J [5].

6.2 Mesh

The mesh size is approximately 140 mm by 140 mm. Figure 6-3 and Figure 6-4 show the mesh for the two different geometries.

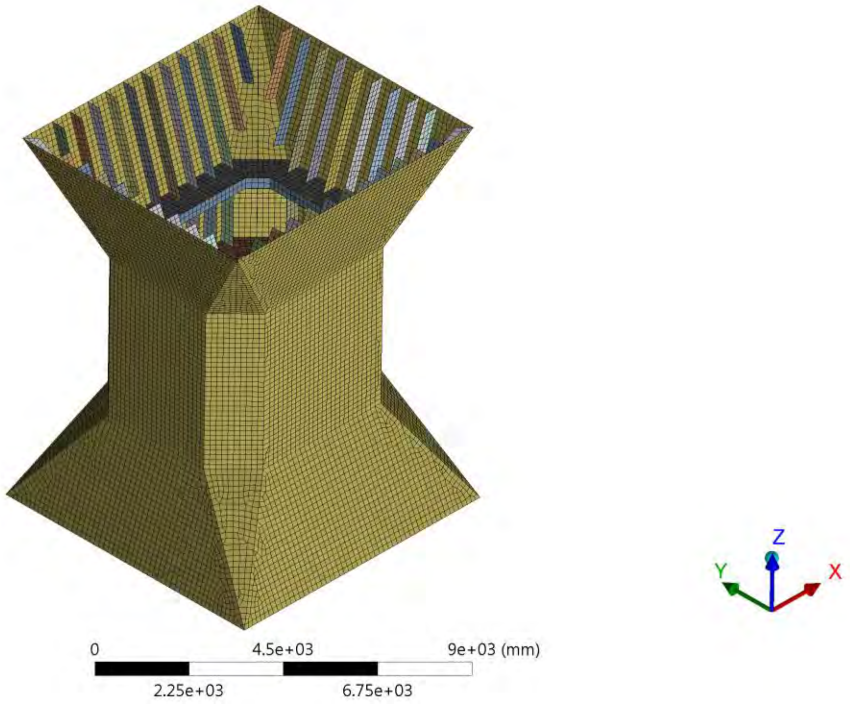

Figure 6-3 Mesh, column with narrow middle part

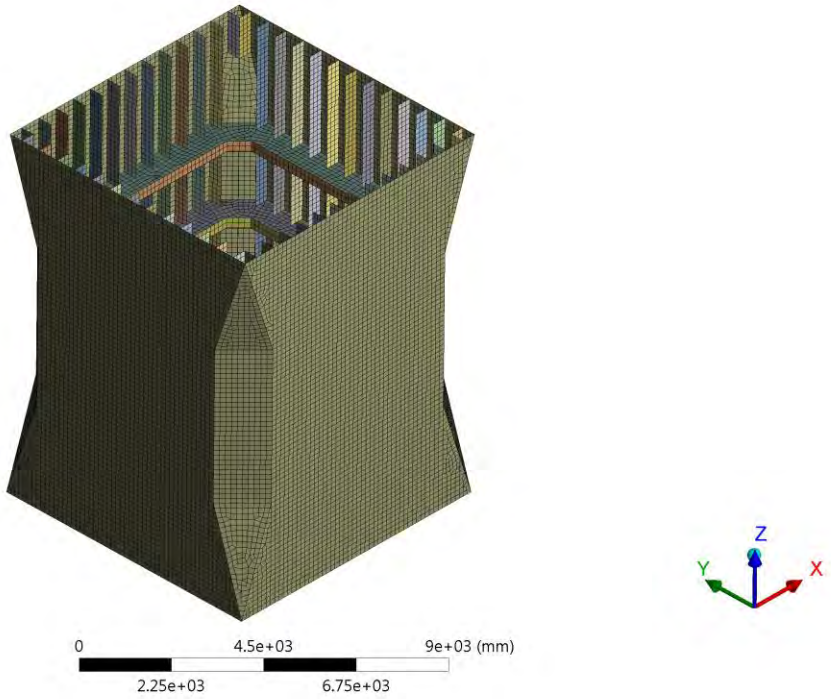

Figure 6-4 Mesh, straight column

6.3 Material properties

Non-linear material properties as documented in Table 1-2 have been used for this analysis.

6.4 Boundary conditions

The analysis is run displacement controlled where a rotation is applied at the bottom of the column. The shape of the bottom is kept rigid, and cannot deform. A rotation of 6 degrees is applied. The top of the column is fixed. Boundary conditions and deformations are summarized in Table 6-2.

Table 6-2 Boundary conditions

	Translation			**Rotation**		
	X	**Y**	**Z**	**X**	**Y**	**Z**
Column top	Fixed	Fixed	Fixed	Fixed	Fixed	Fixed
Column bottom	Free	Free	Free	Free	Free	Time 1: 0° Time 2: 6°

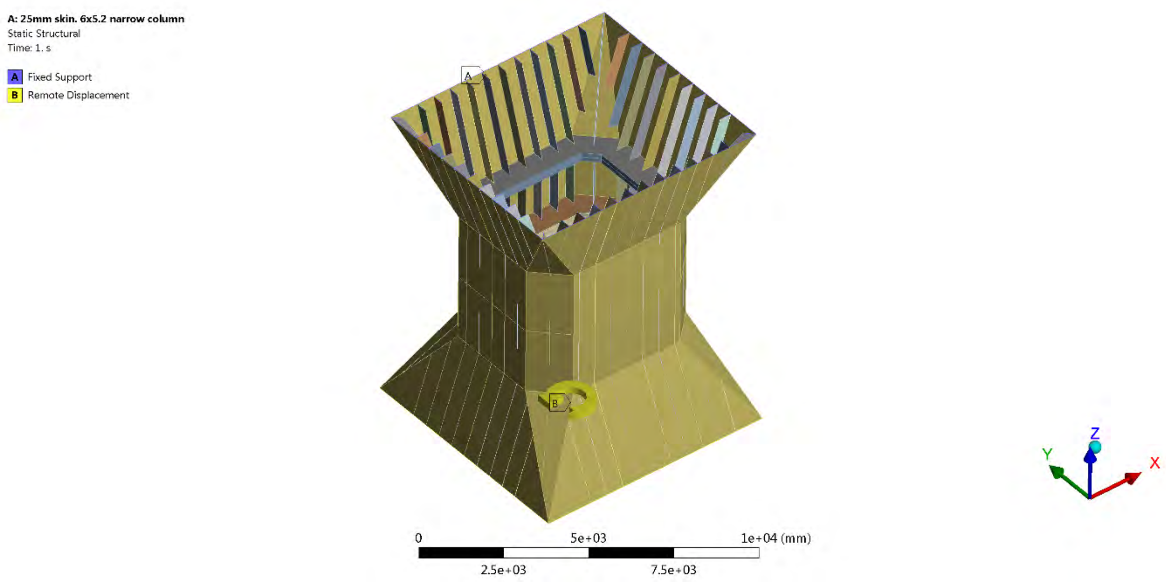

Figure 6-5 Boundary conditions

6.5 Results

Moment about z-axis is probed at the fixed boundary condition at the column top. This is plotted in Figure 6-6. Analysis 1 with 25 mm skin plate and narrow middle part does not converge for a full 6-degree rotation. Analysis 2 and 3 converge at 6-degree rotation, and could have been run further. Maximum torsional force observed for the three variations is presented in Table 6-3.

Table 6-3 Maximum torsional force

Analysis	**Torsion Mz [MNm]**
1	365
2	604
3	750

Figure 6-7 show the energy absorbed (elastic and plastic) vs rotation.

The torsional capacity of the columns is greatly improved by using thick skin plates and/or increase size of the middle part of the columns.

Going from 25 mm plate to 40 mm will increase the torsional capacity by 65.5 % and the weight by approximately 35%.

When keeping the thickness of 25 mm and removing the narrow part of the column so that the walls are straight (chamfered corners are kept), torsional capacity increases by 105.5 % and the weight increase by approximately 28%. This is the most effective way to increase the torsional capacity of the columns.

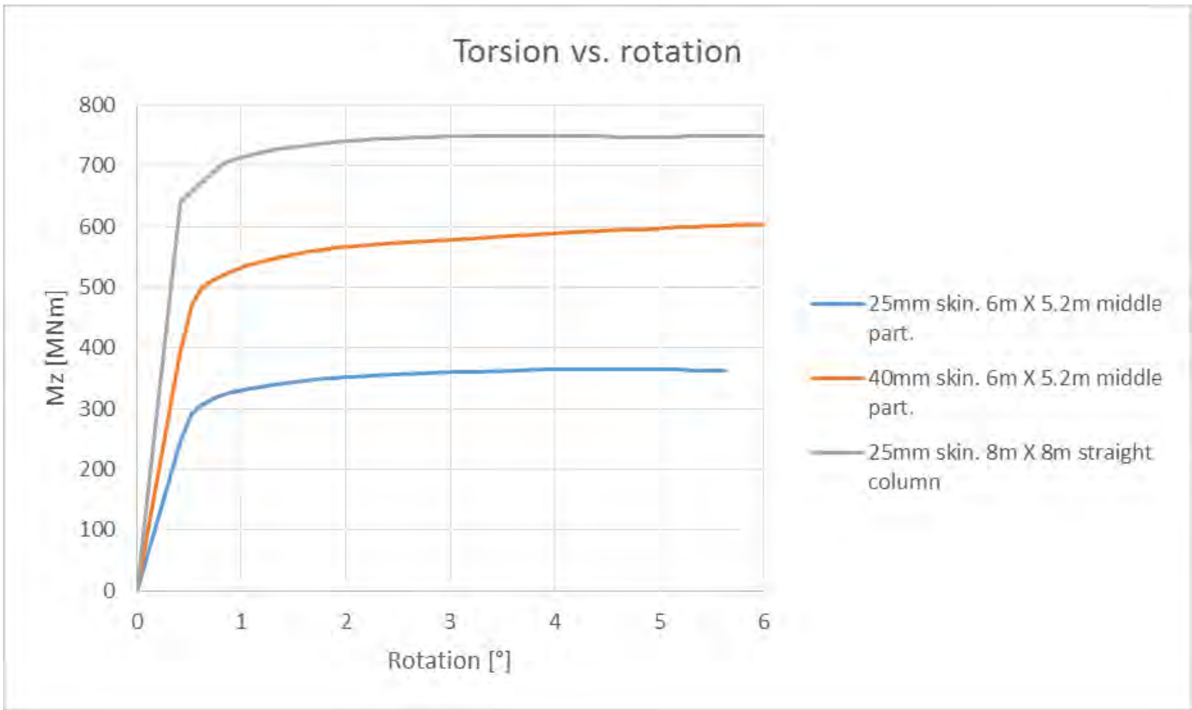

Figure 6-6 Torsion vs. rotation

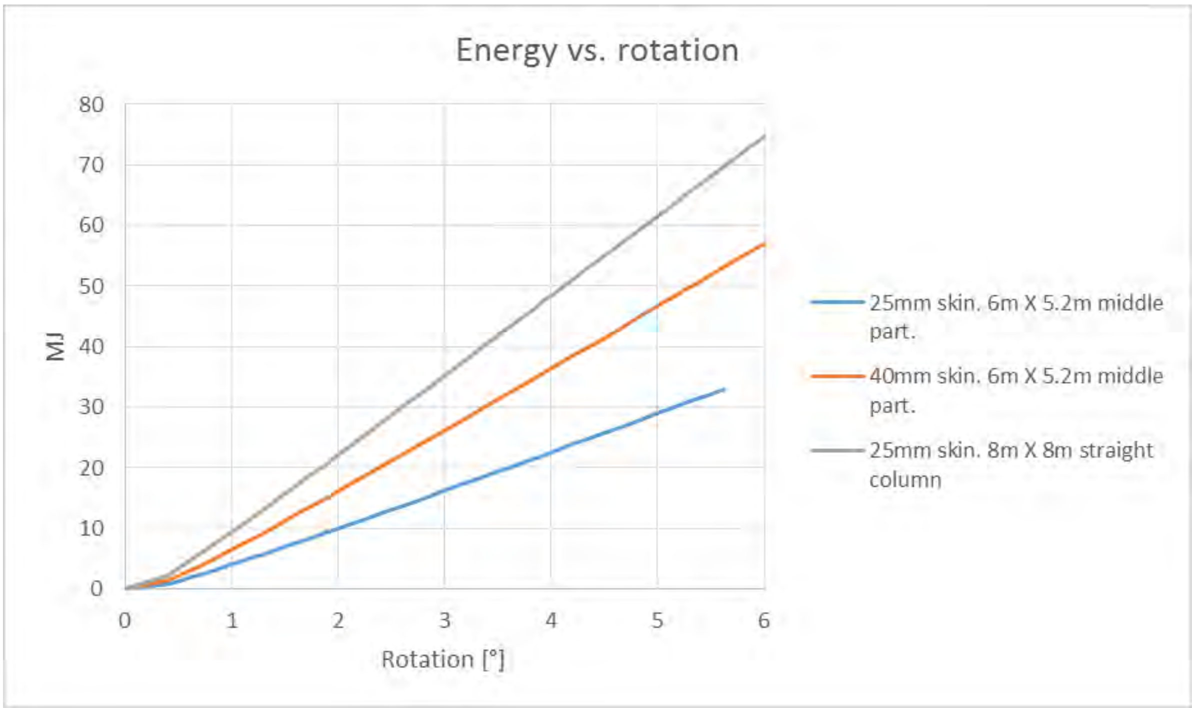

Figure 6-7 Energy vs. rotation

6.5.1 Analysis 1, 25 mm plate, column with narrow middle part

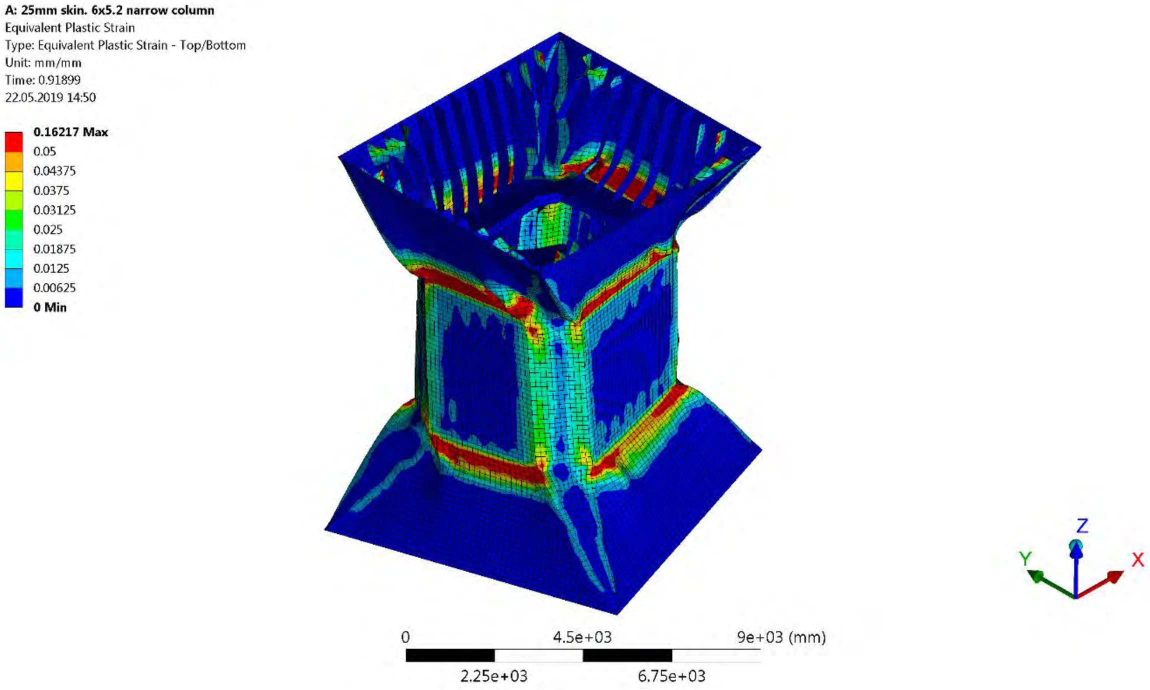

*Figure 6-8 Analysis 1, Plastic strain for last converged step (6 degrees * 0.919 = 5.5 degrees)*

The geometry causes the column to loose torsional capacity and yield of larger parts of the column does not occur. This is unfavorable when trying to absorb as much energy as possible.

6.5.2 Analysis 2, 40 mm plate, column with narrow middle part

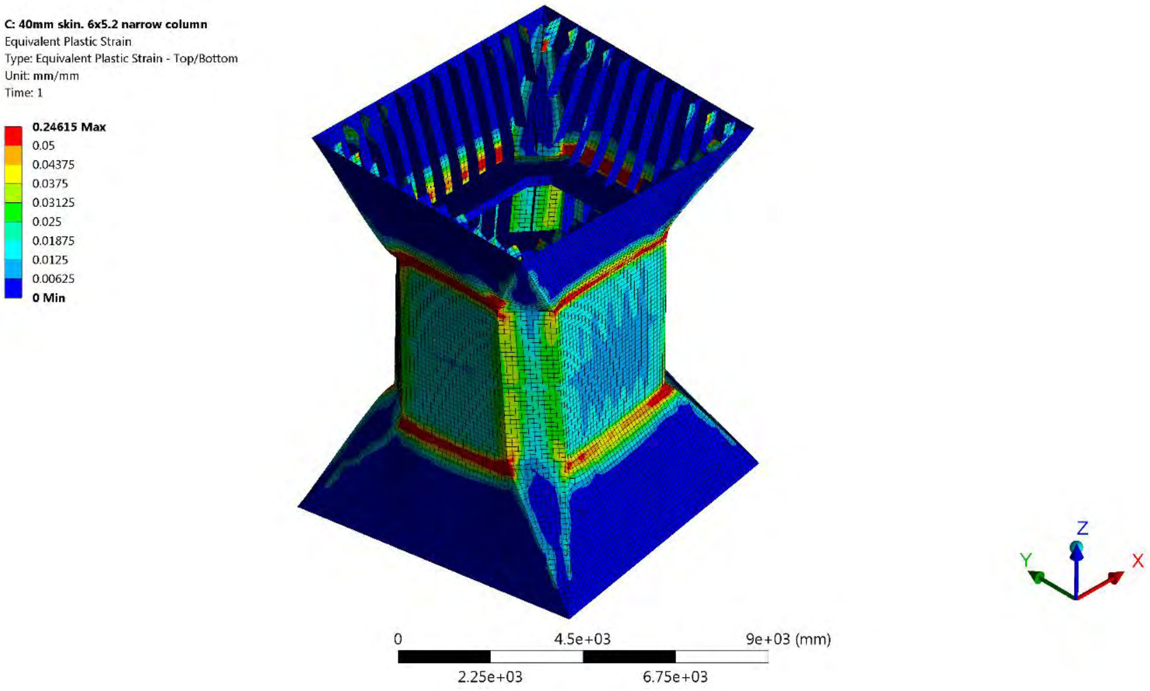

Figure 6-9 Analysis 2, Plastic strain at 6 degrees rotation

Plastic strain for this analysis is higher and occurs over much larger areas, absorbing more energy.

6.5.3 Analysis 3, 25 mm plate, straight column

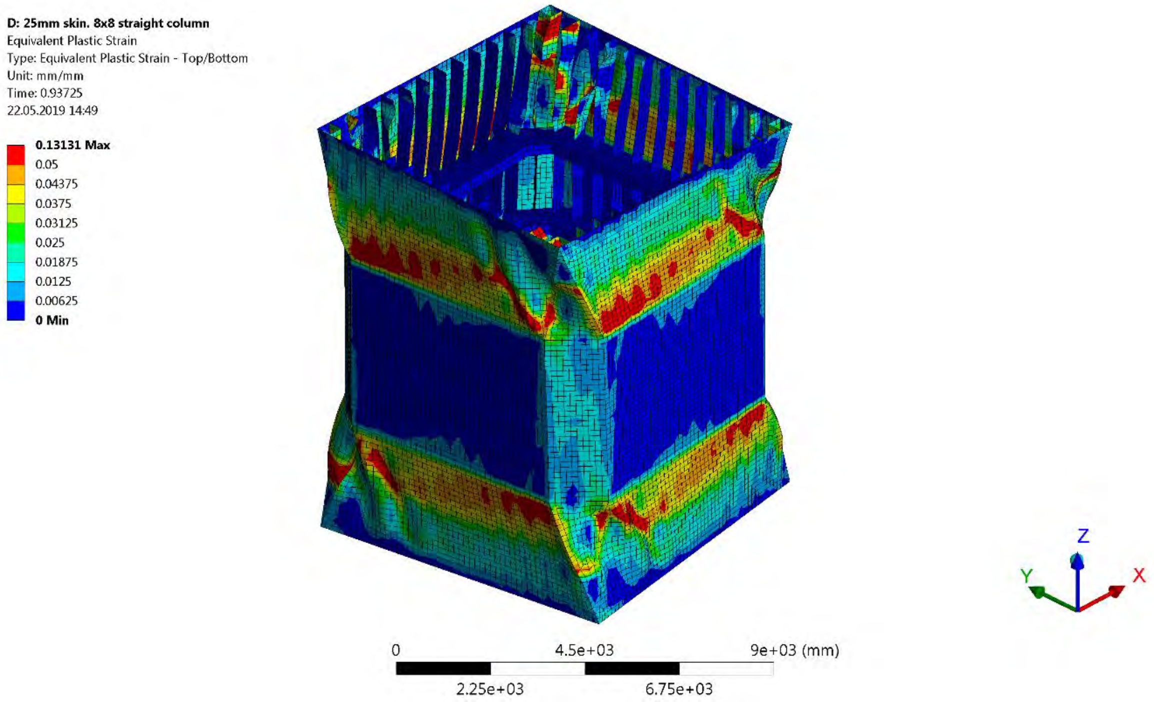

Figure 6-10 Analysis 3, Plastic strain at 6 degrees rotation

7 Ship impact column and bridge girder

The purpose of this analysis is to evaluate the bridge girders ability to take the torsional forces from the column during an eccentric ship impact. The column non-linear capacity is documented in section 6, so the focus here is bridge girder only.

7.1 Material properties

Linear material properties as documented in Table 1-2 has been used for this analysis.

7.2 Mesh

The element mesh is refined at two areas to get better results. The refined mesh has a size of approximately 30 mm by 30 mm.

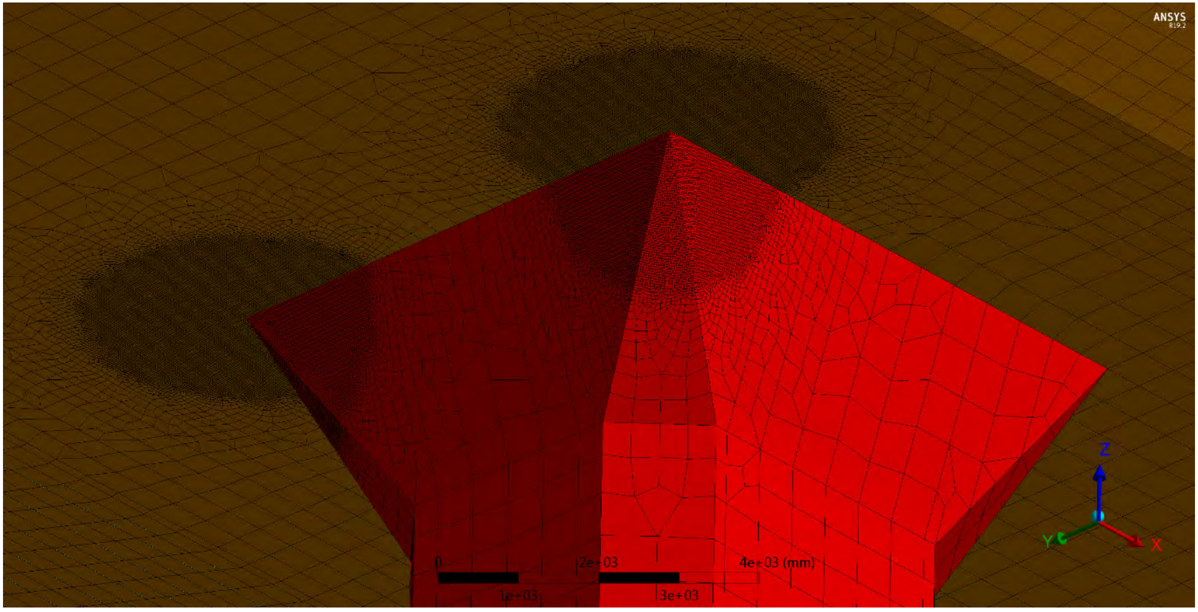

Figure 7-1 Mesh refinement

7.3 Boundary conditions

Boundary conditions and axis definitions are shown on Figure 7-2Figure 2-1 and

Table 7-1.

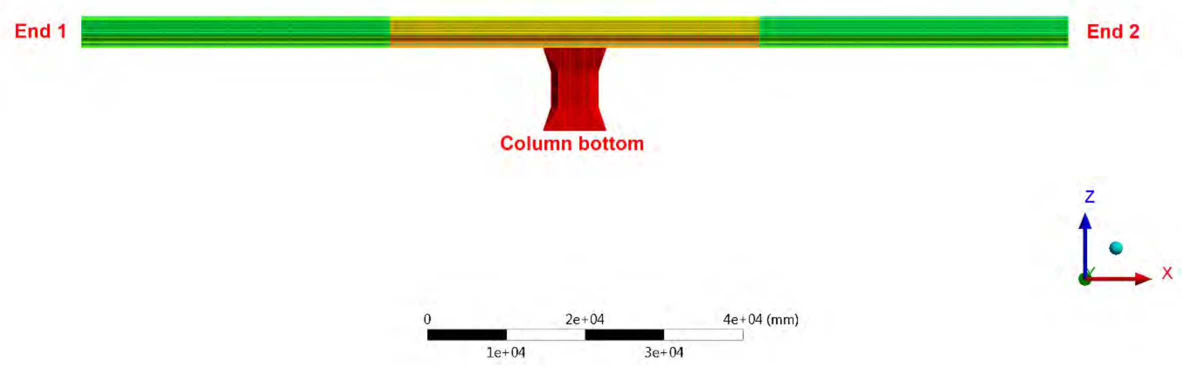

Figure 7-2 Boundary conditions

Table 7-1 Boundary conditions

	Translation			Rotation		
	X	**Y**	**Z**	**X**	**Y**	**Z**
End 1	Fixed	Fixed	Fixed	Fixed	Free	Free
End 2	Fixed	Fixed	Fixed	Fixed	Free	Free

7.4 Loads

Maximum torsional force found for “Analysis 2, 40 mm plate, column with narrow middle part” has been applied to column bottom. Mz = 604 MNm.
The applied force will stress the column well beyond yield. This is documented in section 0.
However, the bridge girder, as can be seen later in this section, have stress in the elastic range. The choice of using linear material properties significantly reduces computational time.

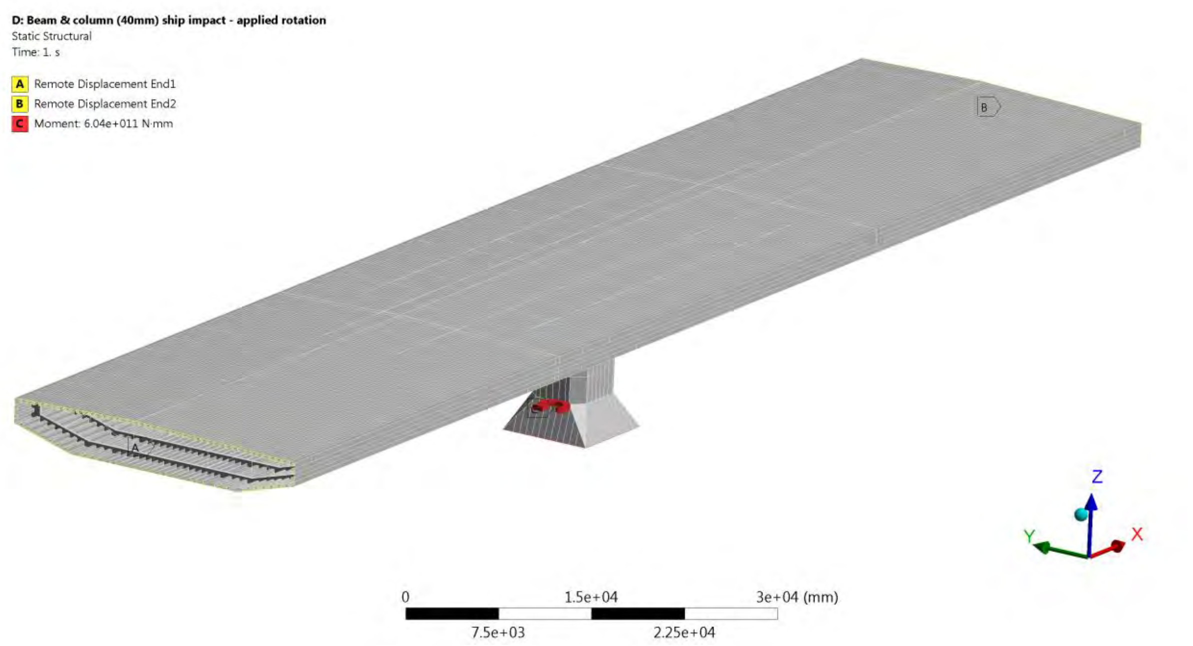

Figure 7-3 Boundary conditions and load application

7.5 Results

Von-Mises stress is as expected well above yield for the column.

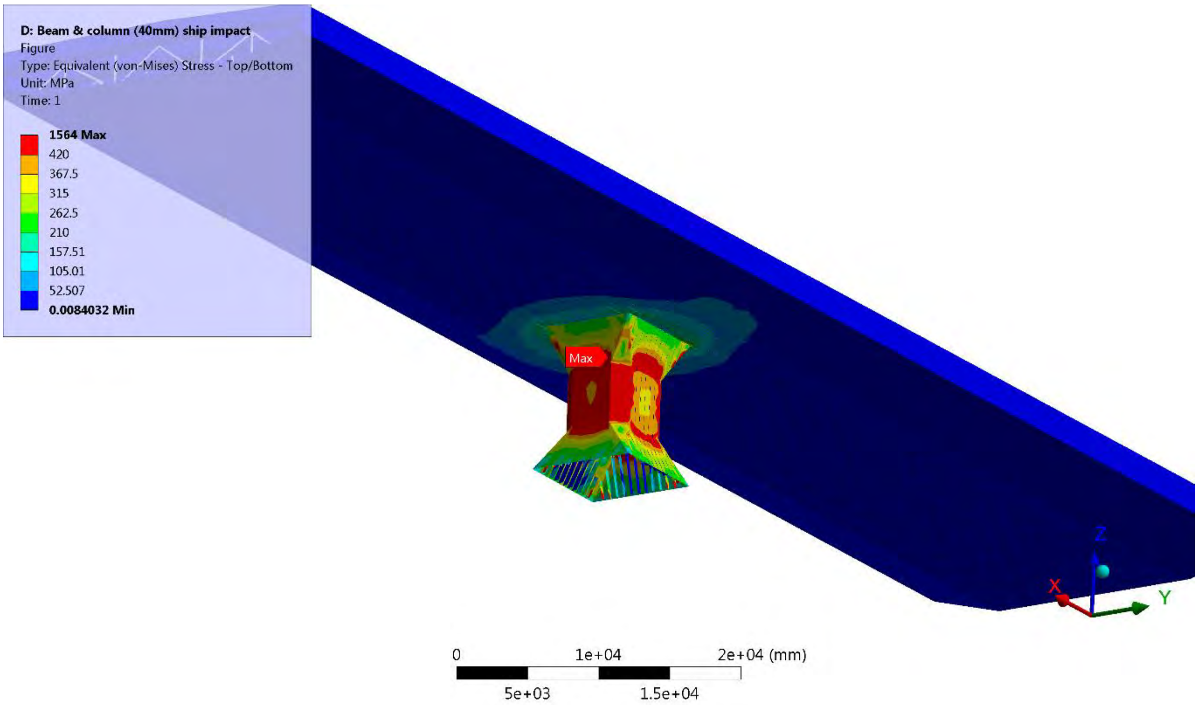

Figure 7-4 Stress (von-Mises) in bridge girder and column

On the following figures the column is removed from the results. The stress color legend is set so that red is higher than yield (420 MPa).

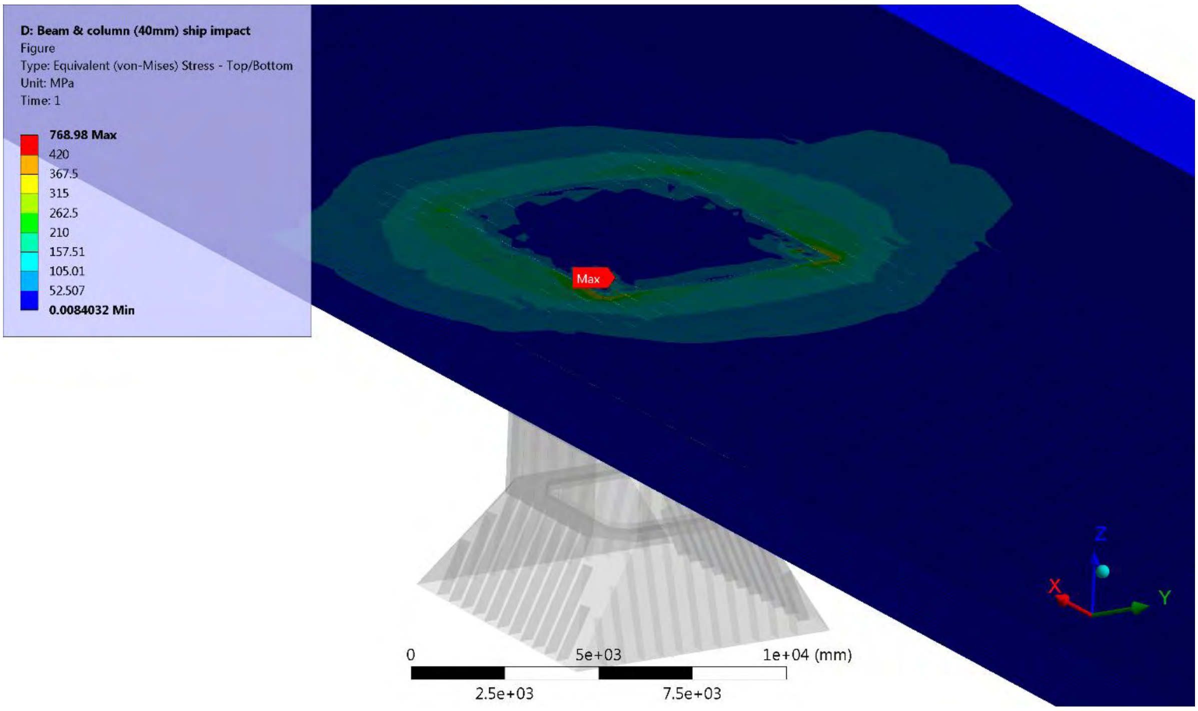

Figure 7-5 Stress (von-Mises) in bridge girder

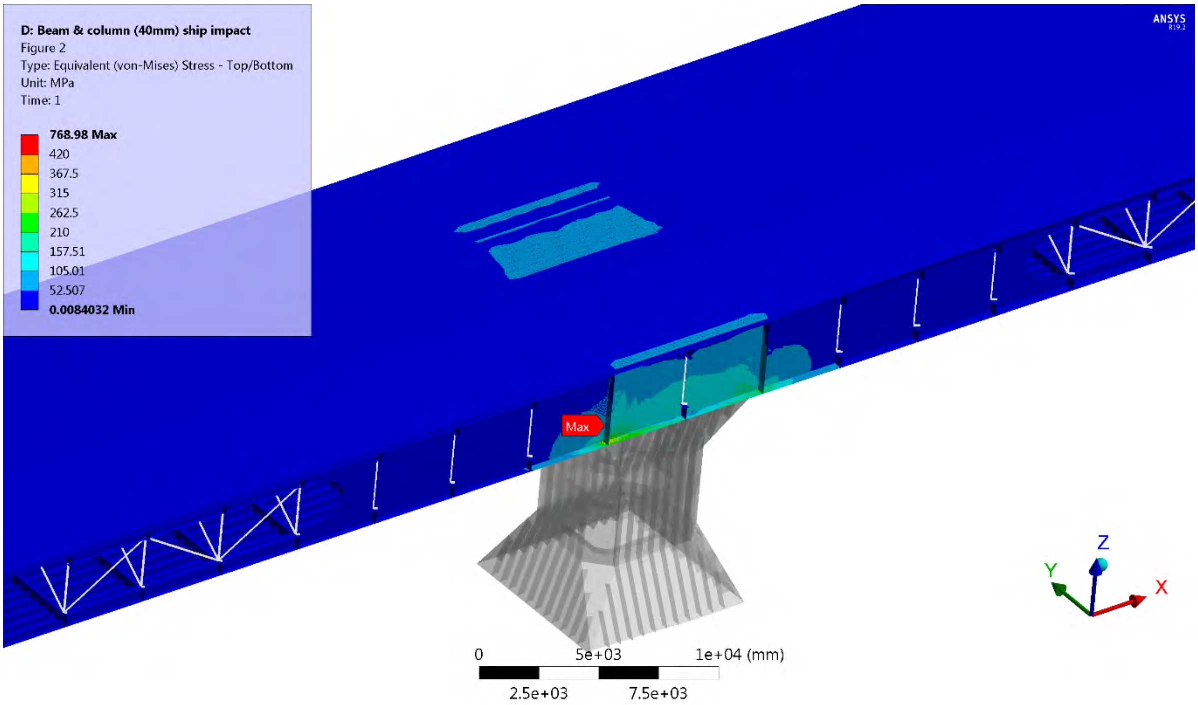

Figure 7-6 Stress (von-Mises) in bridge girder, longitudinal cut

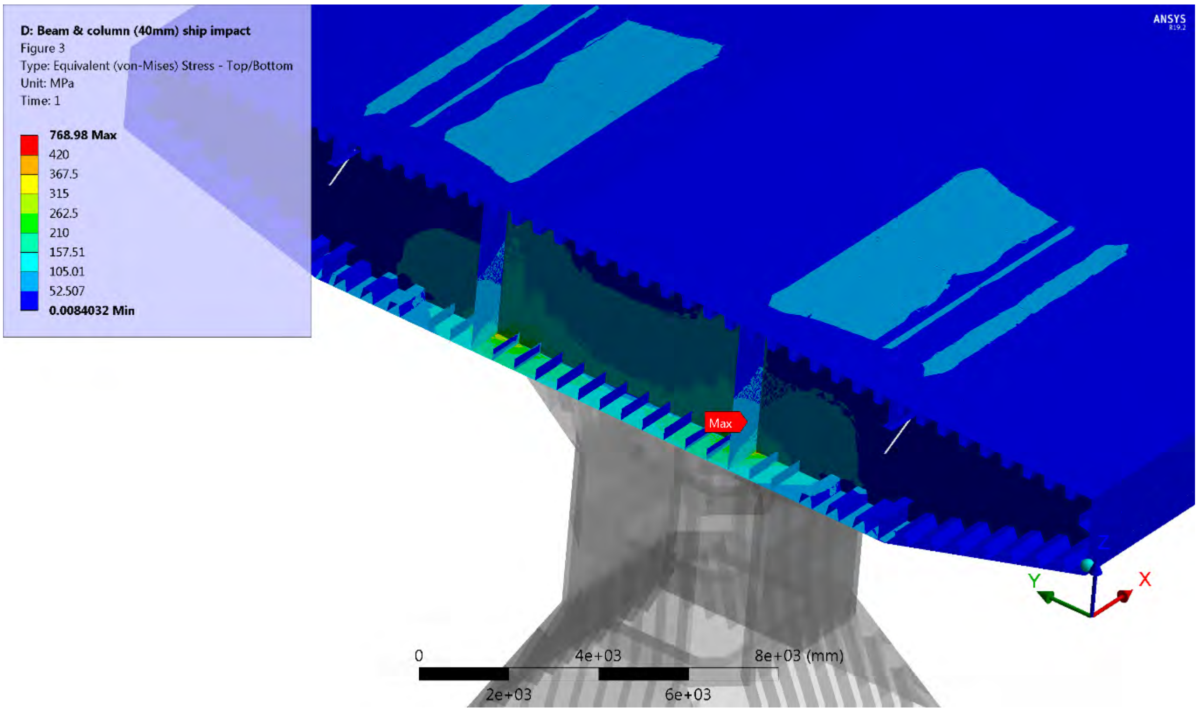

Figure 7-7 Stress (von-Mises) in bridge girder, transverse cut outside column

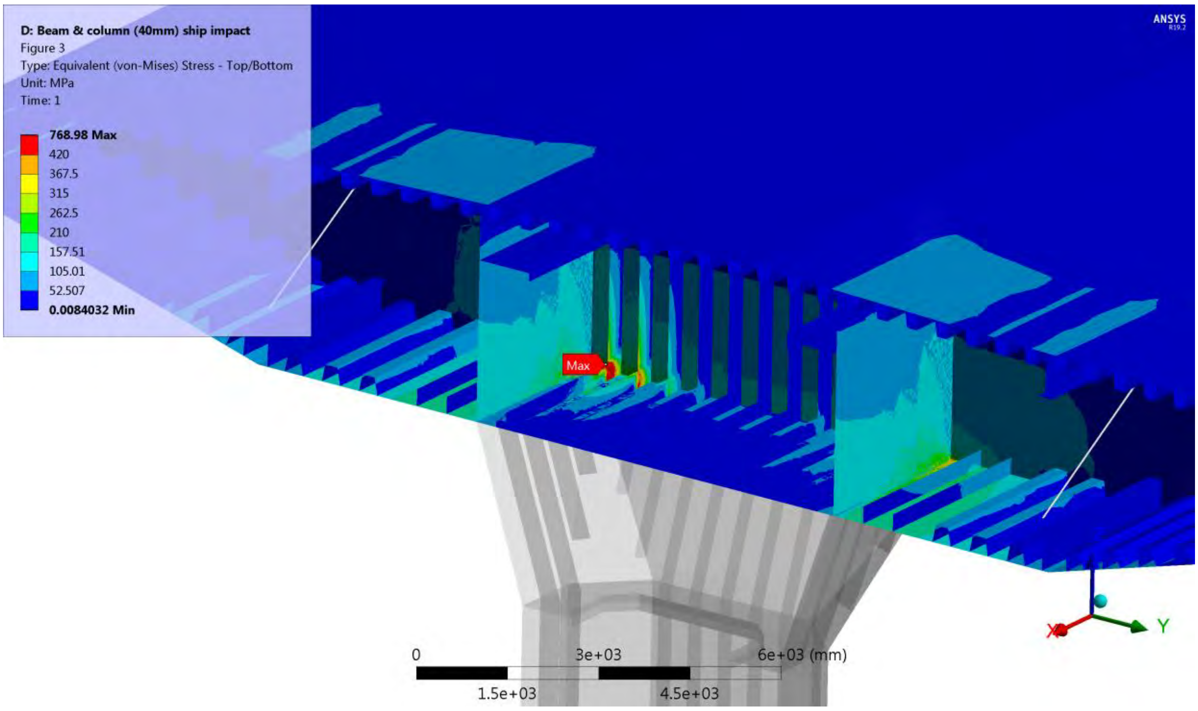

Figure 7-8 Stress (von-Mises) in bridge girder, transverse cut inside column

The overall stress in the bridge girder is acceptable for the maximum torsional force that the column can transfer. Small areas with stress above the yield limit (420 MPa) can be observed on bulbs near the corner of the column. This area is reinforced with a cast part and surrounding area with thicker plates. These reinforcements are not included in this FEM, and stress will most likely be lower due to the reinforcements.

The column has lower Mz (torsion) capacity than the bridge girder, and acts as a weak link between the pontoon and the bridge girder.

8 References

[1] AMC, “10205546-13-NOT-086 : Column design Rev. 1,” 24.05.2019.

[2] CEN, *NS-EN 1993-1-5:2006+NA:2009 Eurocode 3: Design of steel structures, Part 1-5: Plated structural elements,* 2009.

[3] AMC, “10205546-13-NOT-083 : Transverse Trusses in Bridge Girder Rev. 1,” 24.05.2019.

[4] CEN, NS-EN 1991-2 Eurocode 1: Actions on structures. Part 2: Traffic loads on bridges, Standard Norge, 2003+NA:2010.

[5] AMC, “SBJ-32-C5-AMC-27-RE-110 : Appendix J: Ship collision Rev. 0,” 24.05.2019.